THE ROLE OF MECHANOTRANSDUCTION IN THE REGULATION OF HUMAN ALVEOLAR EPITHELIAL CELL FUNCTION

Kathryn Murray BSc (Hons)

A thesis submitted for the degree of Doctor of Philosophy
The University of Edinburgh – 2006

Declaration

I declare that all the work presented in this thesis is my own, and has been composed and performed by myself. All sources of information, including contributions by colleagues, are fully acknowledged in the text.

This work has neither been submitted or accepted for candidature for any other degree or professional qualification.

Kathryn Murray

Table of Contents

Acknowledgements 1

List of Abbreviations 2

Abstract 4

Chapter 1: Lung biology and mechanotransduction 6

1.1 Microanatomy of the alveolus and mechanical forces 7

1.1.1 Alveolar epithelial cells 7

1.1.2 Interstitial cells 8

1.1.3 Alveolar extracellular matrix 8

1.2 Mechanical environment of the alveolus 15

1.2.1 Pulmonary surfactant 16

1.3 Experimental approaches to the study of mechanical stimulation of lung cells 19

1.3.1 Uniaxial systems 19

1.3.2 Biaxial systems and equibiaxial systems 20

1.3.3 Other Mechanical strain systems 20

1.4 Mechanotransduction 21

1.4.1 Mechanoreception 21

1.4.1.1 Integrins 22

1.4.1.2 Stretch – activated /mechanosensitive ion channels 24

1.4.2 Intracellular signalling activated bye mechanical strain 26

1.4.2.1 G – protein coupled receptor signal transduction pathways 26

1.4.2.2 Protein tyrosine kinases 27

1.4.2.3 Map kinases signalling 28

1.4.3 Regulation of tissue remodelling 29

1.4.3.1 Cell proliferation and differentiation 30

1.4.3.2 Extracellular matrix (ECM) turnover 31

1.4.3.3 Surfactant metabolism 32

1.4.3.4 Cytokine, chemokine and growth factor production 33

1.5 Aims and objectives 36

Chapter 2: Materials and methods 37

2.1 Cell culture of human adenocarcinoma cell line NCI-H441 38

2.1.1 Cell counting and viability assessment by the trypan blue dye exclusion stain procedure 38

2.1.2 Coating dishes with ECM proteins 39

2.2 Induction of cyclical mechanical strain **39**

2.3 General immunocytochemistry **44**

2.3.1 Cytospin preparation 44

2.3.2 Immunochemistry of frozen section or cells 44

2.4 Electron microscopy **45**

2.4.1 Processing schedule for tissue cultured cells – cell suspensions 45

2.5 Protein extraction **46**

2.5.1 Lysis of adherent monolayer cell culture 46

2.5.2 Homogenising human lung tissue for protein extraction 46

2.6.1 Sodium dodecyl sulphate poly – acrylamide gel electrophoresis (SDS – PAGE) 49

2.6.2 Electrophorectic transfer of protein to poly vinylidene fluoride membrane 50

2.6.3 Immunoblotting and development of blot using enhanced chemiluminescene – plus (ECL – plus) 50

2.6.4 Stripping and reprobing western blots 51

2.7 Sandwich enzyme – linked immunosorbent assay of extracellular surfactant protein – B (ELISA) **52**

2.8 Reverse transcription polymerase chain reaction (RTPCR) **54**

2.8.1.1 Ribonucleic acid (RNA) extraction from adherent monolayer cell culture 54

2.8.1.2 Homogenising human lung tissue for RNA extraction 54

2.8.1.3 Spectrophotometric analysis of RNA 55

2.8.1.4 DNase treatment of RNA 55

2.8.2.1 Reverse transcription reactions –complement deoxynucleic acid (cDNA) synthesis 57

2.8.2.2 Polymerase chain reactions 57

2.8.3 Agarose gel electrophoresis 59

2.8.3.2 The purification of PCR products for automated DNA sequencing 60

2.9 Taqman® real time polymerase chain reactions **61**

2.9.1 Preparation of cDNA for Taqman® reactions 61

2.9.2 Taqman® realtime polymerase chain reactions 61

2.10 Electrophysiology **62**

2.10.1 Preparation of microelectrodes 62

2.10.2 Filling of microelectrodes 62

2.10.3 Electrophysiological recording 62

2.11 Statistical analysis **68**

Chapter 3: Human type II pneumocyte isolation and characterization **70**

3.1 Human type II pneumocyte isolation and characterization **71**

3.2.1 Primary human sample collection and storage 73

3.2.2 Isolation of primary human type II pneumocytes 73

3.2.2.1 DNase – free isolation method utilising trypsin 73

3.2.2.2 Isolation utilising trypsin and DNase 74

3.2.3 Results 77

3.2.4 Discussion 84

3.3 Type II pneumocyte characterization **87**

3.3.1 Alkaline phosphatase staining 89

3.3.1.1 Results 90

3.3.2 Modified haematoxylin staining 90

3.3.2.1 Results 92

3.3.3 Cytokeratin and common leukocyte antigen (CD45) immunocytochemistry *95*

3.3.3.1 Pan – cytokeratin and CD45 immunocytochemistry results 95

3.4 Modified haematoxylin staining and immunocytochemistry discussion **99**

Chapter 4: The development of an in vitro model system to study type II respiratory epithelial cell mechanotransduction **103**

4.1 The development of an in vitro model system to study respiratory epithelial cell mechanotransduction **104**

4.2 NCI – H441 cell line characterization **105**

4.2.1 Alkaline phosphatase staining of NCI – H441 cell line 105

4.2.1.1 Results 105

4.2.2 Gene expression and production of surfactant specific protein 107

4.2.2.1 Surfactant specific protein – A mRNA expression in NCI – H441 107

4.2.2.2 Results 107

4.3. *Surfactant specific protein A and B expression* 110

4.3.2. Cytokeratin expression within NCI – H441 110

4.3.3 Electron microscopic analysis and comparison of NCI – H441 and type II pneumocytes 114

4.4. The electrophysiological response of primary type II pneumocytes to cyclical mechanical stimulation **117**

4.4.1 The effect of time in culture on the electrophysiological response of NCI – H441 cells 120

4.4.1.1 Results 120

4.4.2 The effect of serum supplementation on the relative percentage change in membrane potential of cyclic mechanical stimulated NCI – H441 cells 120

4.4.2.1 Results 124

4.5 The effect of extracellular matrix substrate on electrophysiological response of cyclic mechanical stimulated NCI – H441 cells **126**

4.5.1 Resting membrane potential of the NCI – H441 cell line cultured on collagen IV and fibronectin 126

4.5.2 Cyclic mechanical stimulation elicits significant membrane hyperpolarisation responses in NCI –H441 cultured on collagen IV and fibronectin 127

4.5.3 Relative change in NCI – H441 cells' membrane potential, cultured on BSA, CIV, FN, following cyclical mechanical stimulation 129

4.6 Discussion **132**

Chapter 5: The effect of cyclic mechanical strain on gene expression and surfactant specific protein levels in the NCI – H441 cell line **137**

5.1 The effect of cyclic mechanical strain on gene expression and surfactant protein levels in the NCI – H441 cell line **138**

5.2 Basal gene expression levels of NCI – H441 cell line **139**

5.3 The effect of culture on fibronectin coated substrata on NCI – H441 cell line gene expression **141**

5.4 The effect of cyclic mechanical stimulation on gene expression levels in NCI – H441 ..... **146**

5.5 The effect of cyclic mechanical stimulation on gene expression levels in NCI – H441 cultured on fibronectin **153**

5.6 The effect of cyclic mechanical stimulation on surfactant specific protein – A in NCI H441 cells **159**

5.6.1 Cytoplasmic levels of SP – A in cyclic mechanical stimulated NCI – H441 159

5.6.2 The effects of cyclic mechanical stimulation of SP – B secretion by the NCI – H441 cell line 162

5.7 Discussion **163**

Chapter 6: Final summary and discussion 168

Appendices

Appendix 1: Reagent Recipes 172

Appendix 2: Original data 184

References 190

Acknowledgements

I would like to thank my supervisors Professors Donald Salter and David Harrison, for their encouragement and support, without which I would never have finished these studies. Also, to my early supervisors Drs Jane Millward-Sadler and Shirley O'Dea, who ventured out to pastures new, but were more than happy to come to my aid.

I am also grateful for all the technical support and advice from staff of the Pathology division and the Centre for Inflammation Research. In particular, Stuart McKenzie, Mike Heriot, Frances Rae and Anne Grant for all their expertise and advice. Not forgeting Drs Gareth Clegg and Stuart McKechnie for helping with gathering patient consents for the project.

Many thanks to everyone who has been and gone from the Osteoarticular Research Group over the years, you kept me cheery both inside and out of the lab. I have fond memories of the third floor Phd office and the students, staff who 'lived' there. Although I am not sure it taught me much professional office etiquette. A special thanks to Kerry, the three Sharons, Nicola, Lynsey, Georgia, Renald, Carolyn, Becca, Kirsty, Caroline, Carrie, Juls, Malcy, Mark, Lou Fairbairn, K', Pam and everyone else I have not mentioned.

Most of all to my family, without their love and understanding I would not have continued and got this far. So thanks to my big sis Louise, Gran, Auntie Marleen and Uncle Donald, Ian, Emz, Frazer and Carolynn. To my father Campbell Murray my gratitude is endless.

List abbreviations

AP	alkaline phosphatase
AT1	type I pneumocyte
AT2	type II pneumocyte
ATP	adenosine monophosphate
BSA	bovine serum albumin
cAMP	cyclic adenosine monophospate
CD	cluster of differentiation
COX-2	cyclooxygenase-2
CIV	collagen IV
cDNA	complete or complement deoxynucleic acid
DAB	diamobenzidine tetrahydrachlorite
DAG	diaclglycerol
dH_2O	distilled water
DMEM	dubuccos' minimal essential medium
DNTP	2'deoxynucleoside 5'-triphosphate
DTT	dithiothreitol
EBSA	epithelial basement membrane surface area
ECM	extracellular matix
EDTA	ethylynediamine tetra-acetic acid
ELISA	enzyme linked immunosirbent assay
ERK	extracellular-signal related kinase
FAK	focal adhesion kinase
FBS	foetal bovine serum
FN	fibronectin
F12	Hams' F12 nutrient mix medium
GAPDH	glyceraldehyde phosphate dehydrogenase
G-protein	guanosine trisphosphate – binding protein
HCL	hydrocloric acid
Hz	hertz
IGF	insulin growth factor
IL	interleukin
IMS	industrial methylated spirit
INF – γ	interferon gamma
IP_3	inositol trisphosphate

kD	kilodalton
KCl	potassium chloride
LPA	liphosphatidic acid
mAb	monoclonal antibody
MAPK	map kinase
mRNA	messenger ribonuceic acid
MIP	macrophage inflammatory protein
MS	mechanical stimulation
NO	nitric oxide
NFκB	nuclear factor kappa B
PBS	phosphate buffered saline
PTHrP	parathyroid related hormone related protein
PIP_2	inositol bisphosphate
PK	protein kinase
PMN	polymorphonuclear cell
SOCS	suppressor of cytokine signalling
SP	surfactant specific protein
TLC	total lung capcity

Abstract

Mechanical forces are believed to regulate the structural, functional and metabolic systems of lung. The development of the foetal lung requires in utero breathing movements. Additionally, a single instance of mechanical strain is capable of enhancing the secretion of surfactant from adult type II pneumocytes, the putative stem cells of the alveolar lining. A clear comprehension of how mechanical force transduction into type II pneumocytes and its regulation of the function of these cells is needed if enhanced strategies for dealing with lung injury, infection and disease are to be accomplished. The aims of the study were **i.** to identify whether a reproducible protocol for isolation of type II pneumocytes from human lung tissue could be developed to study mechanical effects on these cells, **ii.** to establish whether an immortalised cell line, NCI – H441, expressed a phenotype similar to that of human type II pneumocytes, allowing its use in an in vitro model system of mechanotransduction and **iii.** to investigate the effect of matrix substrate and mechanical stimulation on the production of inflammatory cytokines and surfactant expression by NCI – H441.

Experiments have been performed to isolate high yield, viable primary type II pneumocytes. Human type II pneumocytes were successfully isolated from clinical resection samples, utilising a trypsin, DNase, discontinuous percoll® gradient and differential attachment procedure. Cell isolates were characterised by electron microscopy, alkaline phosphatase staining, modified haemotoxylin staining, and pan – cytokeratin and common leukocyte antigen (CD45) immunocytochemistry. Isolated cells were found to demonstrate blunt microvilli, abundant lamellar bodies characteristic of type II pneumocyte under electron microscopic evaluation. Positive alkaline phsophatase staining was detected within isolated type II pneumocytes. The percentage of the cell isolations positively identified as type II pneumocyte with the modified haematoxylin staining ranged from 26.50 –71.36 % of the total preparations. Each preparation possessed variable overall differentiation status of the type II pneumocyte. Type II enriched suspensions yielded a range of 44.00 – 64.77 % cells staining for pan – cytokeratin. In addition, 4.50 – 21.56 % of the cells in the preparations expressed CD45.

Phenotypic analysis showed that many of the morphological and antigenic characteristics of type II pneumocytes were shared with the NCI – H441 cell line. In vitro studies of the effects of mechanical stimulation and matrix substrate on cell membrane potential of type II

epithelial and NCI – H441 cells were undertaken. The cyclic mechanical stimulation regime was applied to cells using an in house system with a regime of 20 minutes stimulation at 0.25 Hz, 5000 μstrain. Significant membrane hyperpolarisation responses were elicited in cyclic mechanical stimulated primary human type II pneumocytes seeded on fibronectin and NCI – H441 cells seeded on collagen IV and fibronectin. A significant membrane depolarisation response was demonstrated by NCI – H441 when seeded on bovine serum albumin.

Real time polymerase chain reaction analysis revealed that NCI – H441 cells express interleukins (IL) 4, 6 and 8, suppressor of cytokine signalling – 3 (SOCS3) and surfactant specific protein – A (SP – A). Six hours after the application of cyclic mechanical stimulation NCI – H441 cells seeded on bovine albumin serum demonstrated a reduction in mean relative SOCS3 gene expression compared with controls. Cyclic mechanical stimulation of NCI – H441 cells seeded on fibronectin resulted in an increase in mean relative IL – 8 gene expression levels an hour after stimulation. Three hours after cyclic mechanical stimulation of NCI – H441 cells seeded on fibronectin the mean relative gene expression of IL – 8 fell compared with controls. Pilot investigation of the extracellular levels of SP – B from cyclic mechanically stimulated NCI – H441 cells revealed a decrease in extracellular SP – B compared with controls. No change in the cytoplasmic levels of SP – A were detected by following cyclic mechanical stimulation of NCI – H441 cells seeded on fibronectin.

Current protocols for isolation of type II pneumocytes from human tissue produce a mixed cell population that is unlikely to be useful for study of these cells in vitro. NCI – H441 cells show phenotypic characteristics of type II pneumocytes and similar electrophysiological responses to mechanical stimulation suggesting that they may be useful surrogates for the study of type II pneumocyte mechanotransduction. Provisional studies using these cells suggest that mechanical stimulation and matrix substrata influence cytokine expression by these cells. Such effects in vivo would have important effects on pneumocyte and lung tissue responses to injury.

CHAPTER 1. INTRODUCTION TO LUNG BIOLOGY AND MECHANOTRANSDUCTION

1. Lung Biology and mechanotansduction

Lung cells are subjected to a number of different physical forces, as a direct consequence of respiration (1). Normal foetal lung development requires breathing movements (2). This suggests that mechanotransduction, which is the transduction of mechanical stimuli into biochemical and or electrochemical signals within a cell (3), plays an important role in regulating lung cell function, from an early stage in its history. A single mechanical stretch of adult rat lung alveolar type II epithelial cells has been shown to result in a transient increase in cytosolic Ca^{2+} that is followed by augmented secretion of surfactant for a period of 30 minutes (4) This would appear to implicate strain in the regulation of adult lung cell function. The precise molecular basis of which has yet to be defined in full.

1.1 Microanatomy of the alveolus and mechanical forces

1.1.1 Alveolar epithelial cells

The airways of the two lungs and pathway of gases are arranged in an assymmetrical dicotomous branching pattern and progress from bronchi, bronchioles to the alveoli. The alveolus is a major site of gas exchange within the mammalian lung with the surface area estimated as 70 m^2 (5). There are at least 40 different cell types within the adult human lung (6)). Each alveolar unit is a pentagonal or hexagonal shape continuously lined with two types of epithelial cell, known as type I (AT1) and II pneumocytes (AT2) (7). Briefly, type I pneumocytes are squamous epithelial cells with thin cytoplasmic extensions, which aid rapid gas exchange and prevent fluid loss. ATI cells are extremely thin and in general are no more than 0.2μm in thickness, but can cover an area of 5000μm^2 (6). This means that in some cases a type I cell can contribute to the lining of more than one alveolus. The type II pneumocytes have a cuboidal morphology and reside at the corners of the alveoli. Type II pneumocytes are estimated to cover 4 - 7 % of the alveolar surface area (6; 7). The free apical surface of the AT2 is covered in blunt microvilli. The cytoplasm of AT2 cells, contain secretory vacuoles, which are apparent as lamellar structures under the electron microscope, and contain pulmonary surfactant (8). In addition, many cytoplasmic organelles are present within AT2 cells, mitochondria, endoplasmic reticulum and golgi apparatus (9). Occasionally a third type of epithelial cell is apparent within the alveolus, known as an intermediate pneumocyte as it possess characteristics of both AT1 and AT2 pneumocytes (10). These intermediate pneumocytes present in usually in instances of lung injury (10) and

are inducible in in vivo models of pulmonary injury (11). It is widely accepted that these intermediate cell types are evidence of the stem cell capacity of the AT2 to transdifferentiate into ATI following injury to the alveolus (12; 13). The time taken for transformation from type II epithelial cell to a type I epithelial cell is approximately 2 days and the turnover rate of type II cells is 25 days (14). A summary of the known characteristics of AT2 cells and the significance of each where known, are given within Tables 1.1. - 1.3.

1.1.2 Interstitial cells

The capillary network of the lung parenchyma is in relatively close proximity to the alveolar epithelium. Beneath the cytoplasmic extensions of the ATI cells the basement membrane fuses with that of the endothelium. So called 'thick' interstitial connective tissue separates the endothelium and AT2 pneumocytes at the corners of alveoli. The alveolar interstitium is a connective tissue framework consisting of collagen and elastin fibres, amongst which are located fibroblasts, histiocytes and mast cells (15).

The mesenchymal cell population of the alveolar interstitium is heterogenous with respect to the phenotyes. Two of the phenotypes are the myofibroblast and the fibroblast. A characteristic of the myofibroblast is its expression of α – smooth muscle actin, vimentin and in general the absence of desmin expression. It is presumed the cytokines such as transforming growth factor – β (TGF – β) and interleukin (IL) – 4 induce the differentiation of fibroblast into myofibroblasts (16; 17). Characteristics of the pulmonary fibrosis such as elevated levels of extracellular matrix protein, collagen I deposition, have been associated with the myofibroblast population (18) (19; 20). The myofibroblast is also a source of inflammatory cytokine production, such as TGF – β and monocyte chemotactic factor protein – 1 (19; 21)). In self - limiting models of pulmonary fibrosis upon resolution, signifcant numbers of myofibroblasts disappear (19; 22). However, in instances of human progressive pulmonary fibrosis populations of myofibroblasts are retained (18).

1.1.3 Alveolar extracellular matrix

The extracellular matrix (ECM) of the lung is a variety of molecules that comprise basement membranes and interstitial connective tissue. The ECM contributes to a number of cellular

functions such as proliferation, organogenesis, angiogenesis, metastasis (23), differentiation (23; 24) and protects cells from apoptosis (25).

Within the alveolus the basement membranes of the capillary endothelium and the alveolar epithelium are fused. This provides an extremely thin barrier between alveolar gas and pulmonary blood. The major components of the alveolar basement membrane are laminin, collagens IV and V, heparan sulfate proteoglycan (HSPG), chondroitin sulfate, chondroitin sulfate-proteoglycan, entactin and fibronectin (26; 27). The basement membrane components derive from both epithelial and intersitial cells in vivo. Collagen type IV isoforms, entactin and laminin originate from intersitial cells and epithelial cells (28-30). Within normal lung parenchyma the collagen types IV and V are prevalent within the alveolar and endothelial basement membranes, whereas types III and V are found within the interstitium (31). The immunohistochemical analysis of alveolar epithelium reveals that fibronectin within the basement membrane is less prominent beneath AT2 cells than AT1 cells (32). This has in part lead to the hypothesis that ECM plays a role in the regulation of alveolar epithelial phenotypes (33). Immortilised rat AT2 cells (SV4O – T2) are capable of synthesizing a basement membrane in vitro comprising laminin – 1, collagen IV, perlecan and entactin. To ensure a continuous basement membrane an exogenous source of laminin – 1 is required (34). Following fibrosis of the lung, collagen V is more prominent in the interstitium, whereas collagen III is less prominent throughout the parenchyma compared to normal samples of human lung (31). Samples of human fibrotic lung also demonstrate prominent quantities of fibronectin in the alveolar epithelium and interstium (35). In addition, the ECM protein tenascin has been found around hyperplastic human AT2 cells of cryptogenic fibrosing alveolitis lung samples (36).

Several models involving primary rat AT2 cells have been utilised in the investigation of the affects of ECM components on the phenotype and function of alveolar epithelium. Subunits of gap junctions known as Connexins, within rat AT2 cells in vitro are regulated by the composition of the underlying ECM at the levels of both transcription and translation (37). Primary cultures of AT2 cells rapidly lose differentiation characteristics when cultured on fibronectin – rich substrates and plastic (38) and in the process assume the phenotypic characteristics of the AT1 cells (24; 39). These models are thought to demonstrate methods of how AT2 cells repopulate the alveolus after cell division and differentiation, that occurs following lung injury (10).

Table 1.1: Type II Pneumocyte characteristics (13; 40)

Cell Function	Product	Significance
Surfactant synthesis components	phospholipids	surface tension reduction
	surfactant proteins A B C D	 Tubelar myelin formation, defence Absorption to lipid monolayer Absorption to lipid monolayer Defence
co-secreted with surfactant	Lysozyme Plasmalogens Cathepsin H	Defence Protects against oxidation
Sufactant maturation	Intracellular cathespsin H	SP-B, and SP-C processing
Secretion **Signal receptors**	β-adrenergic receptors P1 purinoreceptors P2Y purinoreceptors	
exocytotic apparatus	microtubules Actin Annexin II AnnexinIV Annexin VII (Synexin)	
Extracellular transformation	α_1-antitrypsin Convertase	Conversion of lipid monolayer into vesicles
Recycling	SP-A receptor	Rat primary tissue
Lamellar body lysosomal enzymes	Alkaline Phosphatase α-glucosidase α-mannose	Type II cell marker

Table 1.2 Type II pneumocyte characteristics(13; 40)

Cell Function	Product	Significance
Alveolar epithelial repair	Cyclin A	
	Cyclin D1, D2	Proliferation/differentiation
	Cyclin dependent phosphokinases	Proliferation/differentiation
Proliferation	PTHRP	
	Calmodulin	Inhibition of proliferation
	Insulin-like growth factor (IGF) binding protein 2	Proliferation/differentiation
		G_1-arrest
Differentiation	Retinoic acid receptor	Inhibition of differentiation
	Aminopeptidase N	
Apoptosis	CD95 (Fas-ligand receptor)	
	Fas-ligand	
	Bax	Pro-apoptotic protein
	Bcl-2	Anti-apoptotic protein
	Caspase-3	Execution protein
Fluid/electrolyte balance	Aquaporin 1	
	Aquaporin 5	
Water channels	Hg-insensitive channel (MIWC)	
	Hg-sensitive channel (CHIP28)	
Ion channels	H^+channel	
	Na^+ channel	
	CL^- channel	
Ion pumps	H^+pump	
	Cl^-/HCO_3 anion exchanger	
	Na^+/H^+ion exchanger	
	Na^+/K^+ ATPase	
Protein clearance	Carbanhydrase II	
Innate defence	SP-A	
	SP-D	
	Lysozyme	

Antigen presentation	MHC class II HLA class I F_c receptor CD80, CD86	Human (adult, foetal) IFN stimulation IFN stimulation A549 cell line only
Complement complex	C2, C3, C4, C5	
Antiproteases	$\alpha_1$antitrypsin Elafin Matrix metalloproteinase (MMP) MMP inhibitors (TIMP)	 A549
Oxidants	NAD(P)H-oxidase Superoxide anion, hydrogen peroxide	
Antioxidants	Glutathione γ-glutyml transferase Plasmalogens Mn superoxide dismutase (SOD) Mn-, Cu-, Zi-SOD	 in vitro In vitro
Xenobiotic metabolism	Cytochrome P-450 mono-oxygenase	
Coagulation / fibrinolysis	Fibrinogen Urokinase-type plasminogen activator (uPA) UPA receptor Plasminogen activator inhibitor (PA-I) Tissue factor	 IL-1β stimulation bleomycin-induced injury

Table 1.3 Type II pneumocyte charateristics (13; 40)

Cell Function	Product	Significance
Cytokines/receptors	GM-CSF	In vitro
	IL-1β	induced with particles
	IL-4	Human interstial lung disease
	IL-6	IL-1, TNFα stimulation
	IL-8	In vitro
	IL-11	Human interstital lung
	HGF	disease
	Interferon-γ	
	MCP-1	Human interstital lung
	RANTES	disease
	Tumour necrosis factor (TNF)-α	In vitro
		post TNF-α stimulation
		Hyperplastic type II cells
Cytokine receptors	IL-2	In vitro
	TNF receptor	In vitro
	Lymphotoxin-β-receptor	Hyperplastic type II cells
Growth factors	Epidermal growth factor (EGF)	In vitro
	IGF-II	
	Platelet derived growth factor	
	(PDGF)	Idiopathic lung fibrosis
	TGF-α,	
	TGF-β, β_1,	
	TGF-β_3	Hyperplastic type II cells
	Vascular endothelial growth	Normal type II cells
	factor (VEGF)	
	Connective tissue growth factor	Idiopathic pulmonary fibrosis
	(CTGF)	myofibroblast differentiation
Growth factor receptors	Basic fibroblast growth factor	
	receptor	
	EGF receptor	
	Hepatocyte growth factor receptor	
	KGF receptor	

	IGF receptor-1 IGF receptor-2	ontogenesis Early postnal phase
Cell-cell interaction	connexin 43	Electric, ionic coupling
Adhesion molecules	CD44s, CD44v Ep-cam E-Cadherin ICAM-1 VCAM-2	 post TNF-α stimulation post TNF-α stimulation
Integrins	$\alpha_6\beta_1$ $\alpha_3\beta_1$	In vitro In vitro
Paracrine mediators	Endothelin-1 Endothelin receptor A Prostaglandin E-2 Prostacyclin Nitogen oxide (NO) Constitutive NO synthase Inducible NO synthase	Human Rat cell line L2 In vitro Human A549 cell line In vitro, rat cell line L2
ECM constituents	Entactin Laminin Fibronectin Tenascin Proteoglycans Collagen type IV	Basal membrane, in vitro Basal membrane, in vitro In vitro Early organogenesis Hyperplastic AT2 cells In vitro
Other	Haemoglobin Serotonin receptor	Primary rat AT2

1.2 Mechanical environment of the alveolus

Adult human lungs are estimated to have over 300 million alveoli (41). It is suggested that the dynamic three – dimensional nature of the lungs means that the assumption that alveoli operate like balloons during breathing is not a sufficient analogy (42; 43). Several attempts have been made to quantify the degree of strain experienced at alveolar level in relation to changes to pulmonary volume (44-46). The history of sample inflation and method of fixation have a bearing on the results achieved within these studies (1; 43). Interestingly upon investigating the relationship between alveolar volume to surface area, within excised rabbit lungs, four general alveolar morphological changes were observed, during the volume changes of 40 to 100 % total lung capacity (TLC)(42). Firstly recruitment and derecruitment of alveoli, balloon – like increase or decrease, uniform spherical changes or anisotropic accordion – like morphological changes. The findings of this study suggested that these methods of changing surface area in relation to volume played various roles at different levels of inflation. At low lung inflation morphological changes were attributed to crumpling of the alveolar septa. At the upper range of inflation, changes in alveolar shape are attributable to full distension of the entire pulmonary fibrous network (42; 43). This illustrates the potential for heterogenous strain upon cells of the alveolus.

Alveolar surface area (44), collagen fibril length (45) and epithelial basement membrane surface area (46) have all been investigated in relation to pulmonary volume changes in vitro to gain insight into alveolar strains experienced during normal, abnormal and artificial respiration. Tschumperlin and Marguiles in 1999 used excised rat lungs and quantified changes in epithelial basement membrane surface area (EBMSA) changes in relation to different pulmonary volumes. Changes in EBMSA of 5, 16, 12 and 40 % in relation to the volume range of 24 % (starting inflation) TLC at lung volumes of 42, 60, 82 and 100 % TLC respectively. These results parallel those provided from collagen fibril experiments where a 16 % change in fibril length was achieved at a volume of 5 cm H_2O, which translates as a 32 % change in EBMSA. Tschumperlin and Marguiles measured a change of 34 % at the equivalent pulmonary volume. These measurements were made with excised tissue samples without the confines of a ribcage so caution should be attributed to in vivo situations (42; 46). Currently among pulmonary researchers the degree of strain thought to be experienced at the apical surface of the alveolus during normal breathing is 1 – 5 % strain (47). Strain is a unit of expressing physical force and is termed as a change in the initial length of cell length and is often expressed as a percentage.

1.2.1 Pulmonary surfactant

Two factors are important in determining the degree of distensibility and elastic recoil of lung tissue, the size of alveoli and the surface tension at the air – tissue interface. An equation known as Laplaces' law describes the relationship between the external forces, size and surface tension within a sphere, and is often used to illustrate the need for pulmonary surfactant. If applying the equation to alveoli the forces acting on lungs are proportional to the alveolar surface tension and inversely proportional to the size of the alveolus.

Laplaces' Law

$$2\Delta p = \frac{2\gamma}{r} \quad \text{or} \quad \gamma = \frac{\Delta p r}{2}$$

Δp refers to the external pressure, and γ the surface tension within the alveolus. According to this relationship, the external collapsing forces of small alveoli would be such that surface tension would be higher than that of the larger alveoli, which implies that greater forces are needed to inflate the smaller alveoli (15), (48). One of the primary functions of AT2 cells is the production and secretion of pulmonary surfactant (surface active agent). Pulmonary surfactant (surface active agent) is a complex mixture of phospholipids and protein, which acts at the alveolar liquid-air interface to reduce surface tension (Figure 1). In addition to maintaining normal lung function, it is thought to also have roles in pulmonary defence mechanisms and local immunomodulation (49). Dipalmitoyl-phosphotidylcholine is the main constituent of pulmonary surfactant and principally responsible for reducing alveolar surface tension. This molecule contains a hydrophobic saturated fatty acid component, palmitic acid and hydrophilic choline component. The palmitic acid residues of surfactant align themselves in parallel and extend into the alveolar air. The choline residues interact with the aqueous phase of the alveolar lining.

Four surfactant specific proteins (SP), A, B, C, and D are currently known. The characteristics and known functions, which are given within Table 1.4: Interestingly, SP – A is reported as possessing cytokine properties. The application of SP –A to primary AT2 cell cultures demonstrates the autocrine capabilities of this molecule. SP – A increases the transcription of SP – A, SP – B, SP – C, SP – A receptor (SPAR), and *c – jun*. An antibody toward the SPAR blocks the activity of SP – A (50).

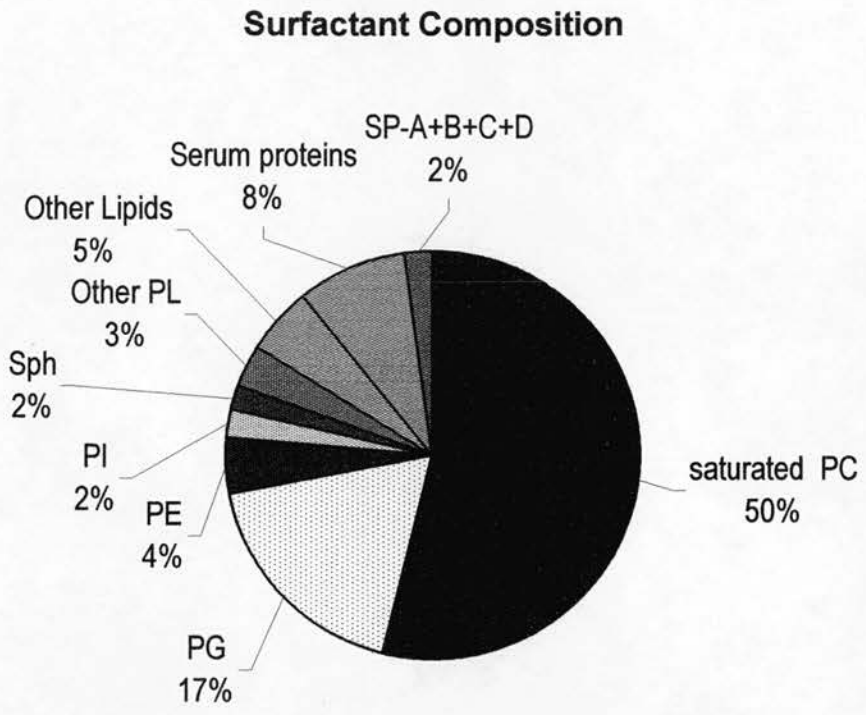

Figure 1. Composition of isolated human surfactant from bronchoalveolar lavage. PC = Phosphatidylcholine, PG -= Phosphatidylglycerol; PE = Phosphatidylethanolamine; PI = Phosphatidylinositol; Sph = Sphingomyelin; Phospholipids; SP = Surfactant protein (49)

Table 1.4. Summary of pulmonary surfactant-specific protein characteristics

SP Molecular Weight (kDa)	Molecular characteristics	Functions
A ~26 -38	Hydrophilic lectin/collagen hybrid	supports alveolar macrophage activities, regulates surfactant secretion cytokine enhances SP transcription
B ~9	Hydrophobic disuphide bridges	optimises surface activity
C ~4	extremely hydrophobic and rich in valine residues	optimises surface activity
D ~43	Hydrophilic lectin/collagen hybrid.	interacts with alveolar macrophages and regulates surfactant secretion.

(49; 50)

1.3 Experimental approaches to the study of mechanical stimulation of lung cells

Due to the degree of three - dimensional complexity the study of the effects of physical forces on cell function has relied heavily on the use of in vitro model system. The two main classes of system used in previous in vitro investigations generate uniaxial and biaxial strain regimes and will be discussed in relation to lung cell mechanotransduction research.

I.3.1 Uniaxial strain systems

Uniaxial strain refers to a pattern of strain within the radial plane, otherwise known as longitudinal strain. The longitudinal strain system most used to investigate the affects of strain on the function of foetal rat lung cells, involves the organotypic 3 – dimensional (3 – D) culture of cells within gelatin sponges. A programmable burst timer, control unit, a DC power supply and solenoid comprise the rest of the apparatus. One end of the sponge is fixed, while the other end of is free, but has a metal bar attached to it. The application of current to a solenoid then draws the metal bar towards it and the removal of current permits the sponge to relax to its original configuration. Investigations of the affects of mechanotransduction foetal rat lung cell proliferation have extensively used this technique (51-54). Within this model system the techniques has also been exploited to gain insight into remodelling events such as extracellular protein gene expression, protein production (54-57) and the release of inflammatory mediators (58).

A major disadvantage of this technique is that in applying strain the cells undergo compression. In addition, accurate evaluation of the quantity of strain experienced by the cultures is difficult (59). In 1995 Liu and coworkers compared 3 - D culture with 2 – D culture of foetal rat lung cells, and the effects of mechanical strain within the respective systems. Two different 2 – D systems were used in the investigation, the first involved an elastic membrane upon which a monolayer of the rat type II cells was cultured and subject cyclic mechanical strain in a longitudinal manner, using the principles of utilised to apply strain to the gelatin sponge 3 – D cultures. Interestingly, no significant increase in proliferation was observed within 2 - D cultures subject to mechanical strain compared to the 3 – D technique. The second of the 2 – D models was a commercially available system known as the Flexercell® system which falls into the biaxial strain methods of applying mechanical strain to cell culture in vitro (52).

I.3.2 Biaxial and equibiaxial strain systems

The term biaxial strain is used to describe the straining of in most cases a circular silastic membrane or substrata and the adherent cells cultured on it, in the radial and circumferential directions. Biaxial strain is often known as non – uniform or out of plane distension.

The first report of this type of system was in 1985 by Hasagawa and coworkers and consisted of the flexing of a plastic cell culture dish onto a convex template. Since, variations of this system have widely been used in the investigation of lung cell mechanotransduction (60-65), most notably the commercial Flexercell® model strain systems (66-69) (70; 71) (72-75), (76-78), (79)). This system employs a vaccum pressure upon the cell culture membrane, with the amplitude and frequency of strain regime readily controlled via a computer. However, these systems are not ideal in that the strain pattern exerted upon cells is heterogenous, with the strain falling to zero at the centre of each test well. Therefore cells at different locations of the wells are subject to different amounts of strain (80). The extent of strain applied to the strained cells is also questionable, as the percentage of strain observed in the membrane does not necessarily correlate to that of the cells (1; 59). Another method of applying biaxial strain patterns to lung cells cultured on deformable membranes, involves the application of hydrostatic pressure beneath the cells under scrutiny. Such a method has previously been of use in applicating of static, single strain to lung cell cultures (4; 81).

Several modifications of the Flexercell® system have been undertaken to solve this problem most notably the development of equibiaxial strain application. Equibiaxial strain is therefore uniform or in plain distension. Cell culture wells are essentially mechanically strained over fixed posts, which assumes frictionless movement of the membrane during the application of strain. This innovation has already been extensively utilised in recent investigations of lung cell (82), (83; 84). Custom built equibiaxial strain systems have been reported, in the study of lung cell mechanotransduction. These systems again use deformable membranes, but staged over an inverted microscope, allowing the determination of strain by fluorescent micoscopy (85-87).

1.3.3 Other mechanical strain systems

Another method of applying mechanical stimulus are known as the 'poke' stimulus, which refers to the deformation of a single cell with a microelectrode, without rupturing the plasma membrane (88). Mechanical stimulus has previously been applied with the twisting of micromagnetic beads attached to the cell surface (89; 90), and the spritzing of culture medium upon the apical surface of cells (91).

I.4 Mechanotransduction

There is a significant interest in the role of mechanical force, normal or abnormal on the biological function of various different cell types and tissues ((92-102)). Model systems of osteoarticular (103) and endothelial cells (104) are the most studied. Similarities between these systems, in the information and energy transfer of mechanical forces exist. However, the amplitude and frequencies of physical force, different tissues experience varies considerably. During normal resting respiration, alveolar tissues are exposed cyclic strain that is punctuated by strains of different frequencies during instances of sighing, yawning and exercise (1). Within a dynamic mechanical environment cells the adaptive homeostatic response can be categorised into four main phases (103).

i. Mechanocoupling – the translation of macroscopic forces into local activity at the cell surface; Mechanoreceptors for example integrins, SACS
ii. Coupling – the transduction or transfer of mechanical information into biochemical signals within the cell; intracellular signalling molecules
iii. Signal transmission from the sensor cell to the effector cells, for example AT2 cells to AT1 cells, fibroblasts, macrophages, and endothelial cells via intercellular signalling molecules.
iv. Extracellular matrix (ECM) – coupling, when the alteration of the extracellular environment modifies the signalling between the effector and sensor cells.

1.4.1 Mechanoreception

The apparatus for transducing extracellular mechanical signals to alveolar epithelium remains unknown. There are several candidate mechanoreceptors, previously investigated within other tissue mechanotransduction models; integrin receptors (105), stretch activated ion channels (106; 106; 107) and growth factor receptors (71).

1.4.1.1 Integrins

Evidence from experiments carried out on a range of different cell types strongly suggests that the integrin family of receptors act as mechanoreceptors. This receptor family are heterodimeric glycoproteins that mediate links between the extracellular matrix and the intracellular environment. Each integrin receptor is comprised of an α and β subunit. There are a minimum of 16 α and 8 β subunits, the various combinations of which determine ligand specificity. There are at present approximately twenty known integrins receptors, with some ligand redundancy existing between this family of receptors. For example, α5β1 and αςβ1 both bind fibronectin, similarly with α6β1 and α6β4 specific for the ECM protein vitronectin (108). Some evidence exists for the normal expression of adult human alveolar epithelial cell expression of integrins. Immunohistochemical analysis of normal regions of human resected tissue, reveal the expression of α 1, 3, 5,6 v and β 1 (Koukilis et al. 1997). Evidence for the role of integrins in the mechanotransduction of adult pulmonary epithelium has yet to be shown. However, a recent report of a role of β_1, α_6 and α_3 in the mechanical – strain induced differentiation of foetal AT2 cells exists (83). This study reports that the ECM protein laminin plays a vital role in differentiation of foetal AT2 cells over other ECM proteins and integrin receptors contribute to the mechanical strain induced differentiation. The protein expression of pulmonary surfactant protein C (SP – C); a differentiation marker was monitored within mechanically stimulated primary cultures of foetal rat AT2 cells, cultured on various matrices. Laminin protein substrata were found to elicit maximal expression of SP – C during mechanical stimulation. Function – blocking anti – integrin antibodies to the integrins β_1 and α_6 were found to alter the adhesion of cells in culture aswell as the differentiation status of the foetal AT2 cell. However, α_3 was found not to be essential to the foetal AT2 adhesion during mechanical strain, but inhibition of this intregin subunit did curtail the accumulation of SP – C protein (83).

Human bone cells that have been subjected to cyclical mechanical stimuli of 0.33 Hz exhibit a membrane hyperpolarisation and depolarisation event following 0.104 Hz stimulation. However the use of antibodies against αV, β1 and β5 integrins could inhibit depolarisation of the membrane. Similarly the hyperpolarisation response was inhibited by the application of gadolinium and antibodies to α5, β1 integrins and the integrin associated protein (CD47). Both responses can be inhibited by; Asp-Gly-Asp

(RGD) containing peptides, genistein; a tyrosine kinase inhibitor and cytochalasin D; which disrupts the cytoskeleton. These results suggest that different frequencies of mechanical strain are involved in activating separate signalling pathways (93).

The hyperpolarisation response elicited following mechanical stimulation of cultured human chondrocytes has also been demonstrated to involve the $\alpha5\beta1$ integrin. This response was also shown to involve intracellular signals by the cytoskeleton, phospholipase C calmodulin pathway, tyrosine protein kinase and protein kinase C. Mechanical stimulation has been shown to influence metabolism, changes in intracellular cyclic adenosine monophosphate and the production of proteoglycans. Therefore from the results it is probable that the $\alpha5\beta1$ integrin is a potential regulator of chondrocyte function (107).

Evidence supporting the role of integrins in transducing mechanical force into biochemical signals has been gathered by an investigation into the relationship between shear stress and endothelium dependent NO-mediated vasodilation of isolated coronary arterioles. The addition of synthetic RGD sequence peptides, competitively inhibit integrin binding to the extracellular matrix proteins containing this sequence and consequently inhibit shear stress-induced vasodilation. An antibody to $\beta3$ integrins significantly inhibited the response to shear stress. Altered levels of tyrosine kinase activity were also found during RGD peptide use. This suggests that the activation of tyrosine kinases in integrin signalling plays a role in endothelial cell mechanotransduction (109).

Vasodilation of vascular smooth muscle cells was found to involve the activation of $\alpha v\beta3$ integrins. Also RGD synthetic peptides have been shown to produce a concentration dependent dilation in conjunction with a marked reduction in $[Ca^{2+}]i$, therefore illustrating the significant role of integrins in mechanotransduction via interactions with the extracellular matrix and cellular signalling involving secondary messengers such as calcium ions (110).

Evidence for the role of integrins in mechanotransduction is strengthening. Mechanical stressing of an osteosarcoma cell line U-205 monolayer by applying physical forces via magnetic beads demonstrated that a central role in the integrin mediated signalling would appear to be fulfilled by the activation of protein tyrosine kinases. The stressing of U-205 monolayer resulted in increased tyrosine phosphorylation , which included mitogen-activated kinase (MAPK). The $[Ca^{2+}]i$ would appear to be of significance as the addition of BAPTA-AM; an intracellular calcium chelator reduced the anchorage of the tyrosine-phosphorylated proteins to the cytoskeleton. Therefore it would seem that some cells can respond to physical forces by integrin mediated signalling which results in an increase in tyrosine phosphorylated proteins. During the course of this signalling process the proteins become physically anchored to the cytoskeleton; an event, which is dependent on intracellular calcium concentration, and ultimately leads to the differential activation of the MAP kinase pathway (111).

Rat cardiac fibroblasts respond to 4% static biaxial stretch with a rapid activation of extracellular signal-regulated kinase (ERK-2) and c-Jun NH_2 terminal kinase (JNK1). Both kinases were differentially regulated when the fibroblasts were plated on different extracellular matrices. ERK-2 could only be activated when plated on fibronectin, whereas JNK-1 could be activated when plated on fibronectin, vitronectin or laminin. Neither kinase was however activated when plated on collagen. At least two integrins were found to be involved in the activation of ERK-2; $\alpha 4\beta 1$ and an RGD-directed non-$\alpha 5\beta 1$ integrin. Results suggested that JNK-1 activation was mediated via an RGD independent integrin or an alternative to the $\alpha 4\beta 1$ integrin (112).

1.4.1.2 Stretch-Activated / mechanosensitive ion channels

Stretch – activated ion channels (SACS) are ion channels with the ability to modulate their intrinsic activity upon the application of mechanical stimulus. In 1984 a stretch-activated ion channels were first identified in embryonic chick skeletal and embryonic Xenopus muscle (102; 113). Subsequently this class of ion channel has been identified in a wide variety of both prokaryotic and eukaryotic organisms (3). There is not always a clearly defined physiological function for such channels in each of the organisms. However, hypothesis exists that stretch activated ion channels are involved in osmoregulation, growth, hearing, balance, and touch. More recently, they are thought to play prominent roles in transforming mechanical stress into electrical responses and or

into fluxes of ions (114; 115). A variety of ion channels demonstrate mechanosensitivity, including the shaker – IR K^+ channel (116)N – type Ca^{2+} channel (117; 118), NMDA channels (119) (120) Ca^{2+} - dependent BK channels (121).

In 1999 Liu and coworkers reported evidence supporting the critical role of stretch activated ion channels in foetal rat lung cell proliferation. It was demonstrated that mechanical strain induced-foetal rat lung cell proliferation, is regulated by both intracellular and extracellular calcium. The addition of the stretch-activated channel blocker, gadolinium was shown to suppress mechanical strain induced-foetal rat lung cell proliferation (106).

A single mechanical stretch of adult rat lung alveolar type II epithelial cells causes transient increases in cytosolic Ca^{2+} that is followed by augmented secretion of surfactant for a significant length of time. The Ca^{2+} was mobilised from intracellular stores rather than allowing Ca^{2+} to enter from the extracellular environment (1). Evidence suggests that the role of calcium ions in human lung epithelial cells is not only restricted to intracellular mobilisation. Ohata and coworkers suggested that lysophatidic acid (LPA), sensitises mechanical stimulation-induced Ca^{2+} influx through stretch activated ion channels, via a mechanoreceptor-linked response (91).

Alveolar epithelial cells actively transport Na^+ via a basolateral located Na^+K^+ ATPase, so that Na^+ and liquid can be cleared out of air spaces. Cyclic mechanical stretch has been found to significantly affect Na^+K^+ ATPase activity. When the murine lung epithelial cell line (MLE-12) was exposed to cyclic stretch of 30 cycles/min by 30 min and 60 min the Na^+K^+ ATPase activity was increased. Blocking amiloride sensitive Na^+ entry into the cells and non-selective cation channels with amiloride and gadolinium respectively, prior to cyclic stretch prevents the increase in Na^+K^+ ATPase activity. It is thought that mechanical stretch stimulates Na^+K^+ ATPase by increasing intracellular Na^+ concentration and by recruiting Na^+K^+ ATPase subunits from intracellular pools to the basolateral membrane (73).

A thoroughly studied model of mechnotransduction is the chondrocyte. Cyclical mechanical stimulation of cultured chondrocytes results in a hyperpolarisation response of the cell membrane and activation of small conductance Ca^{2+}- activated K^+ ion channels. The application of apamin, charybdotoxin and iberiotoxin demonstrated that these stretch activated ion channels were apapmin sensitive, charybdotoxin and iberiotoxin resistant, low conductance channels (107).

1.4.2 Intracellular signalling activated by mechanical strain

Once the reception of mechanical stimulus by alveolar epithelium, the activation of a number of downstream cell signalling events is likely to occur with the result of production secondary signalling mediators for the regulation of the cell function. Molecules such as G protein coupled - receptors, protein kinases transcription factors and signalling molecules.

1.4.2.1 G – Protein coupled receptor signal transduction pathways

Guanine nucleotide binding proteins (G – proteins) associate with cell surface receptors and downstream signalling cascades depending upon the subclass of proteins. G_s interacts with adenyl cyclase to catalyse the production of cAMP and activates protein kinase A signalling pathway. The G_q and G_o proteins activate phospholipase C (PLC). When activated PLC hydrolyses PIP_2 into inositol 3, phosphate (IP_3) and Diacylglycerol (DAG), which act in the release of intracellular stores of calcium ions and protein kinase C signalling.

There are limited reports of research on the role of G protein coupled receptors in alveolar epithelial cell mechanotransduction. Data suggestive of the role of g –proteins in foetal lung mechanotransduction have been reported. The constitutive and regulated section of proteoglycans and glycosaminoglycans in mechanically stimulated foetal rat cells is reliant on the G – protein activity and the integrity of the cytoskeleton (55). The activation of the extracellular regulated kinase 1 /2 (ERK 1 / 2) within adult rat AT2 cells subjected to cyclic mechanical strain is through the action of G – proteins. The inhibition of cyclic strain induced ERK 1 / 2 activity was achievable through the use of pertussis toxin and the use of specific epidermal growth factor inhibitors (71).

Some evidence exists for the involvement of protein kinase B in the regulation of chondrocyte responses to mechanical stimulation. Phosphorylation of PKB is known to anti apoptotic signalling events (122). Interestingly, the activation of PKB in integrin mediated mechanotransduction of human ankle chondrocytes (123). Any involvement of PKB in alveolar epithelial mechanotransduction has not yet investigated.

A mechanotransduction pathway for strain–induced foetal lung cell proliferation has been proposed involving phospholipase C and PKC. Both intracellular and extracellular calcium ions are thought to play a role. Mechanical stimulation causes an increased influx of calcium ions through a gadolinium sensitive stretch activated ion channel, which is thought to contribute to PKC activation and DNA synthesis (51). Tyrosine phosphorylation of phospholipase C-γ is then thought to mediate the hydrolysis of phosphatidylinositol 4,5-diphosphate (PIP_2) to produce inositol 1,4,5-trisphosphate (IP_3) and diacylglycerol (DAG). Intracellular calcium is then mobilised by IP_3 and in the presence of DAG is thought to then activate protein kinase C (PKC) and the following downstream events (53; 124).

Mechanical stimulation of rabbit tracheal epithelial cells leads to Inositol 1, 4, 5 – trisphosphate is formation. This acts as a messenger that can diffuse through the cytoplasm and through gap junctions to release Ca^{2+} from intracellular stores. Diacylglycerol (DAG) is also a product of the hydrolysis of phosphatidylinositol 4, 5 bisphosphate by phospholipase C, and it is a known activator of protein kinase C. Therefore it has been hypothesised that PKC could play an important role in modulating Inositol (1,4,5) P_3- dependent Ca^{2+} signalling. Exogenous activation of PKC by the application of 12-o-tetradecanoylphorborol 13 acetate or 1,2 –dioctanyl 5n-glycerol impede calcium waves and the previously observed increases in $[Ca^{2+}]_i$. The initial positive effect of PKC on calcium mobilisation and the subsequent feedback inhibition is best demonstrated by the application of bisindolylmaleimide. The amplitude of ATP-induced $[Ca^{2+}]_i$ increases are decreased and the following oscillations are blocked. By inhibiting the endoplasmic reticulum Ca^{2+} - ATPase with thapsigargin, PKC activators a reduction in the $[Ca^{2+}]_i$ are also seen. This suggests that PKC could play a role in the mechanical strain induced release mechanism of Ca^{2+} (125).

1.4.2.2 Protein Tyrosine Kinases

Mechanical force induced signalling would appear to be fulfilled by the activation of protein tyrosine kinases in some cell types. Cyclic mechanical stimulation of foetal rat lung cells results in an increase in cell proliferation. After 5 min of mechanical strain tyrosine phosphorylation of proteins can be observed in the band, which corresponds to 110-130 kDa. Some of these proteins have been identified as $pp60^{src}$ substrates; p120, AFAP-110, and cortactin. The amount of $pp60^{src}$ in the cytoskeleton fraction increased

rapidly during the first 5 min of mechanical strain. This is significant to the phospholipase C-γ- protein kinase C pathway as PKC strain–induced activation and translocation to the membrane, and DNA synthesis could be blocked by the use of herbimycin A; a protein tyrosine kinase inhibitor. Interestingly tyrosine phosphorylation of $pp125^{FAK}$ and paxillin did not increase in the foetal rat lung cells. The suggestion is that protein tyrosine kinase activation is an upstream event in the pathway (126). Cyclic mechanical stimulation of the human adenocarcinoma cell line A549 was also found to result in the increase activation of the Src protein tyrosine kinase (79). The tyrosine phosphorylation of focal adhesion kinase in the mechanical strain induced proliferation pathway of foetal rat lung cells bears similarity to human chondrocyte responses to cyclic mechanical stimulation. The dynamic mechanical stimulation of human chondrocytes for 20 min at 0.33 Hz results in the phosphorylation of (pp125FAK), beta-catenin, and paxillin, respectively. These events are integrin mediated and involve the action of SACS (127).

The stressing of U-205 monolayer resulted in increased tyrosine phosphorylation, The $[Ca^{2+}]i$ would appear to be of significance as the addition of BAPTA-AM; an intracellular calcium chelator reduced the anchorage of the tyrosine-phosphorylated proteins to the cytoskeleton. Therefore it would seem that some cells can respond to physical forces by integrin mediated signalling which results in an increase in tyrosine phosphorylated proteins. During the course of this signalling process the proteins become physically anchored to the cytoskeleton; an event, which is dependent on intracellular calcium concentration, and ultimately leads to the differential activation of the MAP kinase pathway (111).

1.4.2.3 Map Kinase Signalling

Mitogen - activated kinases (MAPK) play a variety of vital roles in cell functional response to mechanical stimulation, such as activation of transcription factors, gene regulaion, cell survival and differentation.

Rat cardiac fibroblasts respond to 4% static biaxial stretch with a rapid activation of extracellular signal-regulated kinase (ERK-2) and c-Jun NH_2 terminal kinase (JNK1).

Both kinases were differentially regulated when the fibroblasts were plated on different extracellular matrices. ERK-2 could only be activated when plated on fibronectin, whereas JNK-1 could be activated when plated on fibronectin, vitronectin or laminin. Neither kinase was however activated when plated on collagen. At least two integrins were found to be involved in the activation of ERK-2; $\alpha 4\beta 1$ and an RGD-directed non-$\alpha 5\beta 1$ integrin. Results suggested that JNK-1 activation was mediated via an RGD independent integrin or an alternative to the $\alpha 4\beta 1$ integrin (112).

Following fifteen minutes of equibiaxial cyclic mechanical strain ERK 1 / 2 is maximally activates, within foetal rat lung cells and leads to an increase in SP – C gene expression (77). Tyrosine kinase activity has also been discovered to be necessary in the transduction of strain into a proliferative response in NCI - H441 cells. Mechanical strain was found to increase the phosphorylation of mitogen-activated protein kinases p42/44 and *c-jun*. The activation of the transcription factor activating protein-1, was also detected during the evaluation. The proliferative response to strain was inhibited by the addition of the protein tyrosine kinase inhibitor genistein (76).
The NFκB transcription factor is implicated in the mechanotransduction of chondrocytes (128). However cyclic mechanical stimulation of 18 kPa at 0.5 Hz of A549 cells , was found not to regulate NFκB signalling (79).

1.4.3 Regulation of tissue remodelling

Tissue remodelling processes play an important role in maintaining the normal structure and function of the lung. Little is know about how mechanical forces impinge upon these regulatory processes. The role of mechanical stimulation on lung parenchymal remodelling has to date been surmised from congenital malformations of the lung data and a few experimental models.

1.4.3.1 Cell proliferation and differentiation

It is well documented that respiratory movements occur before birth and these are required for normal foetal lung development to occur (2). In addition, mechanical forces are thought to also affect compensatory lung growth (129), lung structure, function and metabolism (101). During development of the lung, fluid is secreted into the lumen of the tissue, exerting strain on the cells lining the interior of the organs. In a condition such as oligohydramnios where insufficient fluid is secreted into the lumen of the lungs, the lungs fail to grow and differentiate. Complete abolition of foetal breathing movement by transection of the spinal cord of foetal sheep decreases lung growth and leads to an altered ratio of alveolar phenotypes (130). Congenital diaphramatic hernia or experimental tracheal ligation of foetal sheep results in the overexpansion of lung, an increase in growth occurs and leads to a higher AT1 to AT2 cell ratio compared with normal foetal lungs (131). Following Experimental lobectomy or pneumonectomy procedures on animals, an increase in cell proliferation of the residual tissue occurs. Following the same procedures on humans the same phenomena does not occur. There is an increase in DNA synthesis within the residual tissue, but no increase in the cell number (129).

A study of how rat foetal lung cells grown in organotypic culture respond to mechanical stretch found that when cells were subjected to an intermittent stretch pattern of 5% elongation, 60 stretches/min for 15 min of each hour, there was a significant increase in cell proliferation and DNA synthesis. Cell number increased 10% ($p<0.05$), [^{3}H] thymidine incorporation into DNA increased 61% ($p<0.01$) and the [^{3}H] thymidine labelling index increased 2.8 fold ($P<0.001$) compared with non-stretched controls. The intermittent stretch pattern applied possessed amplitude, frequency, periodicity and duration similar to that displayed during normal foetal breathing movements in vivo. Therefore, it was concluded that mechanical forces act directly to stimulate foetal rat lung cell growth. Inhibitors of leukotriene biosynthesis and prostaglandin synthase were found to have no effect on the stretch response shown by the rat foetal lung cells; ruling out a role for these molecules in the response. Hence, this is suggestive of a role for foetal breathing movements in normal foetal lung growth (51).

Human foetal lung fibroblasts (IMR-90) plated on collagen and subjected to cyclical mechanical deformation of 10% increase of the culture surface; 1Hz displayed a

significant increase in proliferation. Two days after cyclical mechanical deformation cell number had increased by 39%. After 4 days cell number had increased by 163% compared to the culture controls. Additionally, medium from mechanically stimulated cells was mitogenic to IMR-90 cells. This is suggestive of autocrine growth factor release from the IMR-90 cells, which then mediate the increase in proliferation (132).

To date a small amount of work has been carried out on mechanical strain effects on human pulmonary cells. The human pulmonary adenocarcinoma cell line NCI - H441 has been recently used to demonstrate that strain, could directly stimulate proliferation in human lung epithelial cells. The NCI - H441 cells were subjected to both a cyclic strain regime of 14kPa (~20% elongation) at 60 cycles/min and a constant tonic strain of 14 kPa for a specified time. The strain conditions were used to imitate the ventilation conditions often used on critically ill neonates (76).

1.4.3.2 ECM turnover

Glycosaminoglycans (GAGs) and proteoglycans (PGs) are agents found within ECM and which are thought to modulate growth factor activities. The production and secretion of these molecules by foetal rat lung cells is affected in response to an intermittent strain regime. It was found that foetal rat lung cells secreted GAGs primarily via a constitutive pathway, which was dependent on the functional integrity of the cytoskeleton and G-protein activity. A pathway that can be regulated was also stimulated by the induction of rapid calcium influx via a stretch activated ion channel. Suggesting that the exocytosis of GAGs and PGs from mixed foetal lung cells, stimulated by mechanical strain can be activated via basal and regulated pathways (55).

During normal lung growth a coordination of cell proliferation and extracellular remodelling is evident. An examination of ECM mRNA and protein levels from foetal rat lung cells at the peak of their capacity for proliferation, which had been subjected to mechanical strain, has been carried out. Results showed that the intermittent mechanical strain regime applied to the foetal rat lung cells differentially regulates mRNA and protein synthesis. Reduction in procollagen-α1 (I) and biglycan mRNA levels were found in cells following the strain regime compared with control cells. Also, collagen-α (IV) and -α2 mRNA levels were elevated however laminin β chain mRNA levels were constant. Despite reduced mRNA levels following intermittent levels of type I and IV

collagen and biglycan within the medium were increased. This uncoordinated relationship between mRNA and protein could possibly arise from an enhanced translational activity of the mRNA. Therefore, the increased synthesis of ECM molecules results in an accumulation of ECM and it is possible that there is no reduction in the activity of degradative enzymes involved in the remodelling process during foetal lung growth (57). An investigation of the affect of cyclic mechanical forces on the turnover of adult human epithelial cell ECM has still to be undertaken. Static mechanical strain of the human foetal pulmonary fibroblast cell line IMR – 90 increases the cells expression of the ECM protein type I collagen. This response is also dependent on the plating substratum of the cells. An increase on α_1(I) procollagen expression is seen only in cells plated on laminin or elastin and not fibronectin.

1.4.3.3 Surfactant metabolism

It is an established fact that mechanical stimulation affects the metabolism of pulmonary surfactant. For example, large tidal volumes induced by exercise or mechanical ventilation result in an increase in surfactant secretion (133). However, the mechanisms of surfactant metabolism are poorly understood at present. Several reports have been made of the effects of mechanical stimulation on the metabolism of pulmonary surfactant in vitro. In 1990 Wirtz & Dobbs reported that a single mechanical distension of primary rat type II cells, can stimulate the secretion of surfactant. Specifically the exocytosis of [^{3}H] phosphatidylcholine (PC) was measured and they found that the magnitude of distension was directly correlated to the magnitude of surfactant secretion. This secretory response to strain was found to be unrelated to cellular damage.

The application of ilprost, a chemical analogue of prostaglandin (PGI_2), to primary rat type II pneumocytes significantly enhances the strain-induced surfactant ([^{3}H]PC) secretory response. The application of a nitric oxide (NO) donor spermine NONOate however does not augment the strain-induced secretion of surfactant and it has been postulated that the NO-cGMP signalling pathway could inhibit surfactant secretion (78).

Tracheal obstruction in the foetal lung leads to increased lung expansion, which stimulates lung growth. In 1999 Lines (134) and coworkers demonstrated that tracheal obstruction of foetal sheep lungs leads to a large simultaneous reduction of SP-A, B and C mRNA expression levels in comparison to control values. In conjunction, there was a significant reduction in the levels of SP-A protein.

Foetal rat lung explants exposed to a single static (tonic) mechanical distension, exhibit a decrease in the mRNA expression levels of SP-B and SP-C. The mRNA levels of SP-A however are unaffected by this type of two dimensional mechanical distension. In the same instance an increase in the mRNA levels of the rat alveolar type I cell marker RTI 40 was witnessed (39). Similarly a static (tonic) mechanical distension of cultered rat type II pneumocytes has been shown to significantly decrease steady state mRNA levels of SP-A and SP-B and an increase in the mRNA levels of RTI 40. The expression of SP-A messenger and 18 S ribosomal RNA levels appear to be undisturbed. (39).

However repeated distension and relaxation: termed cyclic deformation; of the human pulmonary epithelial cell line NCI - H441 for a period of 24 hours significantly increases the levels of SP-A and SP-B by 2 to 4 fold respectively compared with controls. Therefore, cyclic deformation of pulmonary epithelial cells in vitro can alter surfactant specific protein production, substances which are necessary for respiration to occur successfully in the mature lung (72). Phenotypic changes in both the foetal and adult pulmonary epithelium could therefore be stimulated by mechanical strain. (39; 70; 81).

1.4.3.4 Cytokine, chemokine and growth factor production

Cyclic mechanical stimulation of foetal organotypic, rat lung cells enhances the secretion of macrophage inflammatory protein – 2 (MIP – 2) from these cells. MIP – 2 is a rodent homologue of the human pro – inflammatory chemokine interleukin – (IL) 8 (58). The alveolar epithelial cell line A549 when subjected to a mechanical cyclic cell stretch of 30% for 48 hr was found to have significant up regulated production and release of interleukin-8. After only 4hr of cyclic stretch IL-8 gene transcription had increased at least four fold. This is a strong suggestion that alveolar epithelial cells could be involved with the alveolitis associated with ventilator induced lung injury (68).

Other in vitro models of alveolar epithelial cell mechanotransduction demonstrate the cells capacity for inflammatory and differentiation mediator production in response to strain. Cyclic mechanical stimulated A549 exposed monolayers to glass or crocidolite asbestos fibres for a period of 8 hrs significantly increased the production of the pro inflammatory interleukin-8, which is thought to be involved in fibre-induced pathogenic processes (61). Cyclic mechanical stimulation of A549 cells has additionally been

found to lead to the gene expression and protein release of IL – 8, hepatocyte growth factor (63) and transforming growth factor - β (TGF – β) via a PKC mechanism (64).

Strain has also been found to mediate a cell-cell interactive loop within the developing lung vital for maturation. The differentiation factor parathyroid hormone-related peptide (PTHrP) is released by type II cells, which in turn stimulates the production of cAMP in nearby fibroblasts. Mechanical deformation of foetal rat type II cells significantly increases the production of PTHrP. The distension of cultured foetal rat lung fibroblasts also affects the cell's ability to respond to the PTHrP. The effect of this hormone is to affect the differentiation functions of foetal lung fibroblasts by augmenting glucocorticoid binding, increasing the metabolic activity of lipoprotein lipase, the rate of triglyceride uptake and the production of cytokines such as interleukin-6 and interleukin–11. These cytokines can exert their effects on epithelial cells. The result of which is an increase in surfactant production. Inhibition of any of these steps blocks the production of surfactant (135).

Cyclic mechanical strain of A549 cells treated with tumour necrosis factor – □ results in the increased gene expression of a variety of cytokines, chemokines and cell surface receptors. Four hours following stimulation of A549 cells the gene expression of chemokines; CCL2 (MIP – 1), CCL20 (MIP – 3α), CXCL2 (GRO3), inflammatory related proteins; COX-2 and PTX3 and membrane protein IL – 15RA were increased (79).

Interleukin-4 has been suggested to be involved with a mechanotransduction pathway in human articular chondrocytes. Previous work demonstrated that the hyperpolarisation of human articular chondrocytes response to a 0.33 Hz mechanical stimulation, was integrin dependent and that a secreted agent was involved. Antibodies to IL-4 and its receptor were found to inhibit the membrane hyperpolarisation response to mechanical stimulation displayed by the cells and the activity of the medium. Chondrocytes from IL-4 knockout mice did not display a membrane hyperpolarisation response to mechanical stimulation. Therefore, the release of this cytokine may work in an autocrine or paracrine fashion to regulate the structure and function of articular cartilage. Alterations in this pathway could result in the disease osteoarthritis (136).

It has been found that medium conditioned by second-passage lung fibroblasts can stimulate via regulated pathways the accumulation of DNA synthesis in cultures of rat type II alveolar epithelial cells. Cyclic mechanical stimulation would appear to sensitise Type II alveolar epithelial cells to the activity of the fibroblast -conditioned medium. Demonstrating how an interaction between interstitial fibroblasts and epithelial cells could be of importance in lung growth and development (137).

An illustration of the control of inflammatory mediator release used cyclic mechanical stimulation of A549 at 15 % (~64 % total lung capacity) at 20 cycles. Strain induced increase production of IL – 6 and IL – 8 was significantly inhibited when intracellular glutathione was increased. Interestingly the gene expression of IL – 8 was found to be linked to the actions of the transcription factors NFkB and AP – 1 (62). Cyclic mechanical strain of A549 has recently been found to mitogate the non – apoptotic cell death actions of hyperoxia (138).

The arachidonic acid signalling pathway is a vital source of bioactive lipid inflammatory mediators. Cyclic mechanical stimulation of foetal rat epithelial and fibroblasts recently illustrated the rapid regulation of eicosanoid metabolism. Cyclic mechanical regulation of this pathway was restricted to the epithelial cells, and did not involve the fibroblasts. The stimulation of epithelial cells resulted in the release of prostaglandins through an influx of extracellular calcium, activation of phospholipase A_2 and the phosphorylation to p44 /42 MAPK and was dependent on the actions of cyclooxygenase – 2 (139).

A thorough understanding of alveolar epithelial type II cell mechanotransduction is imperative if a better understanding of this cell types' role in maintaining the alveolus is to be achieved. This information will be pertinent to the future development of treatment for human lung disease.

1.5 Aims and objectives

The goal of the work that follows was to gain insights into the role of mechanotransduction in the regulation of human alveolar epithelial cell function. The aims and objectives of this study were as follows:

i. To establish whether or not a reproducible protocol for the isolation of type II pneumocytes from human lung tissue could be developed to study mechanical effects on these cells.

- Obtain human primary lung tissue and optimise the extraction procedure of human primary type II pneumocytes, for use in mechanotransduction studies.
- Characterise phenotype and quality of isolated cell populations.

ii. To establish whether as immortalised cell line, NCI – H441, expressed a phenotype similar to that of human type II pneumocytes, allowing its use in an in vitro model system of mechanotransduction.

- Characterise phenotype of NCI – H441 cell line
- Cyclic mechanical stimulation of NCI – H441 cell line with an established mechanical stimulation system to investigate cell membrane responses; a know endpoint in mechanotransduction studies.

iii. To investigate the effect of matrix substratum, and mechanical stimulation on the production of inflammatory cytokines by NCI – H441.

- Examine the gene expression of inflammatory cytokines: interleukin (IL) – B, IL – 4, IL – 6, IL – 8, suppressor of cytokine signalling (SOCS), and SP – A within cell populations of mechanically stimulated and control NCI – H441 cells cultured on extracellular matrix constituents of the alveolar basement membrane.

CHAPTER 2. MATERIALS AND METHODS

2.1 Cell culture of human adenocarcinoma cell line NCI-H441

The human adenocarcinoma cell line NCI-H441 was obtained from the American Tissue Culture Collection. NCI-H441 cells were grown in Dubecco's Modified Eagle's Medium (DMEM): Ham's F12 Nutrient mixture containing 15 mM HEPES (Sigma) supplemented with 10 % fetal bovine serum (Invitrogen Ltd, Paisley, UK), 2 mM L-glutamine, 100 I.U./ml penicillin (Invitrogen Ltd) and 100 μg/ml streptomycin (Invitrogen Ltd).

The composition of solutions used in experiments are detailed in Appendix I

2.1.1 Cell counting and viability assessment by the trypan blue dye exclusion stain procedure

A Neubauer haemocytometer was used to count and assess the viability of cells. The haemocytometer is a specially designed counting chamber, with nine large squares of a known depth etched onto its surface. Each of these squares has an area of 1 mm^2 and the depth of the fluid is 0.1 mm. Therefore, the volume of liquid covering each of the large squares is 10^{-4} ml (1 x 1 x 0.1 = 0.1 mm^3 = 0.0001 ml).

To count cells a coverslip is placed over the chamber and when the two are in contact with one each other, interference rings (Newton rings) appear at the edges of the coverslip. A mixture of 200 μl of stock cell suspension, 300 μl serum – free medium and 500 μl of 0.4 % Trypan blue solution is prepared. The counting chamber is filled with 10 μl of the diluted cell suspension and the haemocytometer placed on the stage of an Olympus CX2 inverted microscope. The chamber is left to stand for 2 – 3 minutes to allow the cell suspension to settle. The viable cells exude the stain and nonviable cells stain blue. Cells are counted in the four outer large squares and the large central square. When counting the cells crossing the upper and left – hand boundaries are included, whereas those in contact with the lower or right –hand divisions of the chamber are not included in the count. The following equation calculates the total number of viable cells in the suspension:

$$\text{Total number of viable cells / ml} = \frac{\text{unstained cells in the five large squares}}{5} \times \text{dilution} \times 10^4$$

The percentage of viable cells is calculated as follows:

$$\text{Cell viability (\%)} = \frac{\text{total unstained cells}}{\text{total cells (stained + unstained)}} \times 100$$

2.1.2 Coating dishes with ECM proteins

Human placental collagen IV (CIV) (Sigma), fibronectin (FN) (Sigma), and poly-l-lysine (Sigma) solutions were used to coat 58 mm (Nunc) tissue culture petri dishes. Working concentrations of each coating agent were 10 μg/ml in phosphate buffered saline (PBS). Extraneous sites within the surface of the dishes are coated with a 2 mg/ml solution of bovine serum albumin (BSA) (Sigma) in PBS. These solutions were filter sterilised through 0.2 μm pore size Millex®-GP filters (Millipore Corporation Inc, US) before use. To each of the dishes, 1 ml of coating solution was evenly applied and the dish incubated overnight at 4 °C. The following day the coating agent was removed, 1 ml of sterile BSA added to each dish, and the dishes incubated for one hour at 37°C. The BSA blocking agent was discarded, and the dishes either used immediately or stored at –20°C until required.

2.2 Induction of cyclical mechanical strain

The mechanical strain apparatus developed for osteoarticular mechanotransduction studies (92; 107), was used in this study.

Cells of interest are cultivated on 58 mm flexible tissue culture petri dishes (Nunc). These cultures undergo cyclical mechanical stimulation inside specially designed strain vessels. Each of the strain vessels is made of moulded plastic with inlet and outlet valves controlled by an electronic timer. Within the centre and attached to the base of the vessel there is a cylinder which contains a rubber 'O' ring. The cylinder structure forms a firm seal with the base of the culture dish. Eighteen evenly spaced holes of 2.2 mm within this support cylinder allows movement of gas between the main chamber and beneath the dish. When the strain vessel is pressurised with helium gas, a pressure gradient occurs above and the below the dish, which causes the base of the dish to flex downwards, thus straining the adherent cells. This gradient is due to the main chamber, above the dish, being 89 ml and the minor chamber, below the dish being 8 ml in volume and the gas being introduced above the dish not below.

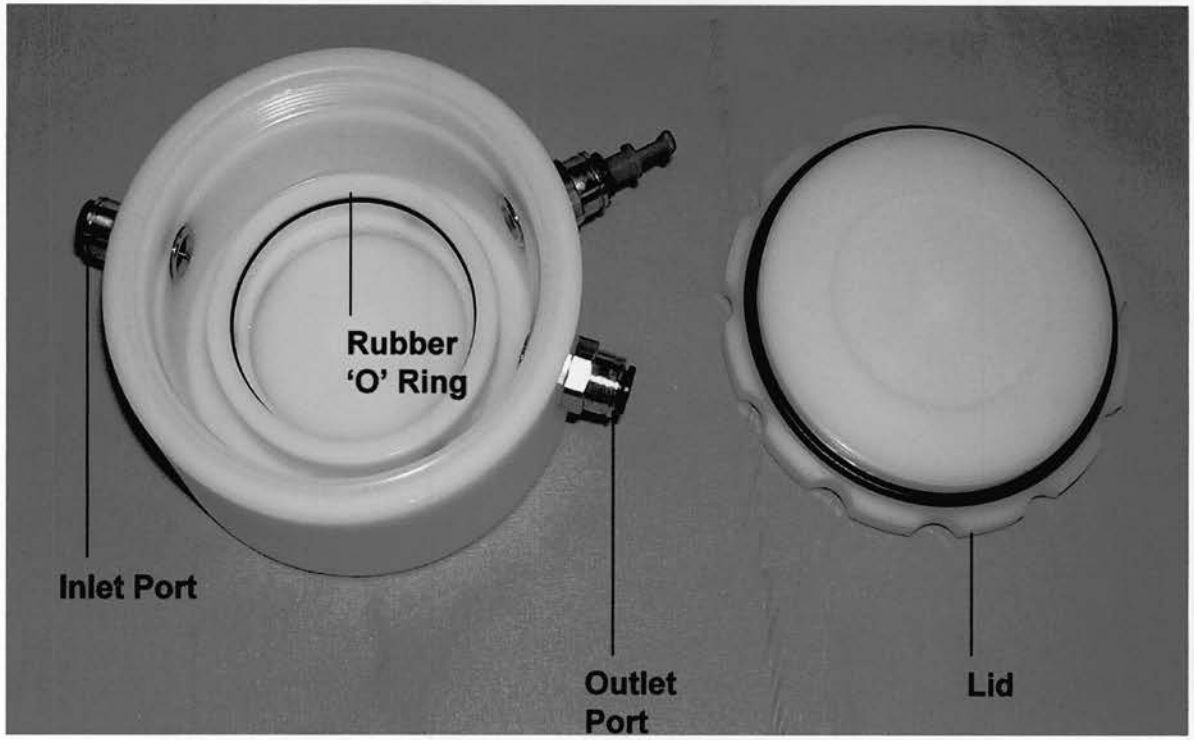

Figure 2.1. Photograph of mechanical Stimulation chamber

Previous studies have ascertained that the degree of gaseous pressurisation has no effect, but that biochemical responses are a direct result of strain experienced on the base of dish by the adherent cells. In these present studies, a pressure of 1.5 Bar above atmospheric pressure was used, which results in a maximum of 5000 μstrain on the base of the dish. The stimulation regime was a frequency of 0.25 Hz (2 seconds on, 2 seconds off) for 20 min at 37 °C. Experiments used NCI-H441 cells from passages 56 to 71 and primary type II pneumocytes from at least three donors. Prior to experiments all cultures were serum starved. The standard growth medium (DMEM:F12, 10 % FCS, and supplements) was removed and the cultures washed twice with serum-free medium. Cell cultures were then an incubated for 30 minutes at 37 °C in serum-free medium before mechanical stimulation

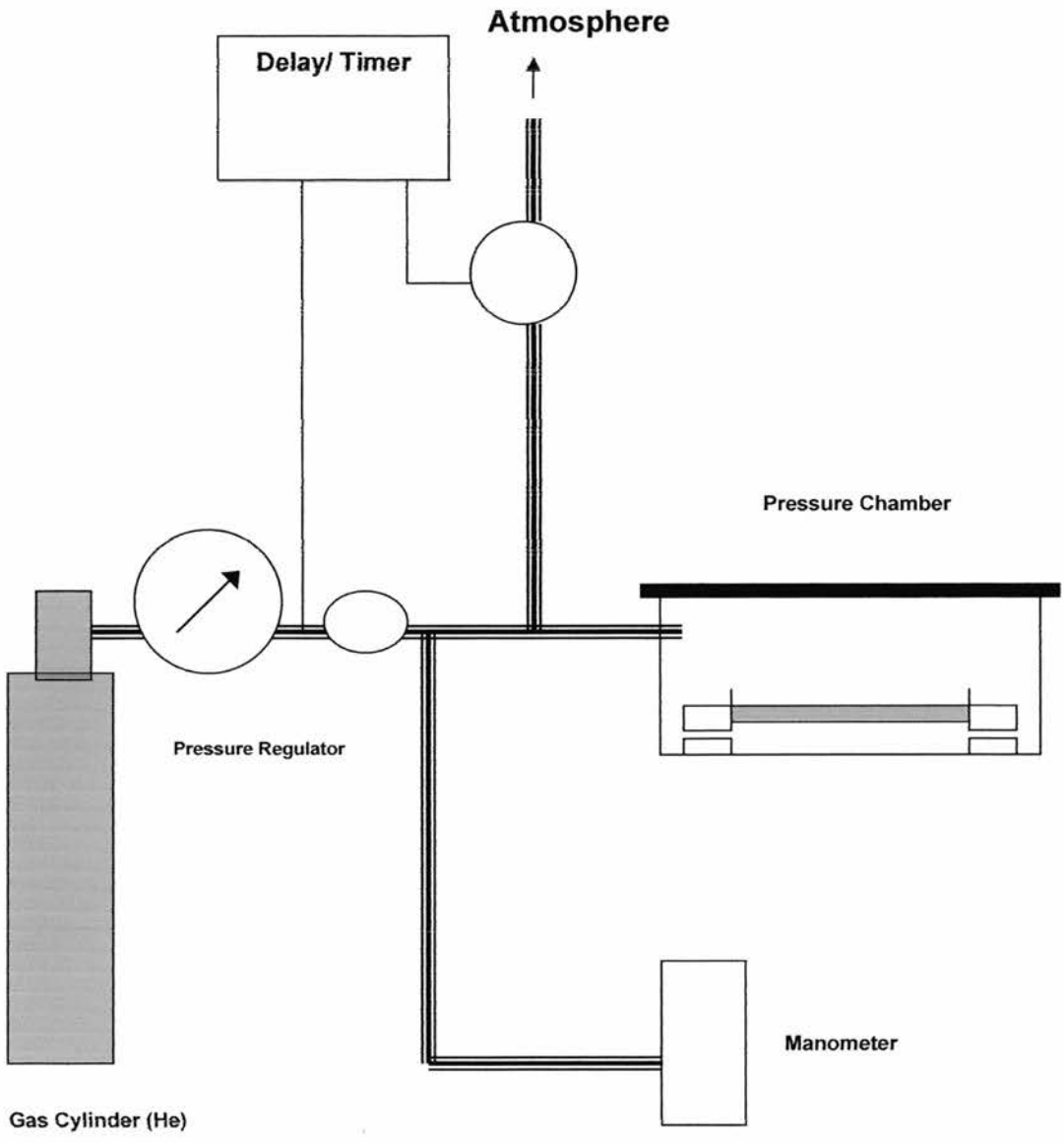

Figure 2.2. Apparatus for the Induction of Cyclic Mechanical Stimulation.
Helium gas entered the system from a gas cylinder, via a pressure regulator, which controlled the inlet and outlet valves of the pressure chamber. A delay/timer allowed the frequency of pressure pulse to be controlled. The pressure in the system was monitored by a manometer.

2.3 General immunochemistry

The specific conditions for antibodies are listed in Table 2.1.

2.3.1 Cytospin preparation

Cytospins of NCI-H441 cells, human primary type II pneumocytes or human peripheral blood mononuclear cells (PBMC) were prepared using a cell suspension containing 2 x 10^6 cells/ ml in serum-free DMEM: F12 medium. PBMC preparations were courtesy of Sonia Wakelin. Cells were spun using a Shandon cytocentrifuge at 300 rpm for 5 minutes. The cell cytospins were allowed to dry at room temperature for 5 minutes, then fixed by immersion in chemically dried acetone:methanol (9:1 vol:vol) for 5 minutes. Slides were air dried for 5 minutes then stored at –20°C until required. Frozen sections of human lung tissue were fixed in a similar manner to the cytospins.

2.3.2 Immunochemistry of frozen section or cells

The fixed slides were allowed to come to room temperature. Following this, sample slides were washed in PBS for a period of 5 minutes. Endogenous peroxidase activity was blocked by incubating sections or cytospins in 0.15% v/v H_2O_2 for 10 minutes at room temperature. The slides were then subjected to a further two 5 minute washes in PBS. Subsequently, the slides were loaded onto Shandon Sequenza staining racks (Shandon Inc, Pittsburgh, USA) with PBS. Potential non – specific binding sites were blocked by incubating for 15 minutes with a serum – free protein block (Dako). The samples were then incubated with the primary antibody for an appropriate duration of time and dilution, according to the conditions required (Table 2.1). The primary antibody was removed by washing the slides three times in PBS, 10 minutes for each wash. The slides were incubated in an appropriate secondary antibody solution for 30 minutes at room temperature. Subsequently, the slides were washed thrice with PBS, each wash lasting 10 minutes. Final visualisation was achieved by incubating the slides with diaminobenzidine (DAB) colour reagent (Sigma) (Appendix I) for 5 minutes. After removing the slides from the racks, they were rinsed in running tap water. The slides were counterstained in Harris's haematoxylin for 20 seconds, and rinsed in running tap water. Slides were then incubated in Scott's tap water substitute (STWS) for 20 seconds, and rinsed in running tap water again. Subsequently the slides were dehydrated in ascending grades of alcohol (64%, 74%, absolute). Finally they were cleared sequentially

through four changes of xylene and mounted with Pertex mounting medium (Cellpath Ltd Hemel Hempstead, UK).

2.4 Electron microscopy

2.4.1 Processing schedule for tissue cultured cells – cell suspensions

Suspensions of NCI-H441 and primary type II pneumocytes were processed for electron microsopy by the same technique. Two millilitres of 1.5 - 4 x 10^6 cells/ml cell suspension were added to 8 ml 0.1 M sodium cacodylate buffer containing 3 % glutaraldehyde (Appendix I), and centrifuged at 2000 rpm, 4 °C for 30 minutes in a Mistral 2000R bench top centrifuge. The pellet was washed in 0.1 M sodium cacodylate buffer at 4 °C for 15 minutes. The pellet then was post fixed in 0.1 M sodium cacodylate buffer containing 1 % osmium tetroxide for 30 minutes at 4 °C.

Mr Stuart M°Kenzie carried out the processing of samples detailed below.
Following fixation, the rest of the processing was conducted at room temperature in a fume hood. The pellet was subjected to sequential dehydration by exposing it to increasing grades of ethanol for 10 minutes each. The grades were as follows; 10 %, 50 %, 70 % and 90 % of absolute ethanol (Hayman Ltd, Essex, UK), followed by three immersions in absolute alcohol for 15 minutes each. The pellet was washed twice with propylene oxide for 15 minutes, followed by incubation in Aladrite oxy resin (TAAB Laboratories Ltd) for 2 hours. The cells were embedded in polythene capsules in fresh araldite epoxy resin. The resin was polymerised at 56 °C for 2 – 3 days and 50 nanometer ultrathin sections of the cell suspension were cut on a LKB Nova Ultratome.
Sections were stained with Uranyl Acetate and Lead Citrate and viewed on a Jeol 100 CXII electron microscope.

2.5 Protein extraction

2.5.1 Lysis of adherent monolayer cell culture

Following experimental manipulation culture medium was discarded to a cell culture waste bottle and the adherent cells washed with ice cold wash buffer (Appendix I) containing 0.1 mM sodium orthovanadate (Na_3VO_4) (2 ml/58 mm plate). This wash buffer was then discarded. The remaining traces of wash buffer were removed by pipette and 350 µl/plate of ice-cold lysis buffer added to the dish. The plates were incubated for a minimum of 15 minutes on ice. The plates were scraped using sterile cell scrapers and the resultant lysate pipetted into microfuge tubes. Cell lysates were then spun at 13 000 rpm for 15 minutes in a microcentrifuge at 4 °C. The supernatants were transferred to fresh microfuge tubes and the pellet containing nuclear debris discarded. Aliquots of 20 µl from each of the different samples were reserved for protein assays.

2.5.2 Homogenising human lung tissue for protein extraction

Primary (fresh/frozen) human lung tissue was homogenised with the use of small dissecting scissors, pestle and mortar (previously stored –70 °C) and a ground glass homogeniser. This technique was carried out on ice within a class I laminar flow cabinet. The small pieces of sample, approximately 2-3 mm^3, were placed in protein lysis buffer [1ml/ 0.5 – 1 g tissue] and sequentially homogenised by use of a chilled porcelain pestle, mortar and ground glass homogeniser. The homogenate was left on ice for 15 minutes, then transferred into a 15 ml centrifuge tube and centrifuged at 13 000 rpm for 30 minutes at 4 °C in a Mistral 2000R bench top centrifuge. Subsequently, the supernatant was frozen at – 70 °C in 500 µl aliquots, with 20 µl of each of the aliquots retained separately so that the protein concentration could be assayed.

2.5.3 Lowry determination of protein concentration

Concentration of protein samples was determined by employing the Lowry protein assay. Known quantities of a 1 mg/ml BSA solution were assayed to construct a standard curve, an example of which is given in Figure 2..x. The equation of a straight line from the graph was utilised for the determination of the protein concentration of the assayed samples.

Table 2.2 shows the protein dilutions used within an assay. Each of the dilutions was set up in triplicate in 1.5 ml microfuge tubes. Then 1 ml of working alkaline carbonate solution was added, the assay samples were vortexed and left to stand for 10 minutes at room temperature. To each of the samples assays 100 ml of working Folin's reagent was added, and the tubes vortexed, then incubated at room temperature for 30 minutes. Aliquots of 200 µl were transferred from each tube into a flatbottomed 96 well tissue culture plate, and the absorbance at 570 nm was determined usining a Dynatech MR500 microplate reader. The final protein concentrations were calculated using Microsoft Excel® software.

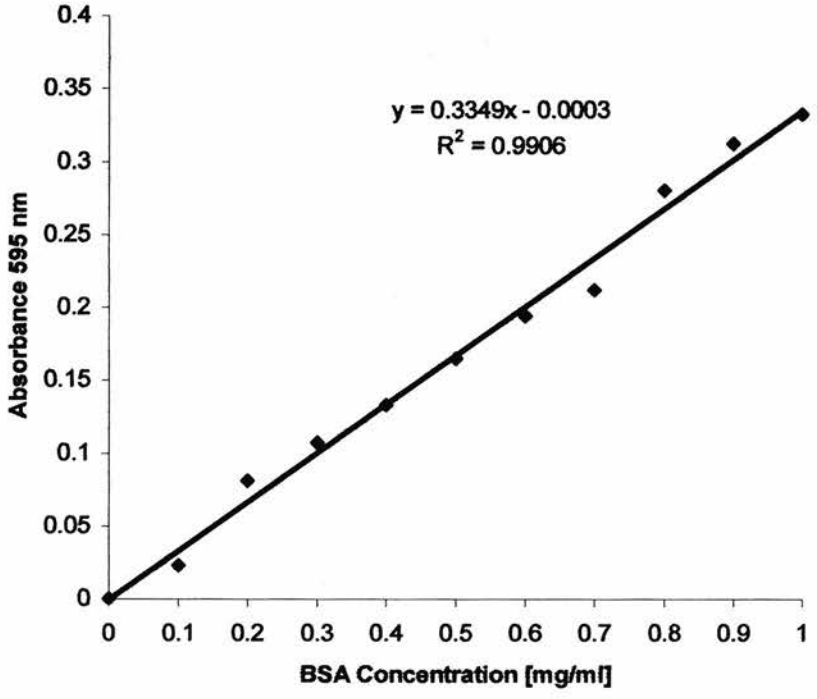

Figure 2.3. Standard curve for Lowry protein assay using BSA

2.6 Western blotting

2.6.1 Sodium dodecyl sulphate poly – acrylamide gel electrophoresis (SDS-PAGE)

Industrial methyl alcohol was used to clean the apparatus (Biorad, mini protean 3), and then it was assembled according to the manufacturer's instructions. The glass plates were marked 0.5 cm below the base of the sample comb space. An appropriate percentage separating gel was made (Table 2.1), and poured between the glass plates to this mark. The separating gel was overlaid with distilled water and left to polymerise for 45 minutes at room temperature. Once the gel had polymerised, the distilled water was poured off and the remaining water adsorbed from the surface of the gel with filter paper. The prepared stacking gel solution was poured onto the separating gel to the top of the glass plates and a 10 well sample comb inserted into the sandwich. The stacking gel was left to polymerise for approximately 30 minutes. Once the gels were set, the combs were removed, the clamp assemblies removed from the casting stand and attached to the inner cooling core. A volume of 500 ml of electrode buffer was prepared from a five times stock solution. The upper chamber was filled with this buffer and the remainder placed in the lower chamber. The protein samples under investigation were diluted with sample buffer (Appendix I) in the ratio of 1:4 vol:vol and boiled for 5 minutes, then placed on ice. Twenty microlitres of the samples and 10 µl coloured molecular weight marker (Amersham Pharmacia Biotech) were loaded onto the gels. Gels were run at 150 V constant voltage, and stopped when the bromophenol blue dye front reached the base of the separating gel.

2.6.2 Electrophoretic transfer of protein to poly vinylidene fluoride (PVDF) membrane

Following SDS- PAGE of protein samples, the separated proteins were transferred to poly vinylidene fluoride (PVDF) membrane. For every gel a piece of PVDF membrane (Sigma) and two pieces of 3 MM Whatmann filter paper of 9 x 6 cm were cut. To aid the efficiency of protein transfer the membrane was initially soaked in absolute methanol for 15 seconds and washed with double distilled water for two minutes. Membrane, filter paper and gels were equilibrated in transfer buffer for 15 minutes, then assembled into the transfer sandwich. From anode to cathode the order of assembly was as follows: fibre pad, filter paper, gel, PVDF membrane, filter paper, fibre pad. This sandwich was placed, with a frozen cooling unit, into a transfer tank. This tank containing transfer cassette and icepack was filled with transfer buffer and the transfer carried out at 100 V for one hour.

2.6.3 Immunoblotting and development of blot using enhanced chemiluminescence – plus (ECL – Plus)

Once the transfer was completed, the PVDF membrane was soaked in absolute methanol for 10 seconds. The membrane was air - dried on filter paper for 15 minutes to allow the excess methanol to evaporate. Extraneous non-specific antigenic sites on the membrane were blocked by incubating the membrane overnight at 4 °C on a shaking platform with 10 ml of 5 % non – fat milk in Tris Buffered Saline containing 0.1 % Tween 20 (TBST). The membranes were incubated with the primary antibody optimally diluted in 2.5 % w/v non-fat milk in TBST blocking buffer at 4°C overnight, or at room temperature for 1 hour with shaking (Table x.x). After removal of primary antibody solution the membrane was washed 6 times for 5 minutes each time with 20 ml of TBST. Goat anti-rabbit HRP-secondary antibody (Dako) diluted 1:2000 in 10 ml of TBST was incubated with the membrane for 1 hour at room temperature with shaking. Then the membrane was washed as before. An enhanced chemiluminescent reaction was used to finally visualise the proteins of interest. The ECL Plus reagents (Amersham) were equilibrated to room temperature, then a mixture of solution A: solution B (40:1) was applied to the membrane for 5 minutes. The fluid was

tipped off the surface and the membrane sandwiched between two pieces of Saranwrap. Care was taken to remove air bubbles trapped between the membrane and the Saranwrap. Inside a dark room, the blotted membrane was exposed to Hyperfilm (Amersham) and then developed by a hyperprocessor (Amersham).

2.6.4 Stripping and reprobing western blots

Pre – blotted, probed membranes were stripped of their detection antibodies and reprobed with an anti - glyceraldehyde –3 phosphate dehydrogenase (GAPDH) antibody. This enzyme is a metabolic housekeeping enzyme, and its detection is used as a protein loading control. This was to ensure that equal quantities of total protein were loaded onto the gel and immunoblotted, therefore testing the validity of resultant band signal intensities. Blots were stripped for 30 minutes at 55 °C in stripping buffer (Appendix I) then washed in copious amounts of TBST before reprobing. Primary and secondary blots were photographed together using a Mitsubishi Video Copy Processor, model K65HM. The instensity of each band was quantified using the Enhanced Analysis software (EASY, Scotlab, Coatbridge, Lanarkshire, UK). This analysis allows a clearer interpretation of visible data from the primary blot as a relative value can be obtained.

The images were saved to floppy disk and printed using the Enhanced Analysis System (EASY, Scotlab, Coatbridge, Lanarkshire, Scotland). This program allows semi-quantitative analysis of protein product. It designates the darkest band on the gel a value of 1000 (background = 0) and thus can designate all the other bands a value between 0 and 1000 depending on their intensity. Therefore this program allows the intensity of the protein bands (which is proportional to the amount of protein) to be semi –quantitatively assessed and a representative assessment of effect of mechanical stimulation on the levels of cytoplasmic protein to be made.

2.7 Sandwich enzyme – linked immunosorbent assay of extracellular surfactant protein – B – (ELISA)

Each sample to be assayed was diluted 1:5 in 80 % v/v isopropanol. A 100 µl aliquot of each sample was applied to 96 well microtitre plates, in duplicate. Mirotitre plates were left overnight, until the samples had fully dried into the wells. The following day, 100 µl 1,1,1 – trifluoroethanol (TFE) was added to the wells, and allowed to evaporate at room temperature. Subsequently, each well was washed with 200 µl methanol for 20 minutes whilst shaking. Wells were again washed with methanol and the methanol discarded immediately. The wells were washed thrice with washing buffer (50 mM Tri – HCl, 0.5 %Tween 20, pH 7.6). Following washing, 200 µl of blocking buffer (50 mM Tris – HCl, 1 % (wt/vol) BSA, pH 7.6) was applied to the wells, and the plate was incubated at room temperature for 2 hours. The wells were again washed thrice with washing buffer. Two hundred microlitres of anti - SP – B (Chemicon USA, Cat No. AB3436, ~0.1mg/ml) antibody at 1/ 10, 000 dilution in blocking buffer, is added to the wells and the plate is incubated overnight at room temperature. Following removal of residual antibody solution, the plate is washed thrice with washing buffer. Two hundred microlitres of secondary goat anti –rabbit – HRP antibody diluted 1/1000 in blocking solution was added to the wells and the plate was incubated at room temperature for 2 hours. Subsequently the wells were washed thrice with washing buffer. Two hundred microlitres of 3,3'5, 5' – tetramethylbenzidine base (TMB) substrate solution (Chemicon, USA) was added to the wells and the reaction is allowed to develop in the dark. The reaction was haltedwith 100 µl of 0.5 M H_2SO_4 and the absorbance of the plate was read at 450 nm.

Figure 2.4 SP - B enzyme –linked Immunoabsorbent assay calibration graph.

Total protein extract from human primary lung tissue sample was assayed at various concentrations of SP - B to construct a protein concentration calibration graph for ELISA examination of experimental samples.

2.8 Reverse transcription polymerase chain reaction (RTPCR)

2.8.1.1 Ribonucleic acid (RNA) extraction from adherent monolayer cell culture

When extracting RNA for future use in analysing gene expression levels the medium was removed and monolayer cell cultures washed with PBS. A volume of 750 µl of working RNA extraction buffer was added to the cells and the dishes rotated to ensure complete lysis of the cells was achieved. The petri dishes were then sealed in parafilm and stored at –20°C. The following day, the dishes were defrosted, the solution pipetted into sterile RNase-free microfuge tubes and 75 µl of sodium acetate solution added to each tube. The tubes were then mixed by inversion, 750 µl of phenol : chloroform (1 : 1) mixture added, mixed by inversion and then vortexed. The microfuge tubes were incubated on ice for 15 minutes, then centrifuged at 13 000 rpm at 4°C for 15 minutes. Approximately 700 µl of the upper aqueous phase was removed into a fresh sterile microfuge tube. An equal volume of RNase-free isopropanol (VWR) was added and the tubes incubated at –20 °C overnight. To pellet the RNA the mixture was centrifuged at 13 000 rpm for 15 minutes and the supernatant removed. The RNA pellets were washed in absolute ethanol, centrifuged for 10 minutes at 13 000 rpm and air – dried for 20 minutes. The final RNA pellets were resuspended in 30 µl double distilled water ($mQdH_2O$) and stored at –70°C.

2.8.1.2 Homogenising human lung tissue for RNA extraction

Primary human lung tissue was placed into RNase-free bijoux, snap-frozen by placing the bijoux into liquid nitrogen, and stored at –70 °C until required. Tissue was homogenised in the presence of RNA extraction buffer and the procedure carried out within a class I laminar flow cabinet. First, the homogeniser was decontaminated with RNase AWAY™ (Molecular Bioproducts, San Diego, CA, USA) then rinsed in RNase –free double distilled water. The tissue was defrosted and kept on ice in an RNase-free plastic universal container. One millilitre of working RNA extraction buffer per 50 – 100 mg of primary tissue was added to the vessel. The container was supported upright by ice with a 250 ml plastic beaker to

ensure the universal was kept in place and did not shatter during homogenising. The homogeniser was run in short rapid bursts until the sample was completely homogenous. The homogenate was transferred into 1.5 ml microfuge tubes in 750 µl aliquots. The aliquots were centrifuged at 13 000 rpm, 4 °C for 15 minutes, then stored at –20 °C overnight before completing the RNA extraction process. The RNA extraction method was the same as the method for RNA extraction of the monolayer cultures, except that the phenol: chloroform step were performed twice.

2.8.1.3 Spectrophotometric analysis of RNA

The concentration of the final RNA solution is determined by measuring the $OD_{260\ nm}$ A 6 µl sample of the RNA is diluted a hundred fold in 594 µl of sterile RNase -free $dmQH_2O$, within a sterile nuclease –free microfuge tube. A BioMate 3 ™ (Thermo Spectronic, Rochester, NY, USA) spectrophotometer measured the absorbance of the solution in UV transparent cuvettes at 260 nm and 280 nm wavelengths. Forty micrograms of RNA per millilitre is known to give an $OD_{260\ nm}$ equal to one. Also the ratio of $OD_{260\ nm}$ /$OD_{280\ nm}$ of an RNA solution can be used to determine if there is significant protein contamination of a sample. A solution of pure RNA will give a ratio if 1.8 – 2.0 and a value 1.6 or below is indicative of contamination and the need for further purification of the sample.

2.8.1.4 DNase treatment of RNA

The majority of RNA isolated from monolayer cell culture was not treated for genomic DNA contamination as the isolation method gave low levels of contaminating DNA. The RQ1 DNase – Free DNase™ (Promega Corp, Madison, USA) was used to treat the contaminated samples. The following was added to a sterile nucleotide and nuclease – free microfuge tube;

RNA in RNase - free $mQdH_2O$	1 – 8 µl
RQ1 RNase – Free DNase 10x Reaction Buffer	1 µl
RQ1 RNase – Free DNase	1 U/ µg RNA
DEPC – $mQdH_2O$ up to a final volume of	10 µl

This mixture was pulse spun at 13 000 rpm for 30 seconds and then incubated at 37 °C for thirty minutes on an OmniGene™ thermal cycler (Hybaid, Teddington, UK). The microfuge tube was put on ice, and 1 µl of RQ1 DNase Stop Solution added to terminate the reaction. Subsequently the sample was incubated at 65 °C for 10 minutes on the thermal cycler to inactivate the DNase. The treated RNA samples were stored at – 70°C until required.

2.8.2.1 Reverse transcription reactions – complement deoxyribonucleic acid (cDNA) synthesis

All materials were purchased from Invitrogen Life Technologies unless otherwise stated. Refer to Appendix I for details of working stock concentrations
Ribonuclease inhibitor, RNAguard™ (3200 U) (Amersham Pharmacia Biotech), 1.5 µg Oligo dT (Amersham Pharmacia Biotech), 3 µg RNA and sufficient DEPC – treated water to make each reaction volume to 33.5 µl, were pipetted into sterile RNase – free 0.5 ml microfuge tubes. The tubes were incubated at 70°C for 10 minutes. Twelve microlitres of stock (5x) reaction buffer, 6 µl 0.1 M dithiothreitol (DTT), 6 µl of 10 mM dNTP mix (Amersham Pharmacia Biotech) and 500 units Superscript II enzyme (Invitrogen Ltd, Paisley, UK) were added to each reaction. The reactions incubated at 42°C for 1 hour, and then 70°C for 10 minutes, on an OMN-E™ (Hybaid, Teddington, UK) hotblock. The reaction products were stored at –20°C until required

2.8.2.2 Polymerase chain reaction

Polymerase chain reactions (PCR) were carried out with Gold *Taq* polymerase kits (Biogene Ltd, UK) using an OMN - E™ thermal cycler. Individual dNTPs were purchased from Amersham Pharmacia Biotech. The following "master mixes" were made up for the amplicon of interest: The volumes stated were multiplied by the number of reactions plus one.

Eight microlitres of the amplicon reaction "master mix" was added to each reaction tube. The cDNA sample was spun at 13 000rpm for 5 minutes prior to the addition of 2 µl (10 % final volume) to the reaction tubes. Two control reactions for every cDNA sample were included, one containing cDNA but not primers and the other with primers but no DNA. The GAPDH primers were designed from the full sequence by Mr Mark Lawson, of the

Rayne Laboratory, Edinburgh and the SP-A, primer pair was designed from the full sequence by myself.

Finally, 2 µl of the Taq DNA polymerase "master mix" was added to each of the reaction tubes. Then all the microfuge tubes were pulse spun in a microcentrifuge for 30 seconds and placed on a OMN - E™ thermal cycler on the following program:

2.8.3 Agarose gel electrophoresis

PCR products were run for analysis on 1 % agarose gels. These were produced by mixing 1.5g of Ultra Pure agarose (Invitrogen Ltd, Paisley, UK) in 150 ml of 1 x TAE buffer (Table 2.4) and boiling at 100°C for 5 minutes in a microwave. The agarose solution was allowed to cool to below 60 °C and poured into a prepared gel tray that had plastic blocks sealing both ends and an appropriate size comb inserted in one end. Once the agarose had solidified, the comb and the end blocks were removed and the gel tray was placed into an Anachem horizontal electrophoresis tank (Anachem Ltd, Luton, UK) which was filled with sufficient 1 x TAE buffer to cover the surface of the gel to a depth of approximately 5 mm. The PCR samples were loaded into the wells of the gel with 1 x PCR loading dye (10 µl PCR sample + 10 µl 2 x PCR loading dye) and electrophoresed at 75 V, constant current for between 30 – 60 minutes.

Minigels for the purification of PCR products were produced in the following manner: 0.6 g of agarose was dissolved in 60 mls 1 x TBE buffer (Table 2.5) by heating at 100 °C for 5 minutes in a microwave. Once the solution had cooled below 60 °C, it was poured into a minigel apparatus (Anachem Ltd, Luton, UK), that had plastic end – pieces and an appropriate sized comb inserted at one end. One the gel had solidified the end pieces and comb was removed and the gel submerged in 1 x TBE buffer to approximately 4 mm aboved the surface of the gel (50 ml of buffer). PCR samples were prepared as before and loaded into the gel, and electrophoresed at 75 V for approximately 10 minutes.

Following electrophoresis, the gels were immersed in a 2µg/ml ethidium bromide solution and left to soak for 20 minutes. The stained gels were then placed on a UVP UV transilluminator, emitting UV light at 320 nm. As standard the gels were photographed

using a Mitsubishi Video Copy Processor, model K65HM, and attached camera, using Mitsubishi Thermal paper.

2.8.2 The purification of PCR products for automated DNA sequencing was achieved by utilising a Qiagen Qiaquick gel extraction kit.

To purify PCR products, they were first run on 1 % TBE mini agarose gels and visualised by staining with fresh ethidium bromide solution. The DNA fragments of the PCR products were excised from the gel using a sterile scalpel, taking care to keep the presence of excess agarose to a minimum. The gel slices were placed in sterile nuclease –free, pre – weighed 1.5 ml microfuge tubes. The weight of the gel was then determined by weighing the tubes. For every 100 mg of gel 300 µl of QX1 buffer was added to the tube. If the gel slice weighed more than 400 mg, more than one microfuge tube was used to purify the product. The samples were incubated at 50 °C for 10 minutes on a hotblock, until the gel had completely dissolved. Every 2 minutes throughout this incubation the tube was inverted to aid the dissolution of the gel. Once this incubation had been completed the buffer was yellow in colour, and the contents of the tube were mixed by inversion. One volume of isopropanol was added and again the tubes mixed by inversion. The samples were applied in 800 µl aliquots to QIAquick spin columns placed in 2 ml collection tubes and centrifuged at 13 000 rpm for 1 minute. The flow through was discarded and the spin columns returned to their collection tubes. A 500 µl addition of QX1 buffer was made to each of the spin columns and they were spun again at 13 000 rpm for 1 minute. The flow through was discarded and the columns returned to the collection tubes. Subsequently, 750 µl of the PE buffer was added to each of the columns and they were left to stand on the bench for a 2 – 5 minutes, then centrifuged for a minute at 13 000 rpm. The flow through was discarded, the spin columns placed back into the same tubes and again spun at 13000 rpm for 1 minute. The spin columns were transferred into fresh microfuge tubes that had had their lids and hinges removed. A volume of 30 µl of sterile mQH_2O was added to the columns and they were left to stand for one minute before they were centrifuged at 13 000 rpm for 1 minute. Finally, the columns were removed and the tubes were capped and stored at –20 °C until they were sent for automated DNA sequencing (Adapted from Promega Technical Bulletin No. 518) Automated DNA sequencing was carried out by Nicola Wrobel, utilising an ABI Prism

Reaction Dye Deoxy Terminator Cycle Sequencing Kit, and analysed using an applied Biosystems 373 automated Sequencer.

2.9 TaqMan® real time polymerase chain reactions

2.9.1 Preparation of cDNA for TaqMan® reactions

Two microlitres of Taqman buffer (10x), 4.4 µl magnesium chloride solution, 4 µl dNTP mix, 1 µl random hexamer, 0.4 µl RNase inhibitor, multiscribe reverse transcriptase (RT), 400 ng of sample RNA and sufficient RNase – free water to make each reaction volume to 7.7 µl, were pipetted, into sterile RNase – free 0.5 ml microfuge tubes. The tubes were incubated at 25°C for 10 minutes, 48°C for 40 minutes, 95°C for 5 minutes and the 4°C for 10 minutes, on an OMN - E™ (Hybaid, Teddington, UK). Twenty – seven microlitres of RNase free - water was then added to the sample to give a final volume of 45 µl of cDNA, and the sample stored at –20°C until required.

2.9.2 TaqMan® real time polymerase chain reactions

All were materials for were purchased from Applied Biosystems unless otherwise stated. Real time polymerase chain reaction were carried out with an AB PRISM® 7700 sequence detection system. Mutiplex comparative PCR reactions were carried out using the following "master mixes "for the amplicons of interest. The volumes stated were multiplied by the number of reactions plus one.

Samples were set up in duplicate with a negative control composed of real time master mix and nuclease – free water on a MicroAmp® optical 96 – well reaction plates. Each plate was spun prior to loading on the real time PCR machine

2.10 Electrophysiology

2.10.1 Preparation of microelectrodes

Fresh electrodes were produced for each experiment. A Narishige microelectrode puller (Narishige, Japan) made the microelectrodes from 10 cm borosolicate glass capillaries containing an inner filament (GC150F – 10, Harvard Bioscience Company). Each capillary had an outer diameter of 1.5 mm, an inner diameter of 0.86 mm, and pulled into two individual microelectrodes. Once cooled, the microelectrodes were stored in a clean container with the tips uppermost until required.

2.10.2 Filling of microelectrodes

Filtered 3 M KCL was used in the preparation of the microelectrodes. Shafts of the microelectrodes were held above the level of 3 M KCL within the rim of a clean beaker, with Blu Tack™. A lumbar needle and 5ml plastic syringe were then used to fill the shaft of the microelectrode with the solution. Consequently the tips of the microelectrodes filled by capillary action along the inner filament. The microelectrodes were left for at least 5 minutes after filling before use. If air bubbles were visible within a microelectrode tip, that microelectrode was discarded, without using.

2.10.3 Electrophysiological recording

These recordings were carried out at room temperature (approximately 20°C). Dishes of pneumocytes were placed on the stage of a Wild M40 inverted microscope, and the cells observed under x200 magnification. An earth electrode, comprised of a non – polarisable silver/silver chloride (Ag/AgCl) wire was placed in the periphery of the dish under examination. This wire was connected to earth via the ground terminal of the input headstage. A pre - prepared microelectrode was connected to the microelectrode holder, so that the central Ag/AgCl wire of the holder inserted into the middle of the microelectrode,

and contacted the 3M KCl. The microelectrode was fixed into the holder so that the blunt end was in contact with the recess and pipette seat of the microelectrode holder. This microelectrode holder was connected to the input of the headstage. Using a Zeiss micromanipulator to manoeuvre the microelectrode and headstage, the tip of the microelectrode is lowered to a level just below the surface of the culture medium with the dish; it appears as if the microelectrode is making a small dimple upon the surface of the medium. To find the microelectrode within the field of view the shaft of the microelectrode must be within the light path. To find the area close to the tip of the microelectrode a defined light spot must be located within the field of view. To do this, swing the micromanipulator vertically until a pale grey shadow is detectable horizontal to the field. Gently lower the microelectrode, and using the coarse control of the microscope focus until the light spot is visible with a more intense shadow spot too. Then, the micromanipulator is used to move the microelectrode horizontally and if needed gently down, until the tip of the microelectrode is visible and in focus. The actual tip of the microelectrode is not visible under these circumstances as it is no more than 0.2 μm in diameter.

After switching on power to the electrophysiology recording apparatus, any voltage registered on the oscilloscope (Gould Advance type OS 4000/4001) was offset to a zero base line, using the input offset potentiometer of the microelectrode clamp (Axoclamp – 2B, Axon Instruments). The microelectrode resistance was monitored throughout experiments using a Wheatstone bridge incorporated into the system. A command current of 5 nA was set with the step command switch. On seeing a voltage pulse on the oscilloscope screen the bridge dial was turned until the voltage step was eliminated, creating a flat line on the screen and balancing the bridge. The resistance of the microelectrode then was read from the bridge dial. The acceptable range of tip resistances was 25 – 50 MΩ. Microelectrodes with tip resistances lower than this range were indicative of tip damage and resistances higher than this indicated air bubbles within the tip of the microelectrode or tip blockage with cellular material.

i. The selection criterion for impaling cells was as follows:

ii. Each cell had to be in isolation not in contact with other cells

iii. They had to be morphologically similar to the eye – i.e. similar size and spread to the same degree (spherical not eliptical or spindle shaped cells)

A voltage - dependent oscillator was used to produce an audible tone that was proportional to the measured voltage. On impaling a cell, the note would change with the change in voltage, which allowed the investigator to monitor entry of the microelectrode into the cell and assess the quality of impalement by the sounds emitted from the oscillator. On cell impalement, simultaneous to the note changing the oscilloscope beam moved vertically on the oscilloscope screen. The digital read out of membrane potential was obtained from the Axoclamp – 2B.

A membrane potential reading was deemed acceptable if, on impaling a cell, there was a rapid change in the voltage which remained constant for at least 30 seconds. Membrane potentials of 5 to 10 isolated pneumocytes were sampled before and after the standard regime of 20 minutes of cyclical mechanical stimulation.

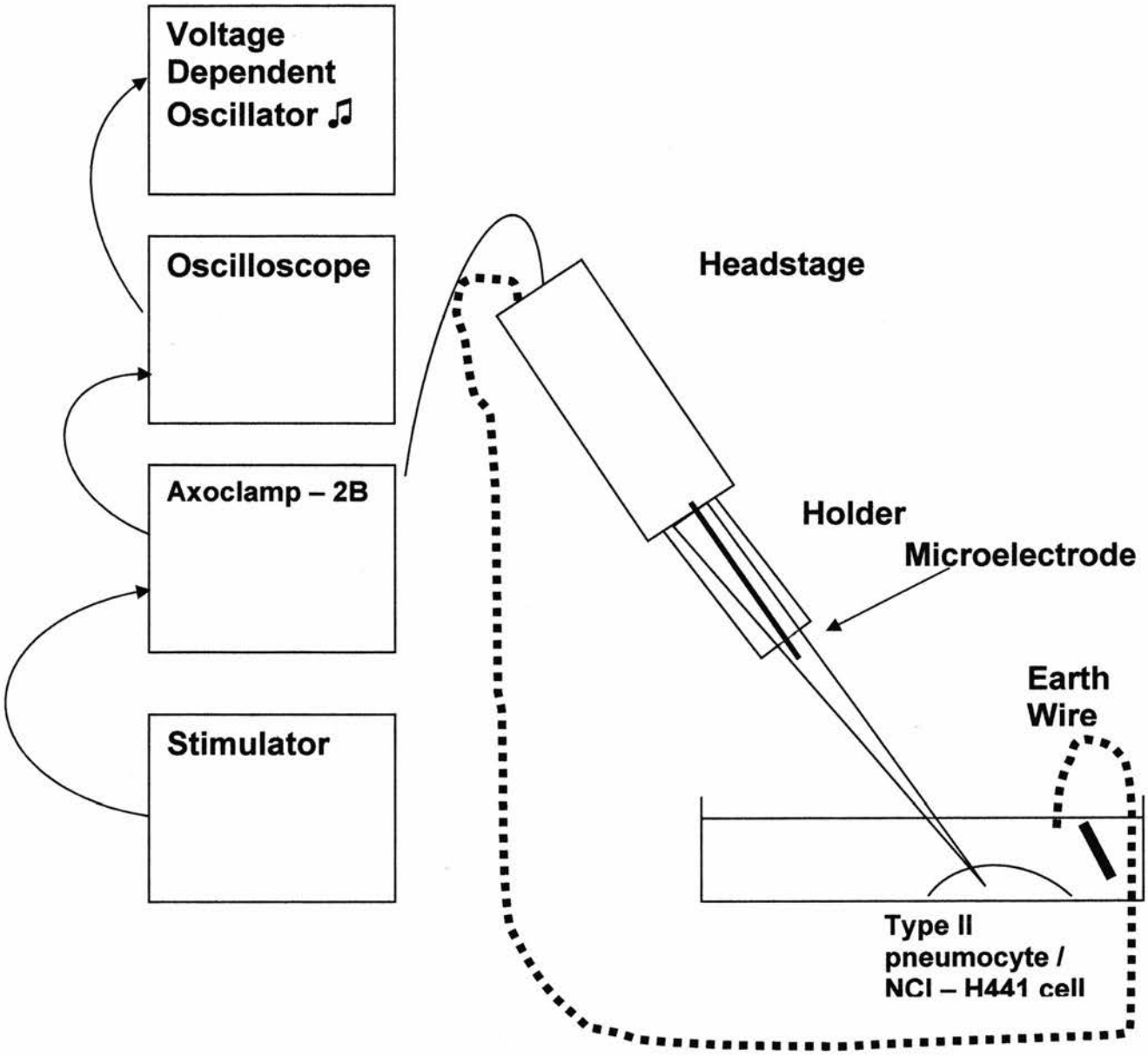

Figure 2.2 Diagram of Axoclamp – 2B System

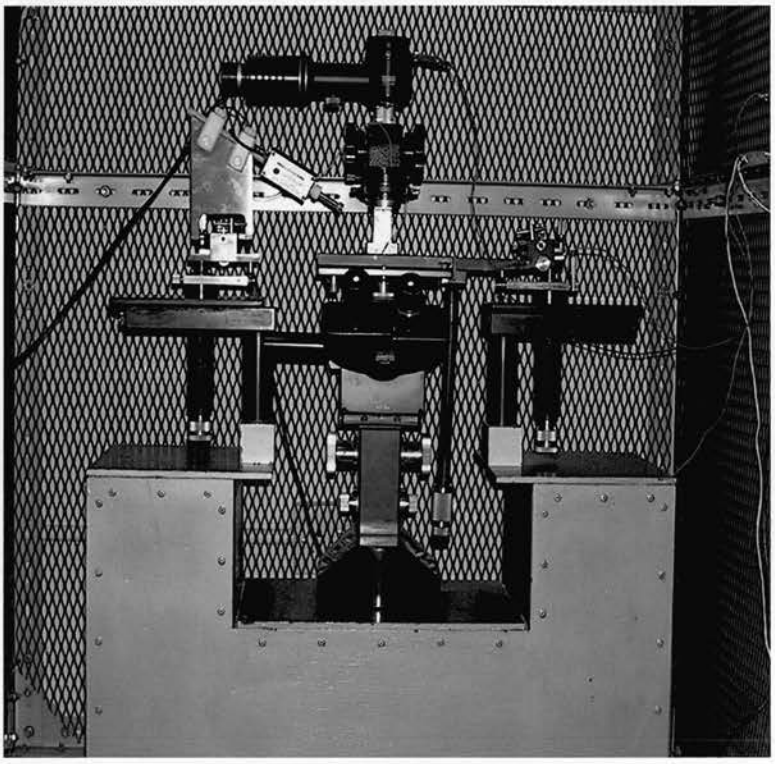

Figure.2.6. Photograph of Wild M 40 inverted microscope and micromanipulation system used in recording membrane potential recording.

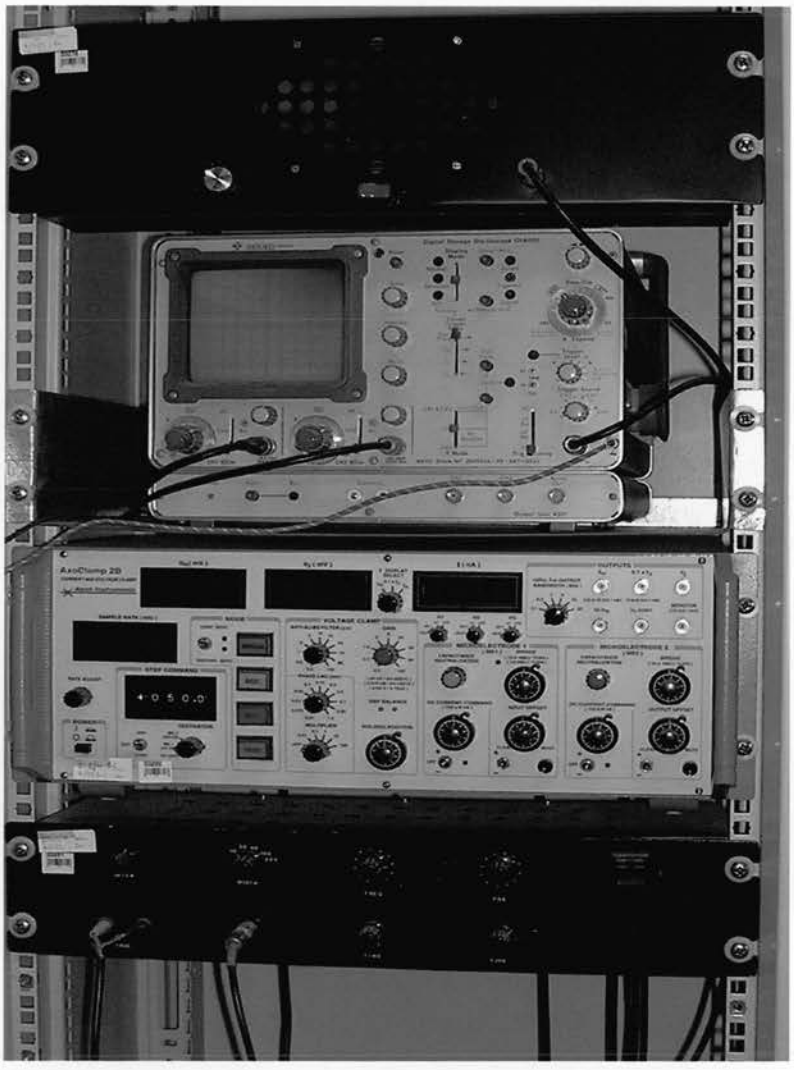

Figure 2.7 Photograph of electrophysiological recording equipment.

2.11 Statistical analysis

Statistical analyses were carried out with the aid of MINITAB™ software package. Basic descriptive statistics; mean, standard deviation of the mean, standard error of the mean were calculated with MINITAB™ software package in Chapters 3 to 5. In Chapter 4 when comparing cell population data F ratios was employed to determine parametric or non – parametric stasis and students' unpaired t- test or Mann U – Whitney tests applied respectively to determine significance of before and after measurements. Utilising a Kruskal – Wallis analysis of the variance of the membrane potential data (Chapter 4) was undertaken.

CHAPTER 3 HUMAN TYPE II PNEUMOCYTE ISOLATION AND CHARACTERIZATION

3.1 Human Type II pneumocyte isolation and characterization

The lung is an extremely complex tissue populated by at least 40 types of cell. The type II pneumocyte constitutes approximately 15 % of the lung parenchyma (6). A major problem when isolating and assessing the purity of type II pneumocyte preparations is the lack of a simple characterisation technique. There is not, at present, an antigen or characteristic that is unique to the type II pneumocyte. Current thought is that the type II pneumocyte is the progenitor cell of the alveolar lining (10). The fact that type II pneumocytes can transdifferentiate into type I pneumocytes following injury highlights this issue. Indeed, during transdifferentiation an intermediate epithelial phenotype appears. The general held consensus today is that the type I pneumocyte population of the alveoli is maintained by this reversible transdifferentiation process (13). In vivo and in vitro models examining the alveolar phenotypes with the electron microscope would appear to support this consensus (10; 11; 141; 142). Pneumocytes possessing characteristics of both the type I and II pneumocytes, often referred to, as the "intermediate" pneumocyte are the main evidence for the process. To date the "intermediate " phenotype has been observed in developing rats (143), cats (144) and sheep (11).

Over the last 30 years published papers have appeared regarding the isolation of type II pneumocytes from a number of different mammalian species; mice, hamsters, rats, pigs, rabbits, guinea pigs, cows and human tissue have all featured (145; 146). Each of these studies, despite different test species, also employed a variety of techniques for enzymatic digestion of tissue and in the purification of the resultant cells. The reported purity of the final isolations range from 60-98 % type II pneumocytes (145). The reported isolations of human type II pneumocytes quote purity ratios of 73 –97 % (Table 3.1). Different proteolytic enzymes, separation techniques, and characterisation methods are all used.

It is not clear what the optimum technique for type II pneumocyte isolation is. The cell density and size of any given population of type II pneumocytes are heterogeneous (6). The rate of sedimentation of a cell varies in direct proportion to cell density and in proportion to the square of cell diameter (147) and different cell types can overlap in cell diameter and size (148) (6), (9; 149). Therefore, the separation of type II pneumocytes from other lung cells by only differential sedimentation is difficult (145). There are also some indications that proteolytic enzymes such as trypsin, when used in the liberation of type II pneumocytes, have a detrimental impact on cellular functions (150; 151). Different proteolytic enzymes

such as trypsin, collagenase, dispase and DNase have been used, and it is difficult to interpret effects of published results for a number of reasons. Disparities exist in the quality of enzymes sold by different suppliers; commercial enzymes are known to vary in purity and activity. In addition, many of the reported type II pneumocyte isolations do not quote the enzyme activity or use different units of activity (145). Dobbs and co-workers suggest that elastase is the most specific proteolytic enzyme at liberating type II pneumocytes (145). However, evidence is emerging that this may not be the case in human type II pneumocyte isolations. Greater yields of type II pneumocytes have been reported with the use of trypsin, compared with elastase (152)). The increasing knowledge of type II pneumocyte biology has also cast doubt on the use of antibodies in the isolation of these cells. Human type II pneumocytes lack Fc receptors, but possess major histocompatibility complex molecules (MHC) I and MHC II molecules (152). Human type II pneumocytes are also known to express ICAM-1, unlike rat type II cells (152)together with a number of other costimulatory T-cell molecules such as CD58, CD54, CD80 and CD86 (153). The paracrine effects of stimulated contaminating immune cells could potentially significantly affect isolated type II pneumocytes (145). Therefore it has been suggested that the final experimental requirements to some extent dictate which combination of techniques are the most appropriate when preparing type II pneumocyte cultures (145). Refer to Table 3.1 for a summary of human type II pneumocyte isolation studies.

The main aim of the following work was to establish whether or not a reproducible protocol for the isolation of type II pneumocytes from human lung tissue could be developed to study mechanical effects on these cells.

3.2.1 Primary human sample collection and storage

Twenty-six human lung specimens were obtained with patient's consent from 21 lobectomy or pneumonectomy procedures for malignant disease. Macroscopically normal tissue was taken from the pleural border and distal from tumours. Samples were immersed in one hundred millilitres of storage medium (Appendix I) within a sterilin jar of known weight. The net mass of the tissue was calculated by reweighing and subtracting the original weight from the total weight of the tissue, jar and media. Samples were then stored overnight. A previous study observed that viable type II pneumocytes are obtainable up to four days post resection (155).

3.2.2 Isolation of primary human type II pneumocytes

All work was carried out within the confines of class I and class II laminar flow cabinets.
A comparison of two isolation procedures was carried out to establish best conditions for successful release of primary human type II pneumocytes. The first procedure was supplied by Dr Shirley O'Dea (Post doctoral research scientist, Lung Pathology research group, University of Edinburgh) and differs from the other procedure (146) predominately by the exclusion of the use of DNase from the protocol.
A full list of solutions and equipment used is given in Appendix I
Isolation of primary human type II pneumocytes

3.2.2.1 DNAse-free isolation method utilising trypsin

The protocol assumes a working mass of 10g fresh lung tissue. The pleura, any large airways, sutures or surgical staples were removed by sharp dissection. This material was weighed to allow assessment of residual lung parenchyma. The residual lung parenchyma was chopped into 2-3 cm^3 pieces and placed inside a 250 ml sterilin jar along with 100 ml of calcium and magnesium ion free PBS (PBS -) (Appendix I). The sample was then washed three times in (PBS –).

Subsequently, the tissue was subjected to enzymatic digestion with 0.25% trypsin solution in an orbital shaking water bath at 37°C for 50 minutes. Following the digestion the tissue was discarded and the enzymatic activity within the supernatant terminated by the incubation of

the supernatant in FCS for 4 min at room temperature. Four millilitres of FCS per original gram of sample was used to quench the enzymatic activity. The cell suspension was then passed through in sequence, a sterile nylon cell strainer of 100 □m pore size and a sterile nylon mesh cell strainer of 40 □m pore size. The recovered filtrate was centrifuged at 250 g for 20 minutes at 10 °C and the supernatant discarded. The cell pellet was then resuspended in 20 ml of serum-free medium before seeding on sterile 75 mm sterilin non-tissue culture grade plastic petri dishes and incubated at 37°C, 5 % CO_2 for 2 hours to allow differential adherence of macrophages and fibroblasts.

Following differential adhesion the medium containing the non – adherent cells was removed from the petri dish and cell suspension was loaded onto a discontinuous Percoll gradient for further purification. The gradients, with cell suspension, were centrifuged at 250 g for 20 minutes at 10 °C. Subsequent to centrifugation the potential type II cells were visible as a white condensed band at the interface of the Percoll gradients (Fig 3.1). This band was recovered by pipetting and washed in (PBS -) before resuspension in maintenance media. In circumstances where significant quantities of particulate matter remained in the suspension, following recovery the band was centrifuged at 250 g for 10 minutes at 10 °C, before washing and resuspension in maintenance media. Cell viability was assessed by trypan blue exclusion assay (Section 2.1.1), cells seeded onto ECM coated substrata (Section 2.1) and incubated overnight at 37°C, 5% CO_2.

3.2.2.2 Isolation utilising trypsin and DNAse

The following protocol is adapted from the isolation method published by Murphy and co-workers in 1999 for the liberation of human primary type II pneumocytes. The major adaptations were modifications in tissue dissection, washing, solution composition, pore size of cell strainers and suppliers of enzymes.

A working sample mass of 10g of macroscopically normal human lung tissue was assumed for the protocol. The sample was trimmed and dissected as described in the previous method and washed three times in 100 ml of Solution A. Subsequently, the tissue was sealed in a 250 ml sterilin jar containing 100 ml of the 0.25 % w/v trypsin in solution B, and the jar incubated in an orbital shaking water bath set at 60 rpm, 37°C for 10 minutes. The enzyme solution was passed through a sterile metal sieve into two new sterilin jars each containing 25 ml (FCS): 12.5 ml DNAse A solution and the tissue retained for further digestion. The

tissue was digested two more times with 100 ml of fresh trypsin solution for a further 20 minutes and on each occasion the filtrate was pooled into FCS: DNAse A solution. Following digestion of the tissue the crude cell suspension sealed in two sterilin jars was shaken vigorously by hand for 4 minutes. The cell suspension was then passed first through a sterile nylon cell strainer of 100 μm pore size into a fresh sterile jar and then through sterile nylon mesh of 25 μm pore size.

Following centrifugation of the cell suspension at 250 g at 10 °C for 20 minutes the supernatant was discarded and the cell pellets pooled in 20 ml of serum-free differential attachment medium containing 2.5 mg of DNAse 1. The cell suspension was seeded on sterile 75 mm sterilin non-tissue culture grade plastic petri dishes at volumes of 3-5 ml of suspension per dish, and incubated at 37° C, 5 % CO_2 for one hour. The cell suspensions were further purified by the use of discontinuous Percoll® density gradients as described previously. The gradients, with cell suspension, were centrifuged at 250 g for 20 minutes at 10 °C. Subsequent to centrifugation the potential type II, cells were visible as a white condensed band at the interface of the Percoll gradients (Fig 3.1). This band was recovered by pipetting and washed in solution B before resuspension in maintenance media. In circumstances where significant quantities of particulate matter remain in the suspension; following recovery, the band was centrifuged at 250 g for 10 minutes at 10 °C, before washing and resuspension in maintenance media. Cell viability was assessed by trypan blue exclusion assay (Section 2.1.1), cells seeded onto ECM coated substrata (Section 2.1) and incubated overnight at 37°C, 5% CO_2.

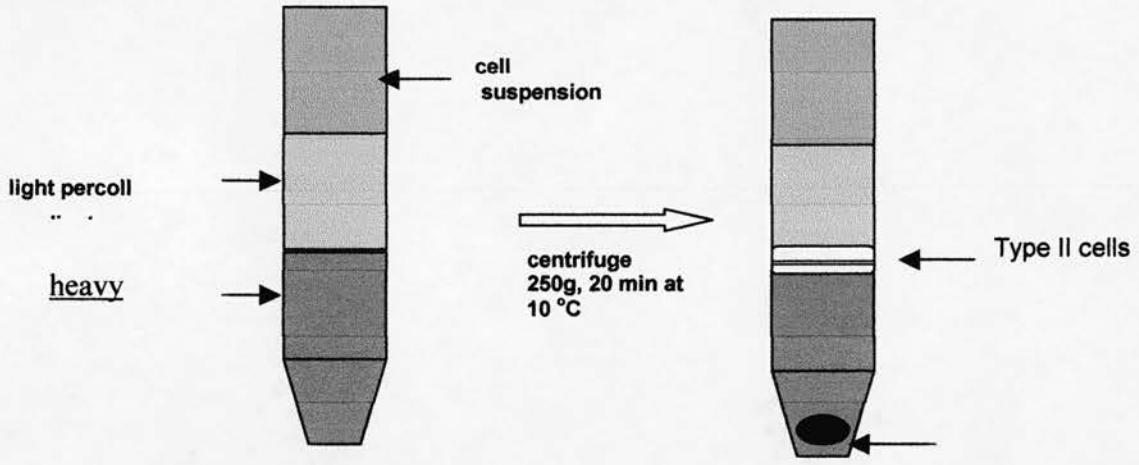

Figure 3.1. Discontinuous Percoll gradient centrifugation. To purify a cell suspension; a light density percoll solution is layered onto a heavier density percoll solution and the cells centrifuged against it. Particles of low density pass through the solutions and the cells of interest condense at a position in the tube where the density is similar to their own.

3.2.3 Results

Twenty-six lung samples were obtained from 21 donors. Two specimens from one donor were recalled by the pathologist and were not further processed. Five samples from four donors were less than 10 g in mass and therefore unsuitable for further use. These samples were snap frozen in liquid nitrogen for later RNA extraction.
Nineteen samples from sixteen donors were available for type II pneumocyte isolation. Four samples from four donors were used for DNase isolation. Fourteen samples from 10 donors were used for DNase- free isolations.
In the isolations including DNase the average mass of lung, tissue used was 14.27 g ± 4.48 g. The average mass of tissue used in the DNase-free isolations was 18.49 g ± 15.93 g

There was a significant difference in the mass of tissue used for the different procedures. A two sample t-test assuming unequal variances yielded a t-value = 0.90, p-value = 0.381. Therefore, the null hypothesis that the two population means are equal did not hold true and significantly, more lung tissue was used in the predominantly unsuccessful DNase-free isolation technique.
In some instances, tissue was weighed following removal of pleura, airways and unnatural material. This resulted in a mean loss of 3.83 ± 2.56 g of the original samples, which is approximately 25.73 ± 9.96.% of the tissue.

3.2.3.1 DNase –free isolation procedure

In 14 of the DNase-free isolation procedures, no cells, very few cells, and cells of an unhealthy appearance displaying membrane blebbing, were obtained.
One isolation yielded 9 x 10^4 cells, equivalent to 1.35 x 10^3 cells/g of tissue. These cells were cultured for 24 hours and stained for alkaline phosphatase activity a type II pneumocyte characteristic (Figure 3.2.).

3.2.3.2 DNase containing isolation procedure

Using the DNAase containing method all four isolations attempted yielded cells. The maximum yield per gram of tissue was 2.92 x10 ^{6}cells. The mean total number of cells liberated during the human type II pneumocyte isolations was 1.37 x 10^{7} ±9.57 x 10^{6} cells and the mean number of cells per gram of tissue was 1.38 ± 1.07x 10^{6} cells. The mean viability of cells immediately after isolation was 93 ± 1.63 % as assessed by trypan blue exclusion assay.

Figure 3.2. Flowchart of sample use throughout duration of project

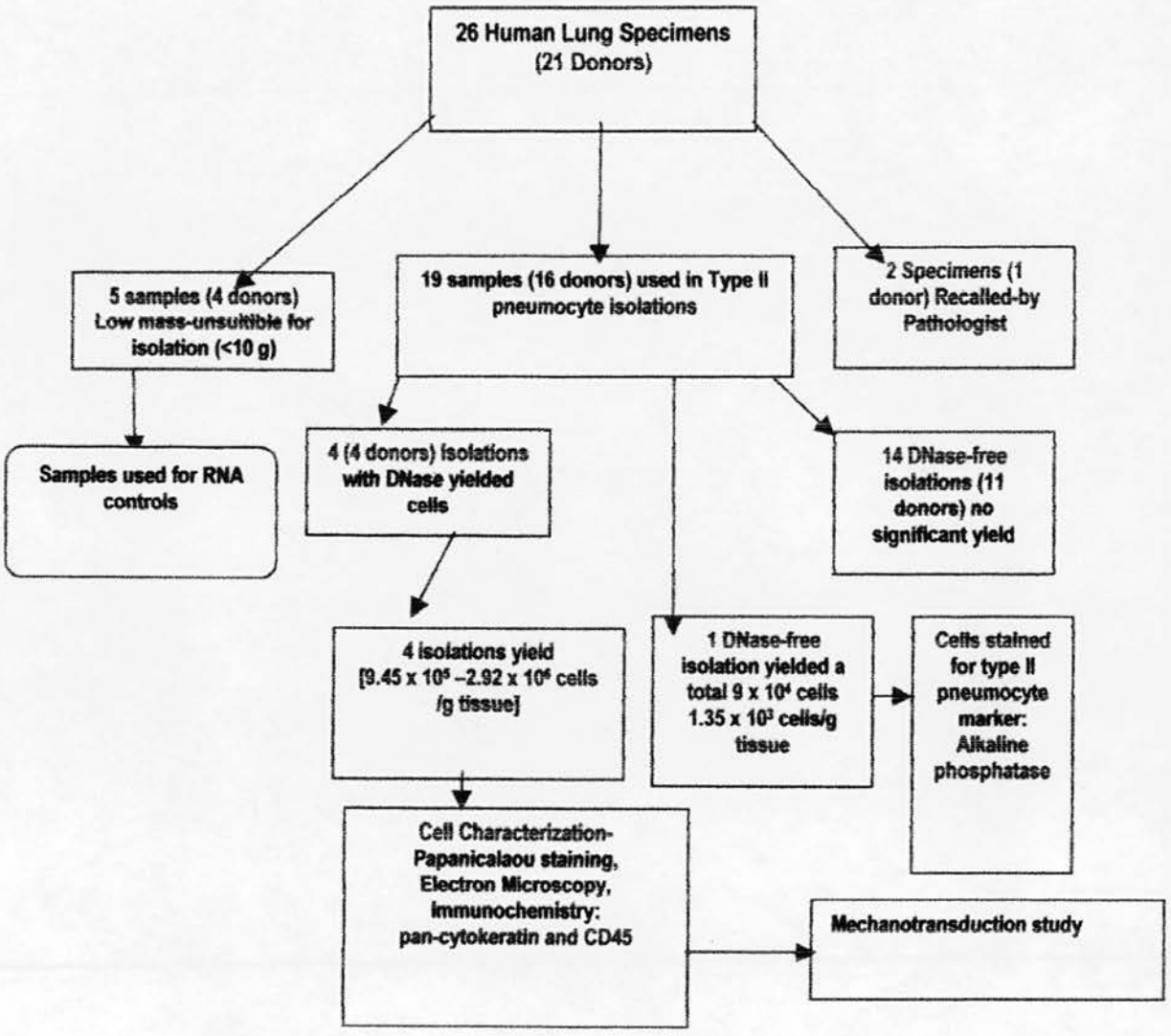

Table 3.2 Human Lung sample data

Sample Number	Pre-dissection Mass (grams)	Post-dissection Mass (grams)	Enzyme solution: Mass tissue ml:g	Total Enzymatic Digestion Duration (min)	Immediate Appearance of Isolated Cells	Observations, notes
1	9.00	/	10x	90	/	Debris collected
2	9.17	/	10x	95	/	Possible over digestion of cells and or inaccurate solution concentrations
3	9.58	/	10x	95	/	Possible over digestion of cells and or inaccurate solution concentrations
4	7.98	/	10x	90	/	Cell Suspension knocked over at final stage
5A	8.20	/	10x	90	/	over digestion suspected
5B	10.90	/	10x	120	Few cells, major membrane blebbing	over digestion suspected
6	13.29	/	10x	30	Few cells, membrane blebbing	Still unclear if duration of digest or solution concentrations inaccurate
7A+B	30.57	/	10x	50/75	Few cells, membrane	Still unclear if duration of digest or solution

					membrane blebbing	digest or solution concentrations inaccurate
8	14.50	/	10x	50	Few spherical granular cells	Fresh solutions used, Cells did not spread after 24 hours culture
9A	**65.00**	**12.19**	**10x**	**30**	**Few spherical granular cells**	**Pleura brittle, difficult to remove staple, sample black, cells spread on CI, CIV, FN proteins**
9B	/	**14.71**	**10x**	**20**	**Few spherical granular cells**	**Pleura brittle, difficult to remove staple, sample black, cells spread on CI, CIV, FN proteins**
10	32.83	/	10x	50	/	percoll gradients disrupted
11	/	37.70	10x	50	/	percoll gradients disrupted
12	/	**66.73**	**10x**	**50**	**Few spherical granular cells-$9x10^4$ cells**	**Percoll solutions made fresh on day and kept 4 °C until needed**
13950	<9.0	N/A	N/A	N/A	N/A	/
13963	<8.0	N/A	N/A	N/A	N/A	/
13971	<8.0	N/A	N/A	N/A	N/A	/

13972	**12.31**	**9.51**	**20x**	**50**	**Spherical, granular**	**Total yield=5.56x10^6 cells yield=2.92x10^5 cells/g tissue Suspension used EM**
13978	**20.60**	**13.00**	**20x**	**50**	**Spherical, granular**	**Total yield=8.78x10^6 yield=6.75x10^5 cells/g tissue**
13979	9.50	N/A	N/A	N/A	N/A	/
13988	**10.23**	**7.19**	**20x**	**50**	**Spherical, granular**	**Total yield=6.45x10^6 cells yield=8.97x10^5 cells/g tissue**
13992	**13.95**	**12.06**	**20x**	**50**	**Spherical, granular**	**Total yield=1.14x10^7 cells yield=9.45x10^5 cells/g tissue**
13994	<8.0	N/A	N/A	N/A	N/A	/

Table 3.3. Human type II pneumocyte DNase –trypsin isolation data

Sample Number	**Sex**	**Age years**	**Mass g**	**Post-dissection mass g**	**Total yield**	**Yield /g tissue**	**Viability Trypan blue exclusion assay %**
13972	F	69	12.31	9.51	2.78×10^7	2.92×10^6	91
13978	M	78	20.60	13.00	8.78×10^6	6.75×10^5	95
13988	F	81	10.23	7.19	6.9×10^6	9.59×10^5	93
13992	F	77	13.95	12.06	1.14×10^7	9.45×10^5	93

3.2.4 Discussion

Using two different isolation techniques, good quality cell retrieval, as assessed by cell number and viability, was obtained more often using the DNase containing procedure. There are many possible reasons for this.

Significantly less tissue was used in the DNase containing, than the DNase-free isolation procedure. The average quantity of tissue used in the DNase-free procedure was 18.49 g ± 15.93 g SD compared to 14.27 g ± 4.48 g in the DNase containing procedure, 2-sample t - value = 0.90, p – value = 0.381. Despite the difference in the mass of tissue used, the DNase containing isolation procedure was the more successful of the techniques at liberating viable type II pneumocytes. The major difference in the techniques was the presence of DNAse in the FCS, differential attachment media and PBS (solution B), used to remove Percoll® from the cell suspension. DNase lyses DNA from ruptured cells and therefore its inclusion could have prevented the cells suspensions of the DNase containing procedures from clumping together. Hence, the DNase containing procedure was the more successful technique due to a more efficient liberation process.
Considering so few cells were obtained with the DNAse-free isolation method, it is impossible to comment on how the exclusion of the enzyme affects the function of isolated type II pneumocytes. Had these isolations yielded cells it may have been possible to compare whether or not the enzyme impairs the quality of isolates.

The final cell yields obtained did not equate to published data. The published method from which the protocol was adapted stated that there is a substantial decrease in the yield per gram of tissue if less than 8 g of tissue is used (146). All the samples used in this method were above the minimum required mass. Therefore it is unlikely that the lower than published yields were due to a lack of tissue. Previously published work that utilised similar methods of isolation of human type II pneumocytes report yields of 2.3 ± 1.1 x 10^6 cells per gram of tissue (146; 157). The average yield per gram of tissue using the DNase containing technique was 1.38 ± 1.07 x 10^6 cells, approximately 60 % of the published yields. This reduction in yield could have been related to the initial tissue sample quality. Localised areas of disease may have influenced the yields. Rat type II pneumocytes are commonly isolated from special pathogen-free animals under a certain age. This is to keep the sample uniformly healthy, and it has been of note (145) that, as the animals age the numbers of type II pneumocytes decrease. Another possible factor wa that variable amounts of tissue were

lost during the initial dissection. There was a mean loss of 3.83 ± 2.56 g of the original samples, which is approximately 25.73 ± 9.96.% of the tissue. The quality of the tissue again potentially affects this percentage loss, as each sample had a different macroscopic morphology. Mechanical dissection of the tissue, with a McIlain tissue slicer as used by Murphy and co-workers, could potentially improve the enzymatic liberation of cells by increasing the surface area of tissue to the trypsin solution. However, the use of mechanical dissection could potentially increase damage to the liberated cells. A further possibility is that during filtration of the crude cell suspension a 25 μm pore size nylon mesh was used instead of the published 30 μm pore size mesh (146). This could explain the lower yields; however the use of this size of mesh did result in very few cell clumps, which is a requirement of the mechanotransduction membrane potential study (Chapter 4).

In conclusion, cells were isolated from primary human lung tissue. A high success rate was achieved using an adaptation of a method published by Murphy et al. 1999, utilising crystalline trypsin and DNAse 1. Four out four isolations yielded cells with a mean number of 1.38 ± 1.07 x 10^6 SD cells per gram of tissue. The cells liberated had a mean viability of 93 ± 1.63 % SD by trypan blue exclusion assay.

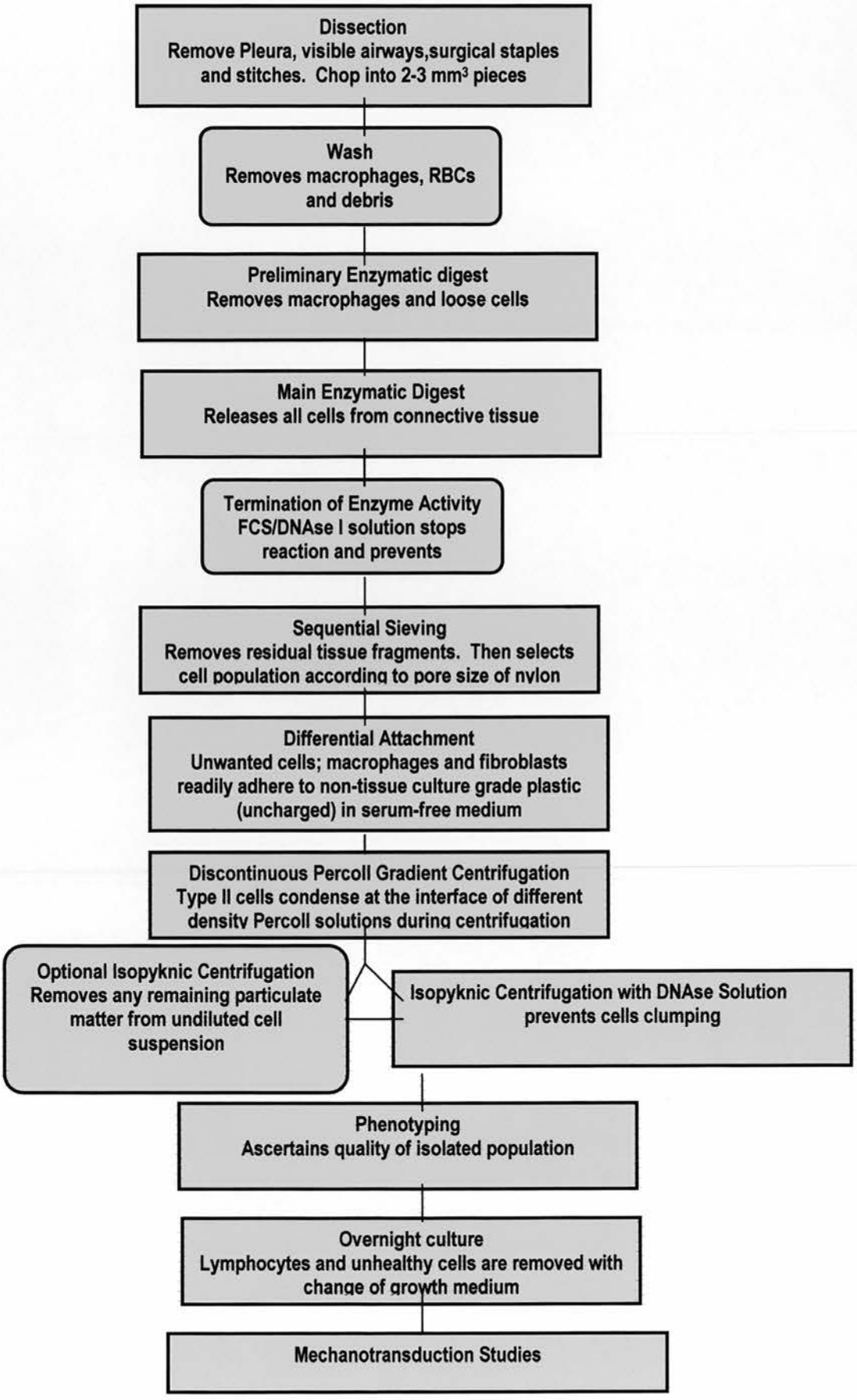

Figure 3.3. Flowchart of human type II pneumocyte isolation method.

3.3 Type II pneumocyte characterisation

Traditionally, to assay type II cell enriched cultures, you must examine the morphological, biochemical and surface marker characteristics (13; 145). The lack of an antigen specific to the human type II pneumocyte has meant that in previous studies a variety of techniques have been utilised in characterising the differentiation status and purity of preparations. Type II pneumocytes have a distinctive morphology in situ which,depending on culture conditions in vitro is retained for a finite period. In vivo they are mononuclear, with blunt surface microvilli, and contain phospholipid – rich lamellar inclusion bodies. This is in sharp contrast to the neighbouring type I pneumocytes, which cover the majority - up to 97 % - of the alveolar surface area. The type I pneumocytes in vivo are extremely thin squamous cells, with no lamellar inclusion bodies or surface microvilli (15).

The fundamental technique to date for characterising human type II pneumocyte preparations is the assessment of cellular morphology by electron microscopy (13; 158). Commonly lamellar bodies are used to identify type II pneumocytes. In general, with respect to the type II pneumocyte, the term lamellar body refers to the phosholipid rich organelles that contain surfactant. In eukaryotic cell biology, other organelles referred to as lamellar include mitochondria and chloroplasts. The phospholipid rich, stacked membranes of these bodies stain intensely with osmium tetroxide in electron microscopy. Type II pneumocyte lamellar bodies have been detected by fluorescent microscopy using acridine orange (159)and phosphrine R stains (160). A lipophilic fluorescent vital stain, Nile red, also identifies human type II pneumocyte lamellar bodies (161; 162). Unfortunately these dyes fade, and the toxic effects of their addition should be considered if the preparations are to be examined further (145) (160). For example the addition of Phosphrine 3R to populations of type II pneumocytes has been noted to decrease oxygen consumption and alter the ultrastructure of mitochondria (160). Other lamellar body staining techniques include the modified papanicalaou (9; 145) and tannic acid fixation with polychrome stain (163). Recently another morphological aspect of type II pneumocytes has been used to assess differentiation status. Caveolae - omega or flask shaped vesicles - and the associated protein caveolin; which are found in abundance within type I pneumocytes and not in type II pneumocytes

(164) et al. 1999, (165), have now been used for the assessment of human type II pneumocyte populations in vitro (157).

The composition of surfactant is not unique to the lung, but the proportions of components are. Phopholipids are found at relatively high quantities within the pulmonary surfactant of type II pneumocytes. The most abundant of these phospholipids are phosphatidylglycerol (PG) and saturated phosphatidylcholine (PC). Previously the abundance of these particular phospholipids has been utilised as a marker for rat type II pneumocyte differentiation (166; 167). The proportion of protein constituents in surfactant is relatively small compared to the phospholipid portion (49). Surfactant proteins, SP-A, SP-B and SP-C have been located in type II pneumocytes. SP-A has also been identified in the gastrointestinal tract, kidney and synovium. SP-A and SP-B are known to be produced within Clara cells of the bronchiolar epithelium (168; 169). Out of the four known surfactant proteins, only SP-C is thought to be type II pneumocyte specific (170) (171; 172) (173). However, macrophages phagocytose surfactant (174; 175), (168), so the production of SP-C but not its presence is specific to lung cells. The production of surfactant also decreases during transdifferentiation in vivo (11; 141) and in vitro (176-178) which reduces its value as a marker (145; 158). The detection of particular enzyme activities known to be prevalent in type II pneumocytes has been used in characterising the differentiation status and quality of cell populations. Alkaline phosphatase and α-glucosidase are two enzymes that have previously been utilised (145).

The majority of investigations of type II pneumocyte surface and antigenic markers have focused on rat cell isolates. To date the only antibody reported to identify human type II pneumocytes is the Ca1, monoclonal antibody (179). The Ca1 antibody only recognises the type II cells and Clara cells despite being raised against a glycoprotein commonly found in malignant cells. Several antibodies have been raised against rat type II pneumocytes. However, these antibodies do not necessarily react against human type II pneumocytes. The mmc_4 (180) or the $RTII_{70}$ (176) antibodies, which identify apical surface antigens of rat type II pneumocytes and Clara cells, do not react towards human cells (personal communication. M. M^{c}Elroy). The human equivalent antibody against an integral apical membrane protein RTI_{42} of the rat type I pneumocyte has been produced and is known as HTI_{56} (181)

The binding patterns of lectins have also been used to investigate cultures of type II pneumocytes (182-184)). The Maclura pomifera (MPA) lectin has been shown to bind to the apical surfaces of rat type II pneumocytes and not the type I pneumocytes (182), whereas the Ricinius communis I (RCA) lectin differentially binds to type I pneumocytes (182). There have been contradictory results regarding type II pneumocytes and lectin binding patterns: RCA has been reported to bind both type I and type II pneumocytes in vivo (185); Buahinia purpurea agglutin (BPA) reportedly binds only to type I pneumocytes in rat lung tissue (183) and in freshly isolated cells (184). However, type I and II pneumocytes in human lung tissue (186) and alveolar macrophages have been described as demonstrating binding to the BPA lectin (185).

Another commonly exploited characteristic of the type II pneumocyte in differentiation studies is the presence of cytokeratins. Cytokeratins are intermediate filament proteins expressed and produced in all epithelial cells (187). Human type I and II pneumocytes in vivo are reported to express the simple epithelium type cytokeratins 7, 8, 18, 19 (188; 189) and possibly the squamous type cytokeratin 4 (189).

3.3.1 Alkaline phosphatase staining

Alkaline phosphatase (AP) staining is a differential method of detecting type II pneumocytes. Adult mammalian type II cells and Clara cells demonstrate a positive AP staining pattern, whereas adult pulmonary macrophages and fibroblasts do not stain for AP. The exact function of this enzyme is unknown, however current supposition is that AP activity plays a role in the differentiated phenotype of the type II pneumocyte (190). Following isolation of primary type II pneumocytes with the DNase-free technique the following method was used to determine the presence of type II pneumocytes. This method was again used to assess the phenotype of the model cell line NCI-H441 (Chapter 4).

The following protocol stains primary human type II pneumocyte and NCI-H441 cell line cultures for AP activity (190).
The final primary type II pneumocyte pellets were resuspended in 2ml of DMEM: F12 media supplemented with L-glutamine (Invitrogen) and penicillin: streptomycin (Invitrogen) and cultured overnight on ECM coated 96 well plates. The NCI-H441 cells were seeded under the same conditions as the primary cultures at 5 x 10^4 cells per ml on ECM coated 58

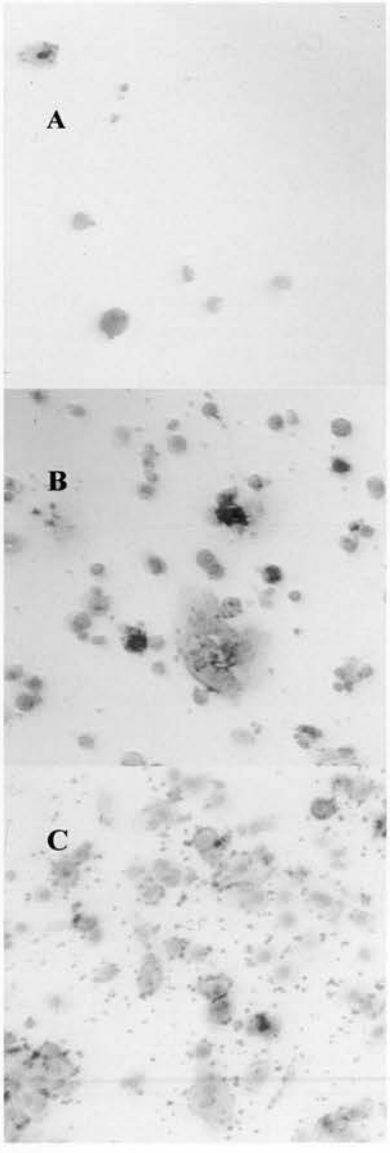

Figure3.2. Alkaline phosphatase stained human type II pneumocyte DNase-free isolations cultured for 24 hours on ECM protein. Typical fields of view representative of cell preparations cultured for 24 hours on A: Bovine serum albumin (BSA), B: Fibronectin (FN), and C: Collagen IV (CIV) coated substratum, stained for alkaline phosphatase activity and counterstained with neutral red. Cell preparations on BSA were typically spherical and stained an intense blue-purple colour. The cells of the FN populations, displayed either spherical or spindle morphologies, again staining with a dark positive blue-purple colour. The cells cultured on CIV were of an eliptical morphology, with a diffuse blue-purple staining apparent within the cytoplasm of cells. A large quantity of debris or particulate was also apparent within the CIV preparation. Original magnification x200.

mm petri dishes. Following the removal of the culture media, the cells were washed twice with PBS. Nitro blue tetrazolium chloride 15-bromo-4-chloro-3-indolyl phosphate, toluidine salt (NBT/BCIP) stock solution (Boerhinger Mannheim) was diluted 1:50 in AP substrate buffer (Appendix I) and 100 µl of working solution added to each well. After covering the plate with aluminium foil, it was subject to incubation at room temperature for 2 hours (120 minutes). Following the incubation period, the plate was washed twice with PBS and the colour allowed to develop in a class I laminar hood for 2-3 minutes. The cells were fixed with 100 µl of 4% formalin per well for 30 seconds. Subsequent to fixation, the cells were rinsed twice with PBS. A 1% solution of Neutral red in PBS was used to counterstain the cells as follows: 100 µl of the counterstain was added to each well and the plate incubated for 1 minute. The Neutral red solution was removed by rinsing the plate in tap water, and the cells were covered with an aqueous mountant (Dako Faramount®). This aqueous mountant forms a hard seal and does not require the use of a cover slip. The cells were visualised using an Olympus CX2 microscope.

3.3.1.1 Results

Positive alkaline phosphatase (AP) staining was demonstrated in the three cultures of the DNase-free pneumocyte isolate. This is indicative of the presence of type II pneumocytes in the initial isolated population. Primary human DNase-free isolated cells were seeded in equal quantities onto a control; bovine serum albumin (BSA), fibronectin (FN) and collagen IV (CIV) coated substrata, cultured at 37°C, 5 % CO_2 for 24 hours, and stained for alkaline phosphatase activity. Fibronectin and collagen IV are two of the major protein constituents of the human pulmonary basal lamina. Following 24 hours, few cells adhered to the BSA substratum. Cells cultured on CIV appeared more squamous than the cells within the other cultures. The cells cultured on BSA and FN appear rounded and stained strongly for AP. The intensity of AP stain was weaker within the cells cultured on CIV (Figure 3.).

3.3.2 Modified haematoxylin staining

Papanicalaou staining is a polychromatic technique routinely used in the examination of cytological smears. This stain has been of use in the examination of primary type II pneumocyte enriched cultures since 1974 (9) (145; 146). Leland Dobbs proposed a "Modified Papanicalaou" stain in 1990, specifically for examining cytospins of type II cells,

which is in fact a modified haematoxylin stain. This technique is by reputation the easiest and one of the most reliable methods of assessing the quality and differentiation status of type II isolations. In essence, the haematoxylin stains the inclusion bodies of type II pneumocytes, which are visible as deep blue granules surrounded by clear halos.

Cytospins of three DNase - containing human type II pneumocyte isolates were assessed with the modified haematoxylin stain and denoted according to their original sample numbers; 13978, 13988 and 13992.

This study based the following method on that used by Leland Dobbs (145). The cell suspensions of 2 x 10^5 cells/ ml were spun in a cytocentrifuge (Shandon) for 5 minutes at 10 g onto Superfrost® slides. The slides were left to air dry inside a class I laminar flow hood for 15 hours. The next day the slides were subjected to an incubation of 3 to 4 minutes in Harris' haematoxylin solution, followed by immersion in three different changes of distilled water (dH_2O), to remove the excess haematoxylin. Subsequently, colouration of cytospun cells was enhanced, by incubating the slides in STWS for 2 minutes. After rinsing with tap water, the slides were immersed in a solution of 50% IMS for 90 seconds. Subsequently, the slides were passed sequentially through IMS solutions of concentrations 80% and 95% for 15 seconds each, and a final, incubation in 100% (absolute) IMS for 30 seconds. Processing of the specimens was then completed by immersion of the slides in an IMS:xylene (1:1) solution for 30 seconds, followed by incubation in xylene for 1 minute and coverslipping the slides with Pertex™ mountant. Once dried, the slides can undergo inspection for the presence of type II-like cells. To inspect the cells the slides were viewed under oil immersion at 630-1000 times magnification, using light microscopy. A minimum of 200 cells were counted taking note of the nuclear morphology and number of inclusion bodies in each cell. Type II pneumocytes are known to be mononuclear, whereas leukocytes possess poly morphological nuclei (PMN). Previous studies imposed a minimum number of four inclusion bodies as a criterion in the identification of type II cells (Richards 1987, }(146). Within this study, the same criteria were adhered to and the data analysed with the aid of MINITAB™ statistical software. MINITAB™ allows the user to easily subset the data according to criteria. Within this project, cells were in either of two categories; mono (1) or PMN (2), which included bilobular cells, and the quantity of lamellar bodies for each noted in MINITAB™.

3.3.2.1 Results

Primary human type II pneumocyte enriched suspensions stained with a modified haematoxylin method clearly display cells with characteristics of the type II pneumocyte and a small proportion with the nuclear morphology of leukocytes (Figure 3.5). Deep blue granules reputed to be lamellar bodies were apparent throughout the cytoplasm of the mononuclear cells, suggesting they were type II pneumocytes. At the periphery of the cells, some lamellar bodies appear to have been released during the preparation of the cytospin.

The criterion for a type II pneumocyte in this method is that it be mononuclear with a minimum of four lamellar bodies. The mean percentage of the three isolations constituted by mononuclear cells was 91.96 ± 4.90 % and PMN 8.04 ± 4.90 %. The mean percentage of the three isolations that were mononuclear with four or more lamellar bodies, and therefore potentially type II pneumocytes, was 49.70 ± 22.47 %.
Population 13978 had an overall percentage of 94.03% mononuclear cells, with the proportion of this preparation potentially being type II pneumocytes 51.24%. The median number of lamellar bodies (LB) in the type II pneumocytes was six, with the first quartile of LB being five and the third quartile 10. The overall percentage of preparation 13988 constituted by mononuclear cells was 95.50 %. The potential type II pneumocytes within 13988 was 26.50%, with a median number of LB of 6 and between the first and third quartiles 5-10. Sample 13992 yielded 86.36% mononuclear cells, with 71.36% of the total preparation potential type II pneumocytes. The median number of LB was 17 and between the first and third quartiles 12-23.

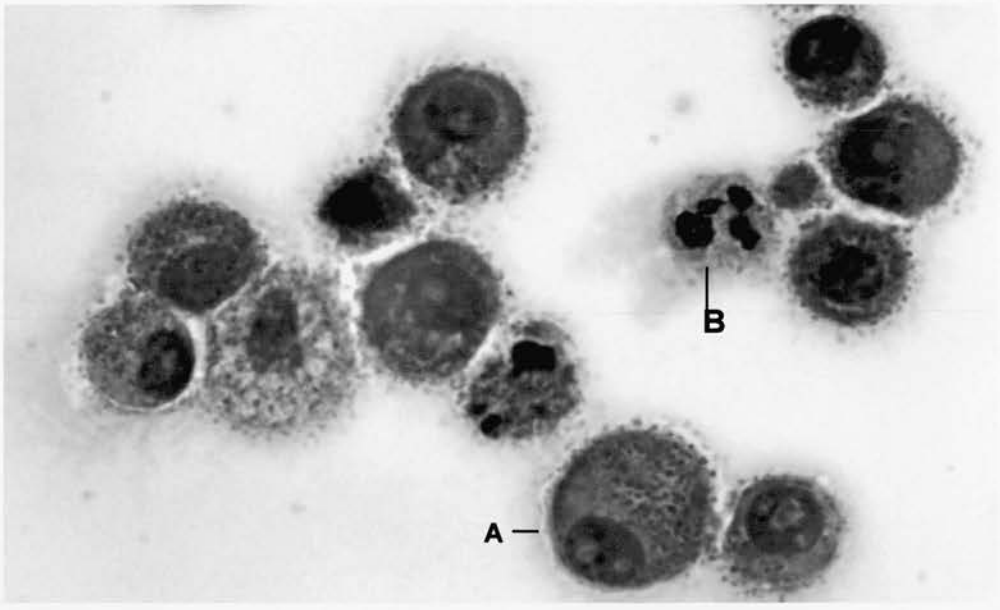

Figure 3.5. Example of a primary human type II pneumocyte enriched cytospin stained by the modified haematoxylin method. **A/** Mononuclear cell containing dark blue stained lamellar bodies. **B/** Polymorphological nuclear cell. Original magnification x1000 oil immersion.

Table 3.4 Modified Haematoxylin Stained Cell Count Data.

Sample	13978	13988	13992
Total cell count	201	200	220
Total PMN cell count	12	9	30
Overall percentage PMN	5.97	4.50	13.64
Total mononuclear cell count	189	191	190
Overall percentage % mononuclear	94.03	95.50	86.36
Total mononuclear cell LB ≥4	103	53	157
Percentage % total count mononuclear LB ≥4	51.24	26.50	71.36
Percentage % mononuclear cells with LB ≥ 4	99.04	98.15	94.01
Mean LB mononuclear LB ≥4	8.46	6.85	17.91
St Dev	10.53	2.90	9.66
Median LB	6	6	17
Quartile 1	5	5	12
Quartile 3	10	9	23

LB, Lamellar body, LB≥4, number of lamellar bodies greater than or equal to 4

3.3.3 Cytokeratin and common leukocyte antigen (CD45) immunocytochemistry

Erythrocytes, fibroblasts, alveolar macrophages, leukocytes, bronchiolar pneumocytes, type I pneumocytes, endothelial cells and smooth muscle cells could all contaminate a type II pneumocyte enriched culture in various ratios.

Simple identification of type II cells is precluded by our current lack of insight into their biology. Strikingly, at present there is no known specific marker for the human type II pneumocyte. Various groups have developed antibodies against rat type II pneumocytes, but these do not necessarily react against human type II pneumocytes. Unfortunately, mmc_4 (M^cElroy); a monoclonal antibody raised against rat type II cells, which has been of much interest within the pulmonary research community does not react against human type II pneumocytes. Immunocytochemical analysis of human type II enriched preparations is still possible, but requires the investigation of more than one characteristic.

Immunohistochemstry is of use in the routine examination of cytokeratin expression profiles in epithelial tissue. Cytokeratins are complex intermediate filaments of eukaryotic cells. Two subtypes of the filament exist; the acidic type I and basic type II. A unique feature of cytokeratin gene expression is that one member of the individual subtype is always coexpressed with a member of the opposite subtype within an epithelial tissue. It is not possible to differentiate between alveolar and bronchiolar epithelium using cytokeratin immunhistochemistry (191) Kasper and Singh 1994). However, this technique can, in theory, detect the presence or absence of cytokeratin expression characteristic of pulmonary epithelium within isolated type II pneumocytes. All cells of haematopoietic origin express the Leukocyte common antigen (CD45) (Thomas 1989). Some of the major contaminants of the pneumocyte type II isolations are of haematopoietic origin.

Cytospins of the DNAse type II pneumocyte isolations 13978, 13988 and 13992 were immunostained with the pan-cytokeratin antibody clone MNF116 and a common leukocyte antigen, CD45 antibody clone preparation (2B11 + PD7/26). The MNF116 clone is specific for the cytokeratins 5, 6, 8, 17 and 19. There are five known isoforms of CD45 and the clones' 2B11 + PD7/26 are thought to react against all of them. Immunostaining methods are detailed in Section 2.3.

Immunostained cytospins of type II pneumocytes were examined under high power light microscopy. Positive and negative cell counts were taken from three representative fields of view and a mean percentage calculated.

3.3.3.1 Pan-cytokeratin and CD45 immunocytochemistry results

Probing cytospin 13978 with the pan-cytokeratin antibody MNF116, demonstrated a mean of 52.16 ± 9.25 % positive staining; sample 13988 a mean of 64.77±10.15% positive staining; and 13992 a mean of 44.00±1.66%, positive staining. The immunostaining pattern for pan-cytokeratin was variable in both the cytospins and paraffin sections of lung parenchyma. In the instance of CD45, probing 13978 revealed a 13.91±4.03% positive staining; the cytospins 13988 and 13992, demonstrated 21.56±1.01% and 4.50±5.60% positive staining for contaminating immune cells respectively. The immunostaining pattern of common leukocyte antigen was diffuse within the cytoplasm of positive cells and more intense toward the cell surface. Variability in staining was apparent within the common leukocyte antigen positive cells (Figure 3.6.).

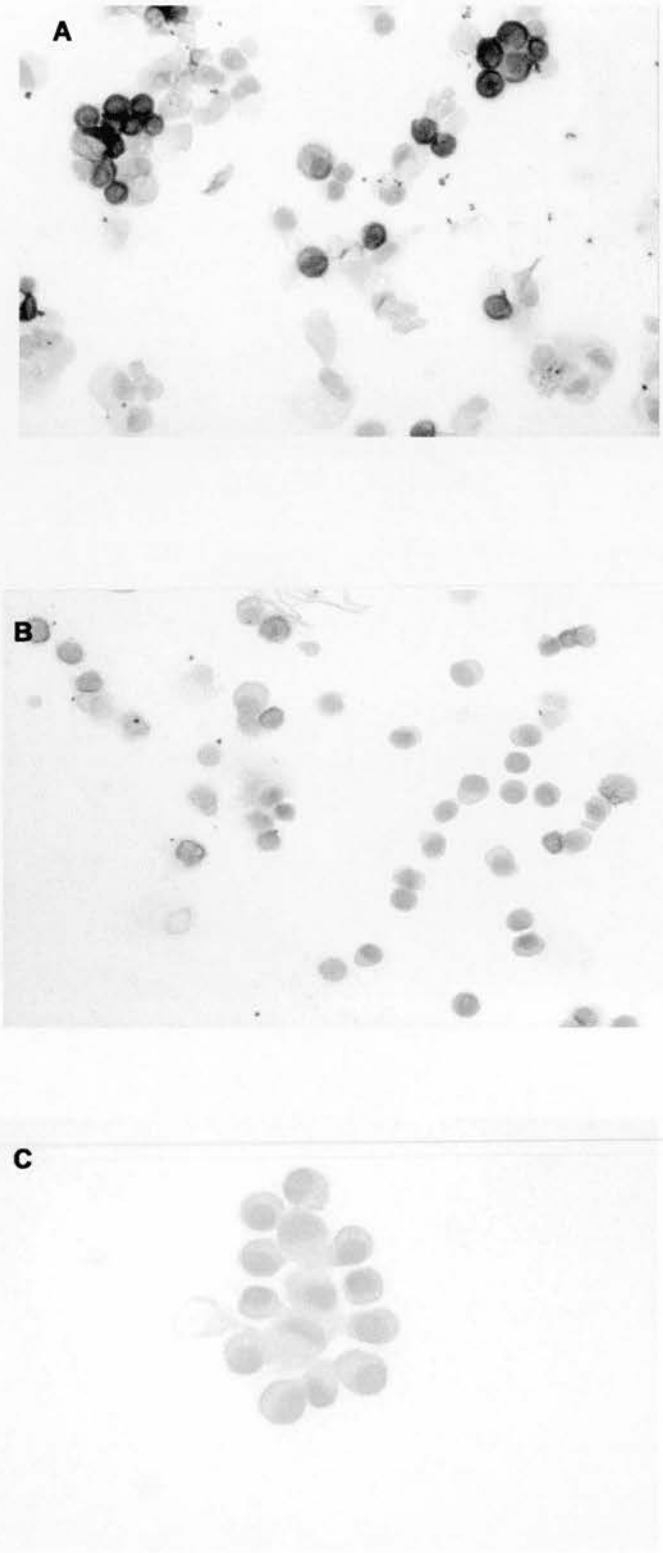

Figure 3.6. Cytospin preparation and immunochemistry of freshly isolated human type II pneumocytes. Typical fields representative of immunostaining with the **A.** MNF116 pan-cytokeratin, **B.** 2B/ll+PD7/26 CD45 and **C.** mouse IgG_k negative control antibodies in human type II pneumocytes. Original magnification x400.

Table 3.5 **Cytokeratin and CD45 expression by primary human type II pneumocytes**

Antigen	Sample	% positive cells /field			Mean	SD	Total Cell Count
Pan-cytokeratin (MNF116)							
	13978	42.62	62.84	51.01	52.16	9.25	419
	13988	66.67	63.64	64.00	64.77	10.16	200
	13992	46.46	51.76	33.77	44.00	1.66	289
CD45 (Dako2B11+PD7/26)	**Sample**	**% positive cells /field**			**Mean**	**SD**	**Total Cell Count**
	13978	14.67	14.29	12.77	13.91	4.03	185
	13988	16.90	27.78	20.00	21.56	1.01	185
	13992	0.00	7.77	5.73	4.50	5.60	418

Sample	Potential Type II pneumocyte characteristics	Proportion of isolation mean ± SD (%)	Immune Cell Characteristics	Proportion of isolation mean ± (%)	Accounted Population (%)
13978	**MNF116**	**52.16 ± 9.25**	**2B11 + PD7/26 (CD45)**	**13.91 ± 4.03**	**66.07**
	Mono	51.24 ± 22.47	PMN	5.97 ± 4.91	57.21
13988	**MNF116**	**64.77 ± 10.16**	**2B11 + PD7/26 (CD45)**	**21.56 ± 1.01**	**86.33**
	Mono	26.50 ± 22.47	PMN	4.50 ± 4.91	31.00
13992	**MNF116**	**44.00 ± 1.66**	**2B11 + PD7/26 (CD45)**	**4.50 ± 5.60**	**48.50**
	Mono	71.36 ± 22.47	PMN	13.64 ± 4.91	85.00

Table 3.6. Summary table Immunocytochemistry and Modified Haematoxyilin Stain data. Characterisation of the three primary human type II pneumocyte enriched isolation samples 13978, 13988 and 13992 were examined with immunocytochemistry and a modified haematoxylin stain. The pan-cytokeratin clone MNF116 was used to identify potential type II pneumocytes. The monoclonal preparation of 2B11 + PD7/26 for the common leukocyte antigen CD45, was employed to identify contaminating cells of haematopoietic origin. The criterion for identifying potential type II pneumocytes in haematoxylin stained samples was that. Potential Type II pneumocytes (Mono) were only designated such if they possessed a mononuclear morphology with four or more lamellar bodies .in haematoxylin stained samples. Contaminating leukocytes and bilobar cells were also assigned according to their nuclear morphology (PMN). The above table summarizes the representative data characteristics within three isolations. The proportion of the total isolation constituted by each characteristic is expressed as a mean percentage ± SD. The percentage of an isolation accounted for in each method is depicted by the sum of the two proportions.

3.4 Modified haematoxylin staining and immunocytochemistry discussion

In theory the combined count data from the modified haematoxylin stain and immunocytochemical assessment should account for the majority of the cell populations of the three DNase type II pneumocyte isolates (Table 3.6.). Overall, a comparison of the data from the techniques yields conflicting results as to which of the two is better for the characterisation of human type II pneumocyte isolations (Figure3.7).

In the case of 13978, 66.07 % of the total population was accounted for with immunocytochemistry. Whereas within the modified haematoxylin stain, 57.21 % of the 13978 cell population could be accounted for. Immunocytochemistry accounted for 86.33 % of the 13988 isolate population, compared to 31 %, accounted for by the modified haematoxylin stain. Staining and analysis of 13992 with the modified haematoxylin technique was able to account for 85 % of the isolate. Assessment of 13992 by immunocytochemistry accounted for 48.50 % of the isolated cellar population. A likely explanation for these conflicting results is the heterogeneity of tissue samples. It is worth considering the benefits and limitations of the two techniques. In the immunocytochemical analysis, two broad categories of characteristic were investigated; epithelial and immune cell.

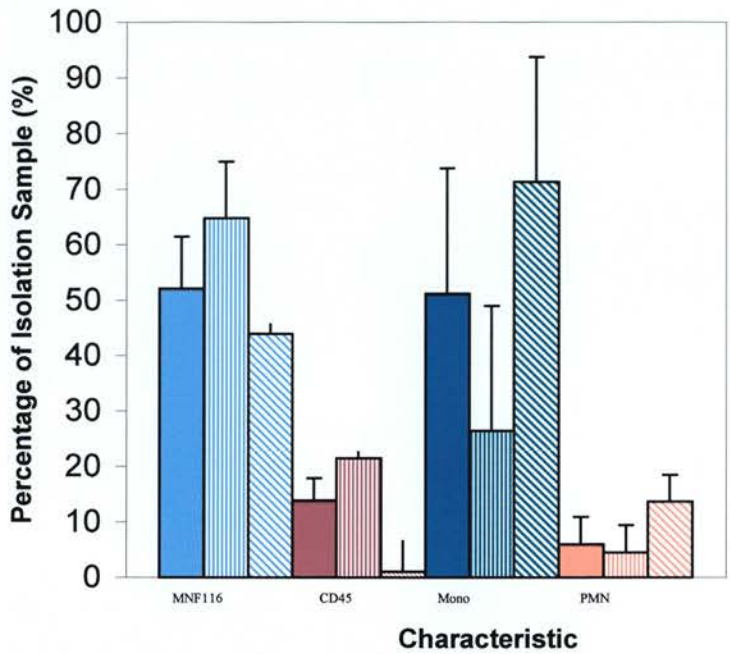

Figure 3.7. Graph of immunocytochemical, and modified haematoxylin stain analysis of primary isolated type II pneumocytes.

Samples 13978, 13988 and 13992. MNF116 = Pan-cytokeration, CD45 = Common leukocyte antigen. Modified haematoxylin stain data: Mono = mononuclear cells with four of more lamellar bodies, PMN = Cells with polymorphological nucleus.

MNF116 13978 sample MNF116 13988 sample. MNF116 13992 sample.

CD45 13978 sample. CD45 13988 sample. CD45 13992 sample

Mono 13978 sample. Mono 13988 sample. Mono 13992 sample. PMN 13978

PMN 13988 sample. PMN 13992 sample

CD45 (2B11 + PD7/26). The pattern of cytokeratin expression changes during epithelial development and differentiation in both Xenopus Laevius (192) and rats (193). Variability of staining in the cytospins could be a reflection of the expression profile of the cells. Filaments of each subfamily of cytokeratin are antigenetically related (187). This means that, depending on the degree of cytokeratin gene expression and protein production, the level of positive staining may vary. Also probing with a pan –cytokeratin antibody such as MN116 potentially includes the detection of other epithelial cells such as Clara cells. In the instance of CD45, variable staining of antigen has previously been documented in cells of haemopoeitic origin. Macrophages and eosinophils are reported to stain variably, with polymorph cells staining less strong. The majority of plasma cells do not react with the anti-CD45, 2B11 +PD7/26 preparation (194) (195). Therefore, the differentiation status of the cells under investigation can have a misleading effect on the purity assessment of isolations. The modified haematoxylin stain in one step assesses purity, differentiation and contamination. However, for example in sample 13988 the proportion of the isolate assigned as type II pneumocyte by modified haematoxylin stain is approximately one third the value assigned by immunocytochemistry. If this is a true reflection of the purity of the isolate, then potentially the isolation was contaminated by large numbers of fibroblasts, macrophages, lymphocytes and epithelial cells. The criterion for type II pneumocytes used was that the cells be mononuclear with four or more lamellar inclusion bodies. Macrophages ingest surfactant material (174) (175), and this could pose a problem when using the haematoxylin stain as they could be mistaken for type II pneumocytes (190). Also, mechanical strain is known to enhance the release of surfactant (1; 86), and during the isolation procedure the cells are subject to significant strains, which could result in a loss of inclusion bodies indicative of the type II pneumocyte (157). Therefore a number of cells of interest could be excluded in the analysis.

When considering the best technique for characterising human type II pneumocyte isolations it would be the modified haematoxylin staining procedure, based on its simplicity and qualitative assessment of type II pneumocyte differentiation. To test further for contaminents immunochemical analysis of fibroblast content of isolations is possible with the use of antibodies against the intermediate filament protein vimentin, but the antibodies are not specific (196). Levels of fibroblast contamination have successfully been monitored in cultures of keratinocytes by assaying the mRNA expression of keratinocyte growth factor (KGF) with RTPCR (197). To assay endothelial cell contamination by immunochemistry, antibodies against factor XIII could be of use (196). However, due to the limited availability of cytospins from each isolation, it was concluded that the immunocytochemical analysis

should be confined to cytokeratin and common leukocyte antigen (CD45).

Until a specific type, II pneumocyte antigen is discovered the difficulties of characterising isolations will remain. Alkaline phosphatase staining correlates closely with modified haematoxylin staining in rabbit and rat type II pneumocytes (190). However the human type II pneumocytes cultured for 24 hours and stained for alkaline phosphatase activity demonstrated that it can be difficult to differentiate between positive and negative staining cells depending on the degree of cell spreading, such as that seen in the cells cultured on CIV (Figure 3.4). The few isolated type II pneumocytes cultured on BSA stained AP activity stained intensely purple, but had a rounded morphology. The type II pneumocytes cultured on FN presented with a variety of morphologies, and intensities of stain. However the morphology and AP stain intensity was uniform within the culture of type II pneumocytes on CIV. The AP stain intensity could be attributed to the cell morphology presented within these three cell populations. Isolated human type II pneumocytes have previously been reported to preferentially adhere to collagenous substrata (155). Therefore, the less adherent and more rounded the cell, the more intense the AP staining pattern. This presumes that all the cells of interest possess the same AP activity.

CHAPTER 4 THE DEVELOPMENT OF AN IN VITRO MODEL SYSTEM TO STUDY TYPE II RESPIRATORY EPITHELIAL CELL MECHANOTRANSDUCTION

4.1 The development of an in vitro model system to study type II pneumocytes respiratory epithelial cell mechanotransduction

Mechanical forces are important for normal lung development and function (1). Foetal lung development requires breathing movements and an in vitro study demonstrates that a single episode of mechanical strain is capable of enhancing surfactant secretion and transiently increasing $[Ca^{2+}]_i$ of adult rat type II pneumocytes (4). Significant evidence is accumulating to suggest that mechanical forces play an important role in regulating type II and type I pneumocyte phenotypes (11). Type II pneumocytes are thought to differentiate into type I pneumocytes through an intermediary cell type, which exhibits characteristics of the two phenotypes of cell (10), (11; 13; 157). Following a period of increased lung expansion in lungs of foetal sheep, the numbers of phenotypic type II pneumocytes and type I pneumocytes are altered (11).

Tracheal obstruction in foetal lungs, either experimentally or via congenital abnormalities leads to an increase in lung expansion, which stimulates lung growth. In 1999 Lines and coworkers (134)demonstrated that tracheal obstruction in foetal sheep lungs leads to a large simultaneous reduction of SP – A, B and C mRNA expression levels in comparison to control values. In conjunction with this, there was a significant reduction in the levels of SP – A protein.

The human adenocarcinoma cell line NCI – H441, has been used to investigate in vitro the potential of mechanical strain to stimulate proliferation in human lung epithelial cells. Both tonic and cyclic patterns of mechanical strain stimulate proliferation within this model. Mitogen – activated protein kinases p42/44 and *c - jun* phosphorylation increases, and the transcriptional protein activating protein –1 is activated in response to strain (76). The application of cyclic mechanical strain of 22% using the Flexercell® strain unit in vitro on primary rat type pneumocytes demonstrates that strain can induce both apoptosis and secretion of phosphotidyl choline (PC), a major component of surfactant (198)

To date the mechanisms of pulmonary epithelial cell mechanotransduction have largely been unexplored. I decided to examine the usefulness of an in – house developed system that had been previously utilised in the investigation of mechanotransduction in chondrocytes and bone cells. The unpredictable availability of suitable primary human tissue necessitated the use of an alternative model for primary human type II pneumocyte cultures. Therefore, I also investigated the potential usefulness of the human adenocarcinoma cell line NCI – H441 in this model system. As this cell line has undergone a limited amount of phenotyping it was important to do some additional characterisation to assess the similarity with the human primary type II cells.

The main aim of this chapter was the development of an in vitro model system to study type II respiratory epithelial cell mechanotransduction

4.2 NCI-H441 cell line characterization

The NCI-H441 cell line (H441) is derived from a papillary adenocarcinoma, and is known to display characteristics similar to type II pneumocytes and Clara cells (American Tissue Culture Collection)(199). NCI – H441 cells are reported as expressing the surfactant specific proteins SP-A and SP-B, and at electron microscopic level display multi-lamellar bodies (200). Traditionally the human A549 adenocarcinoma cell line has been used as a model for human type II pneumocyte studies. However, despite previous demonstration that the A549 cell line produces the phospholipid components of pulmonary surfactant (145) SP- A, mRNA was not detected by RT – PCR (201) and Northern blot analysis in these cells (200).

4.2.1 Alkaline phosphatase staining of NCI-H441

The method of alkaline phosphatase staining utilised is given in Chaper 3. The H441 cell line was seeded in 55mm petri dishes on BSA, fibronectin (FN), collagen (CIV) at a concentration of 2×10^5 cells/ml, as had previously been undertaken in primary type II pneumocytes. The seeded petri dishes were then incubated overnight at 37°C, 5% CO_2, before testing for alkaline phosphatase activity.

4.2.1.1 Results

Strong alkaline phosphatase staining patterns were evident in all the H441 cultures tested. In some examples the intensity of staining was so great that, instead of blue purple staining witnessed within the primary type II pneumocyte culture, the cells appear black: brown. Various morphologies of cell were apparent on the different sustrata. There were instances of polygonal cells on collagen IV, which results in a diffuse alkaline phosphatase staining (Figure 4.1.). NCI – H441 cells adherent on FN were spindle (Figure 4.1.). The majority of NCI – H441 cells seeded on BSA remained round and stained darkly for alkaline phosphatase (Figure 4.1.)

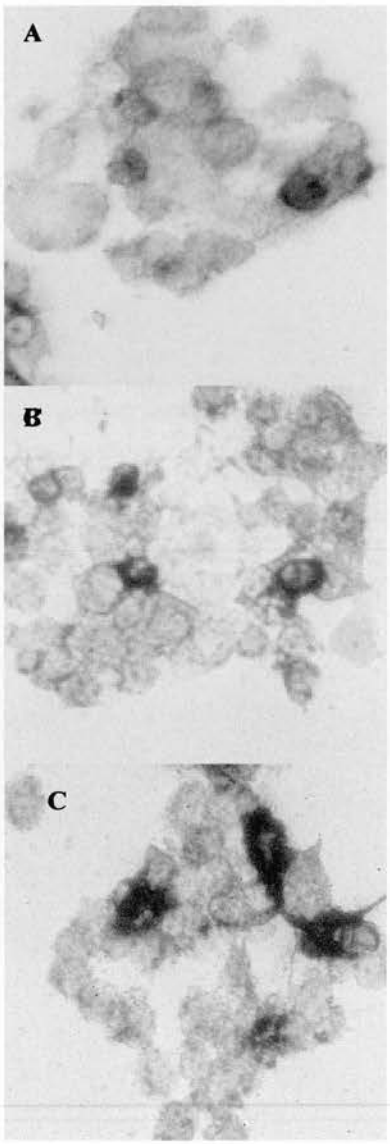

Figure 4.1. Alkaline phosphatase staining of the NCI – H441 cell line cultures on bovine serum albumin (BSA), Collagen IV (IV) and Fibronectin (FN). Typical fields of view representative of NCI-H441 cells cultured for 24 hours on A: BSA, B: CIV and C: FN coated substratum, stained for alkaline phosphatase activity and counterstained with neutral red solution. Positive staining for alkaline phosphatase activity was apparent in all the cell culture conditions. Original magnification x200.

4.2.2 Gene expression and production of surfactant specific protein

4.2.2.1 Surfactant specific protein – A mRNA expression in NCI – H441

Nine investigative RT-PCR reactions were carried out for SP – A mRNA using primary human lung total RNA which was isolated according to the method detailed within Chapter 2.

To optimise the primer specific conditions the concentration of the reaction component (dNTPs), and enzyme cofactors ($MgCl_2$ and BSA) were varied.

Three subsequent SP – A RT – PCR reactions were carried out on primary human lung and NCI-H441 total RNA using the optimised primer specific conditions

Details of the exon spanning SP-A primer sequences are given in Chapter 2.

4.2.2.2 Results

The optimised SP – A mRNA primer specific conditions were as follows:

3 μg cDNA, 1.75 - 2.5 mM $MgCl_2$, 100 μM dNTPs; the addition of 0.001 % BSA solution had no detectable benefit. These conditions operated efficiently with the standard GAPDH mRNA RT –PCR (Figure 4.2).

A positive signal for SP –A mRNA was detected in both primary human lung and NCI – H441 samples. A stronger signal was detected for SP – A mRNA in the human lung sample compared to the NCI – H441 samples (Figure 4.3).

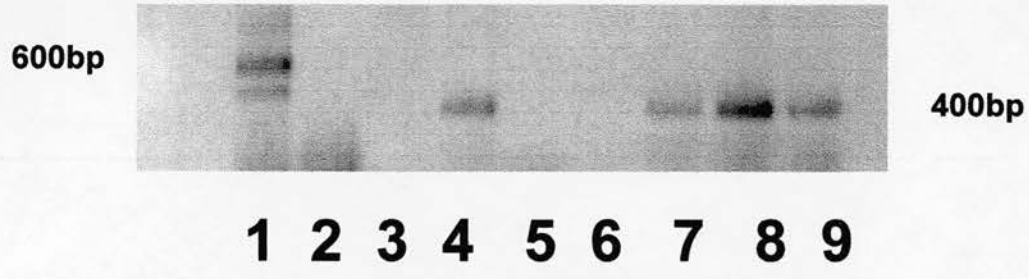

Figure 4.2. Human pulmonary surfactant specific protein A RT-PCR conditions. 1. positive GAPDH cDNA control. 2. negative GAPDH cDNA control. 3. negative GAPDH primer control. 4. SP –A, 1.5 mM$MgCl_2$, 100 μM dNTP, +BSA, 5. empty lane. 6. empty lane. 7. SP –A, 1.5 mM$MgCl_2$, 100 μM dNTP, +BSA. 8. SP –A, 1.5 mM$MgCl_2$, 100 μM dNTP, +BSA, 9. SP –A, 1.5 mM$MgCl_2$, 100 μM dNTP, +BSA. Reaction temperature 60°C.

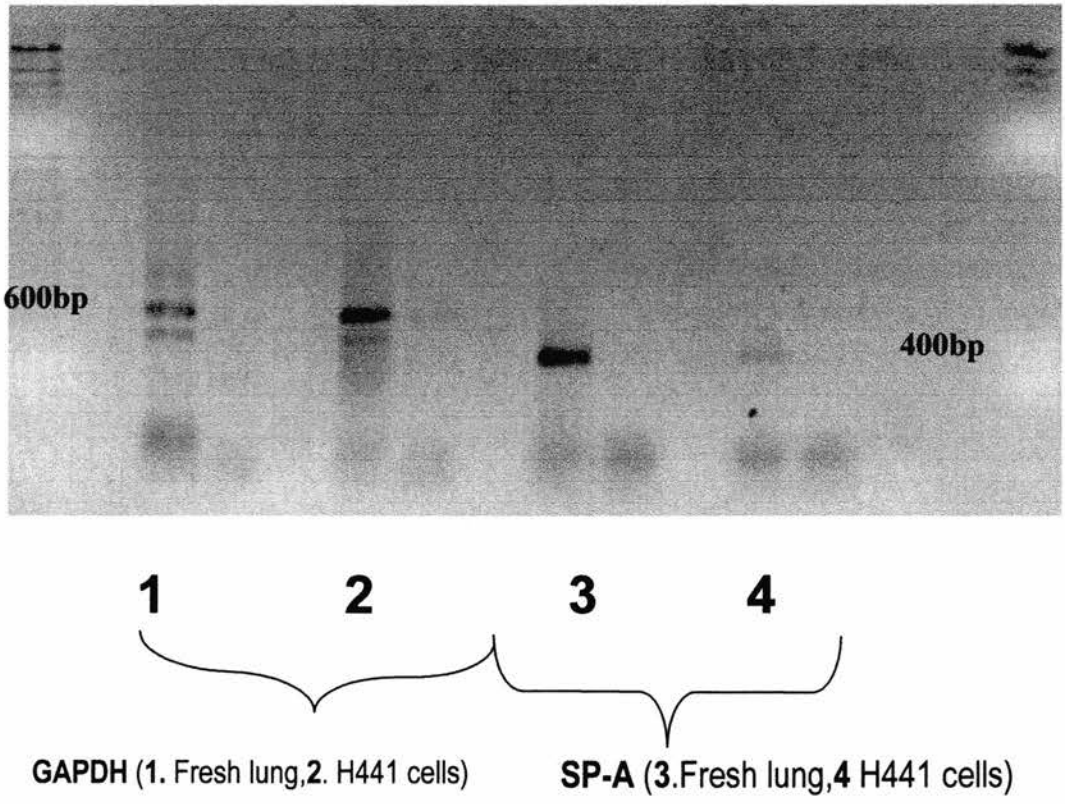

Figure 4.3. Surfactant protein A expression by NCI – H441 and human lung. Comparison of human primary lung tissue and NCI – H441 SP –A. 1. Lung tissue GAPDH positive cDNA control. 2. NCI – H441 GAPDH positve control. 3. Lung tissue SP –A. 4. NCI –H441 SP –A.

4.3. Surfactant specific protein A and B expression

The preparation of cytospins and immunocytochemistry were undertaken as described in Section 2.3. Cytospins of NCI – H441 were probed with the polyclonal antibodies for SP – A (AB3420), or SP – B (AB3436), or normal rabbit IgG (AB – 105 –C) as a negative control.

Probing of NCI – H441 cytospins for SP –A and B was untaken on three separate occasions. Positive cytoplasmic staining for SP –A and SP –B is evident within the NCI – H441 cytospins. On two occasions, there was background staining, but positive staining was still apparent. However, only a minority, less than 10 %, of cells, stain positive for the surfactant specific proteins (Figure 4.4).

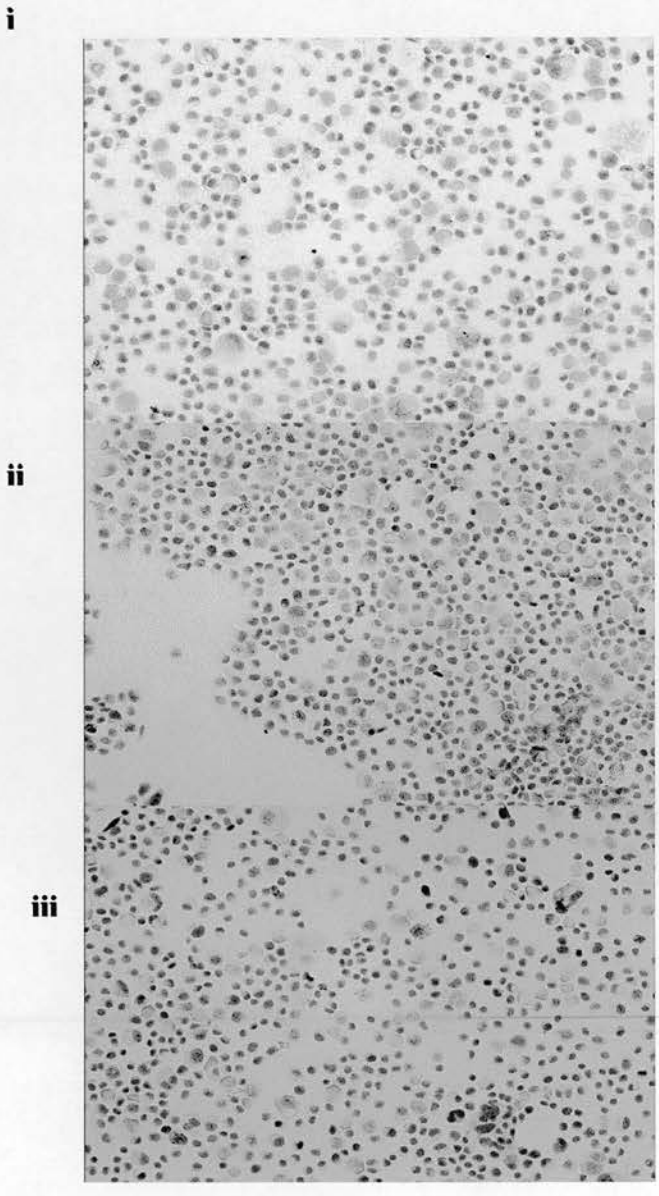

Figure 4 NCI –H441 surfactant specific protein A and B immunocytochemistry. Original magnifications x 200.

i). Normal Rabbit IgG (AB – 105-C) immunocytochemistry negative control

ii) NCI – H441 cell line SP - A polyclonal (AB3436) immunocytochemistry.

iii) NCI –H441 cell line SP –B polyclonal (AB3434) immunocytochemistry.

4.3.2 Cytokeratin expression within NCI-H441

The preparation of cytospins and immunocytochemistry were undertaken as described in Section 2.3. Cytospins of NCI – H441 were prepared and probed with the pan – cytokeratin antibody, clone MNF116, or the mouse IgG1κ negative control.

NCI – H441 cytospins were probed for expression of cytokeratins twice. Positive cytoplasmic staining was apparent within the cytoplasm of the NCI – H441 cells probed with MNF116 on both occasions in more than 90 % of the cells (Figure 4.5).

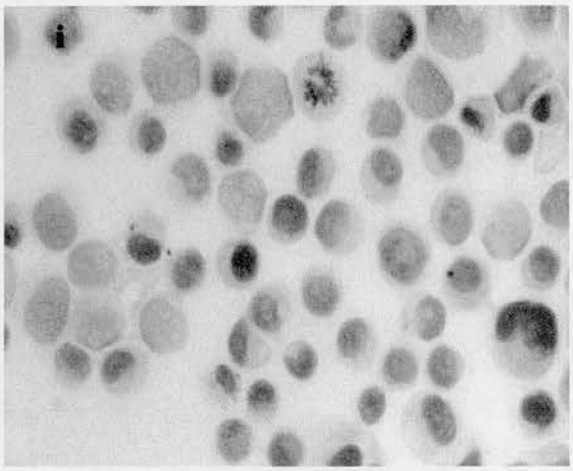

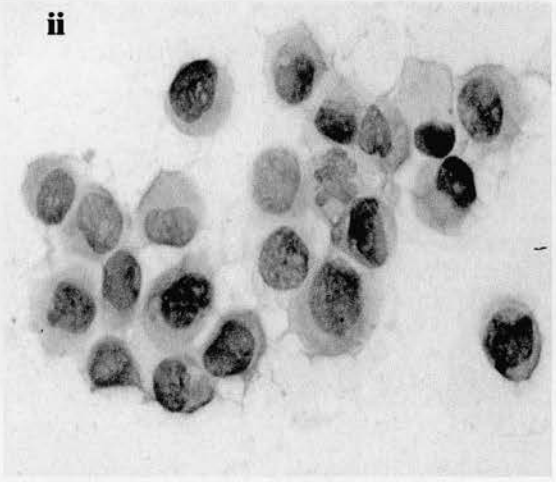

Figure 4. Pan – cytokeratin immunocytochemistry of NCI - H441 cell line cytospins. Original magnifications x 400

i) IgG negative control.

ii) Pan – cytokeratin MNF116 Immunocytochemistry of NCI – H441.

4.3.3 Electron microscopic analysis and comparison of NCI-H441 and type II pneumocytes

The lack of a specific marker for human type II pneumocytes means that assigning the phenotype may rely on the analysis of the cells' morphology by electron microscopy. Mononuclear cells with apical microvilli, lamellar bodies, abundant organelles and no caveolae vesicles are all typical morphological characteristics of the type II pneumocyte (145; 146) (153; 157). The preparation of cells for electron microscopy was undertaken as detailed in Section 2.4. Electron micrographs were taken of a type II pneumocyte enriched cell population (Section 3.3.6) and a NCI – H441 cell line sample.

Microvilli characteristic of type II pneumoctyes are evident on the surface of the NCI – H441 cells examined by electron microscopy. Dark osmiophillic lamellar bodies are present within the cytoplasm of the NCI – H441 cell line (Figure 4.7.). Cells characteristic of type II pneumocytes are apparent within the electron micrographs of the primary human pneumocyte population (Figure 4.6.). The cells possess blunt surface microvilli and dark cytoplasmic lamellar bodies. The type II pneumocyte, shown in Figure 4.2.4.2., appears to be expelling material from a lamellar body by exocytosis. The lamellar bodies within the cytoplasm of the primary type II pneumocyte, in comparison with the lamellar bodies of the NCI –H441 cell, appear larger. Another cell type apparent within the isolation is the phagocyte (Figure 4.2.4.). The phagocyte of Figure 4.6. demonstrates pseudopodia and internalised inorganic material, which is most likely Percoll from the isolation procedure.

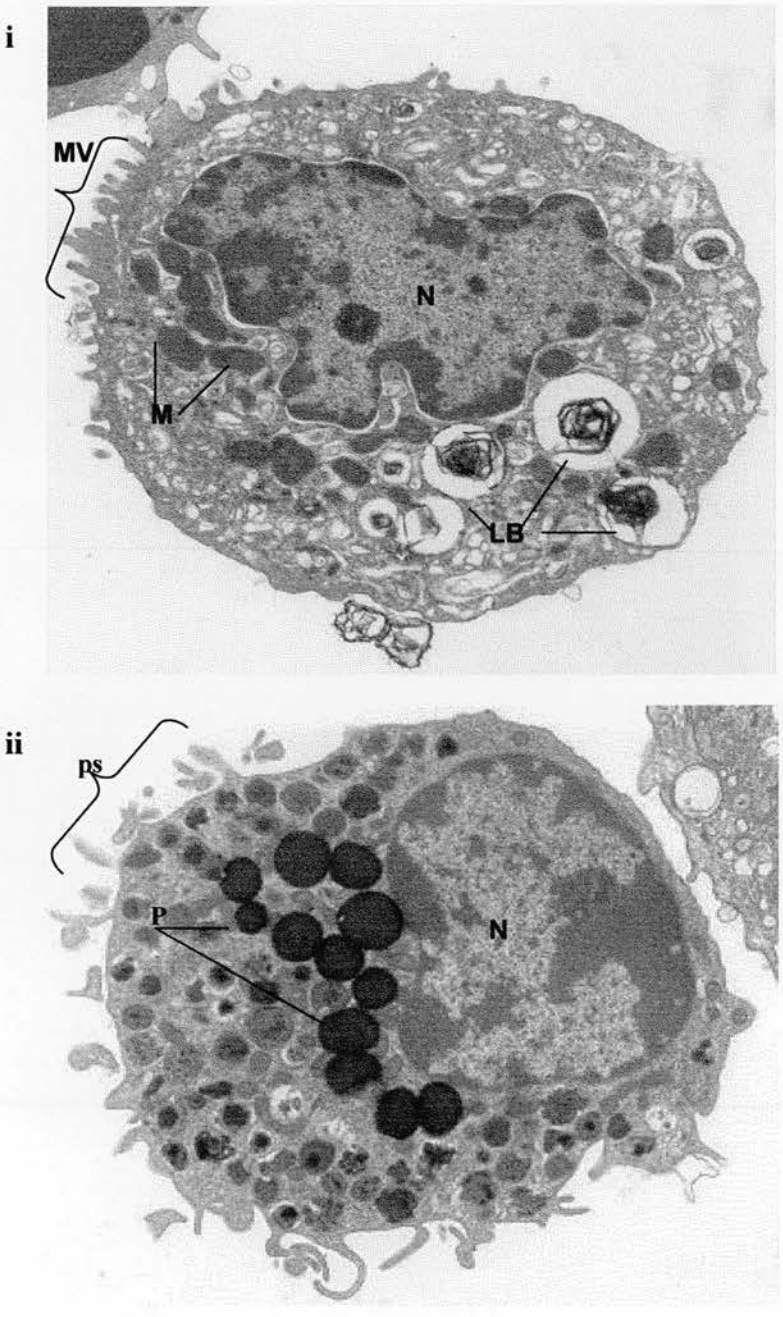

Figure 4.6. Electron Microscopy.of Primary Type II Pneumocyte Enriched Suspension. **i** Primary Human Type II Pneumocyte original magnification x 9936. MV = microvilli, LB = lamellar bodies; M = mitochondria, N = nucleus. . **ii** Primary Pulmonary Phagocyte original magnification x.9936

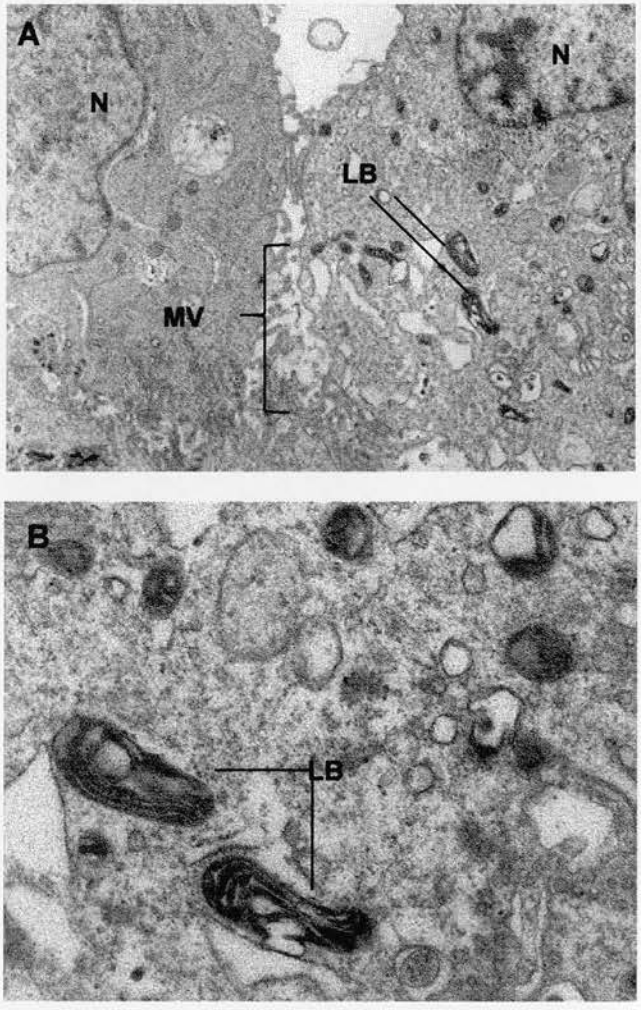

Figure 4.7. Electron microscopy of NCI – H441 cell line.

A N = nucleus, LB = lamellar bodies, MV = microvilli.

Original magnification x 7920.

B N = nucleus, LB = lamellar bodies. Original magnification x 27000.

4.4. The electrophysiological response of primary type II pneumocytes to cyclical mechanical stimulation

Previously, a pilot study undertaken by Dr Malcolm Wright, a principal investigator in osteoarticular cell mechanotransduction, demonstrated that primary type II pneumocytes that were subject to cyclic mechanical stimulation display a significant membrane hyperpolarisation response. The details of this pilot study are given below.

Details of the electrophysiological procedure are as in Section 2.9 and isolation of primary type II pneumocytes in Section 3.3.6. Primary human type II pneumocytes were isolated by courtesy of Dr Shirley O'Dea and seeded at 5 x 10^4 cells ml^{-1} on fibronectin (FN) coated 58 mm petri dish. Subsequent to overnight culture at 37 °C, 5 % CO_2, measurements of resting membrane potentials of the type II pneumocytes were taken by Dr Malcolm O Wright via the single cell impalement method detailed in Chapter two. The culture was subsequently subject to cyclic mechanical strain at 5000 μstrain (με), 0.25 Hz (2 seconds on 2 seconds off) for 20 minutes.

Cyclic mechanical stimulation at 5000 με, 0.25 Hz, for 20 minutes, resulted in a statistically significant membrane hyperpolarisation response in primary type II pneumocytes cultured on FN. The primary type II pneumocyte culture demonstrated a mean resting potential of 22.00 ± 7.03 (-mV) and a relative percentage change of 90.90 ± 68.00, $p = 0.006$ (Table 4.3.). Note was taken that the cells appeared to degranulate following mechanical stimulation.

A similar series of experiments was undertaken by myself to analyse NCI – H441 cells under similar conditions. A summary of membrane responses elicited by NCI – H441 are given in Table 4.1

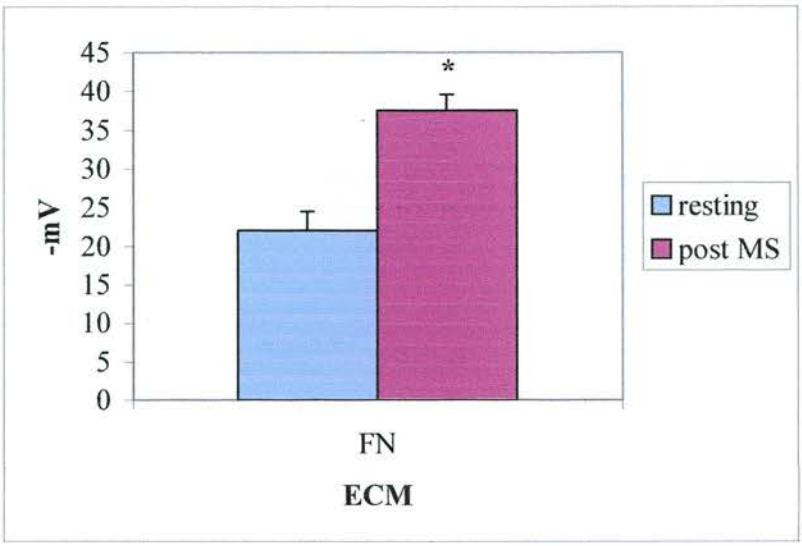

Figure 4.8. The electrophysiological response of primary type II pneumocytes to cyclic mechanical stimulation. Primary human type II pneumocytes were isolated from resection specimens and cultured on fibronectin. Cell membrane potentials prior and following cyclic mechanical stimulation, of 0.25 Hz, 5000με, were measured. Graph is representative of one experiments, + 1 Stdev, n=10. $p < 0.05$ *paired t-test.

Table 4.1 The effect of 0.25 Hz, 5000 με mechanical stimulation on the membrane potential of primary human type II pneumocytes

n		Membrane Potential (mean ± SD) (-mV)			
Resting	Post MS	Resting	Post MS	% Relative Change	P value
8	7	22.00 ± 7.03	37.57 ± 5.50	90.90 ± 68.00	0.006

n = number of cells sampled, Post MS = membrane potential following cyclic mechanical stimulation, % relative change = percentage change in membrane potential relative to the resting membrane potential. p value = calculated with a paired t – test

4.4.1 The effect of time in culture on electrophysiological response of NCI – H441 cells

NCI-H441 cells were cultured at 5 x 10^4 cells ml^{-1} on CIV coated substratum in DMEM: F12, 1 % penicillin/streptomycin, 1 % L-glutamine, and were incubated for of four or twenty –four hours prior to mechanical stimulation to examine the effect of culture duration on mechanical cell responses. A cyclic mechanical strain regime of 0.25 Hz (2 seconds on, 2 seconds off) for 20 minutes was used with pressure pulses of 1.5 atm above atmospheric pressure, which resulted in a maximum of 5000 microstrain (με) on the base of the 58 mm plastic culture dish. Sampling of resting and post mechanical stimulation membrane potentials, and statistical analysis, were carried out as mentioned in Section 4.3.1.

4.4.1.1 Results

In experiment i) NCI-H441 cells cultured on collagen IV (CV) in serum –free medium for four hours had a mean resting membrane potential of 25.20 ± 2.86 –mV. Subsequent to cyclic mechanical stimulation the mean membrane potential was 46.40 ± 6.80 – mV; the mean relative change in membrane potential was 86.90 ± 41.20 %, $p = 0.0122$. NCI-H441 cells subjected to an incubation of 24 hours in serum – free medium similarly displayed a significant membrane hyperpolarisation responses to cyclic mechanical stimulation. The resting membrane potential of NCI – H441 cell s cultured on CIV for 24 hours was 15.00 ± 1.23 -mV and following cyclic mechanical stimulation was 29.00 ± 3.42 –mV. This represents a mean relative change of 89.0 ± 27.80 %, $p = 0.001$ in membrane potential. In experiment ii), following 4 hours of culture on CIV in serum – free, NCI – H441 cells had a resting membrane potential of 14.83 ± 3.76 –mV. Following cyclic mechanical stimulation the membrane potential fell to 29.29 ± 4.86 –mV. This is represents a mean relative change in membrane potential of 124.00 ± 45.80 %, $p \leq 0.001$. Following 24 hours of culture in serum – free conditions the resting membrane potential of NCI – H441 cells was 15.38 ± 3.43 –mV and subsequent to mechanical stimulation the membrane potential was 20.17 ± 8.28 –mV. This represents a mean relative change in membrane potential of 141.20 ± 41.20, $p = 0.003$. This shows that mechanical stimulation induces a consistent membrane hyperpolarisation in NCI – H441 cells cultured on CIV for 4 or 24 hours (Table 4.2).

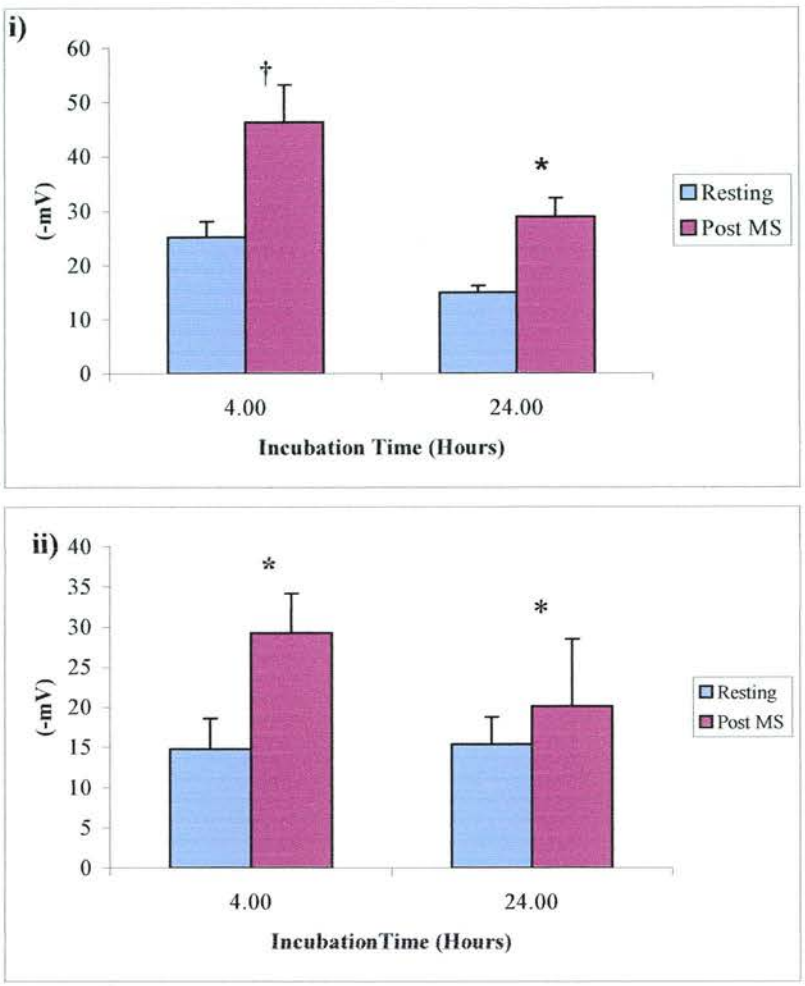

Figure 4.9. The effect of time on electrophysiological response of NCI-H441 cells. Electrophysological responses of NCI-H441 cells prior and following cyclic mechanical stimulation of 5000 με, 25 Hz, for a period of 20 min, were measured. The effect of seeding experimental populations for 4 and 24 hours, on the cellular membrane potentials at rest and following mechanical stimulation were examined. The graphs are representative of two experiments i) and ii), + 1 Stdev, n=5. $p < 0.05$ *paired t-test, † Mann-U-Whitnney test

4.4.2 The effect of serum supplementation on the relative percentage change in membrane potential of cyclic mechanical stimulated NCI – H441 cells

NCI-H441 cells cultured at 5 x 10^4 cells ml^{-1} on CIV coated substratum in DMEM: F12, 1 % penicillin/streptomycin, 1 % L-glutamine, were subject to incubations of twenty –four hours with and without 5 % FCS prior to mechanical stimulation to examine the effect of serum culture on mechanical cell responses. Cell culture medium was changed to serum – free medium 30 minutes before mechanical stimulation. A cyclic mechanical strain regime of 0.25 Hz (2 seconds on, 2 seconds off) for 20 minutes was used with pressure pulses of 1.5 atm above atmospheric pressure, which resulted in a maximum of 5000 microstrain (με) on the base of the 58 mm plastic culture dish.

Sampling of resting and post mechanical stimulation membrane potentials, and statistical analysis were carried out as mentioned in Section 2.3.1.

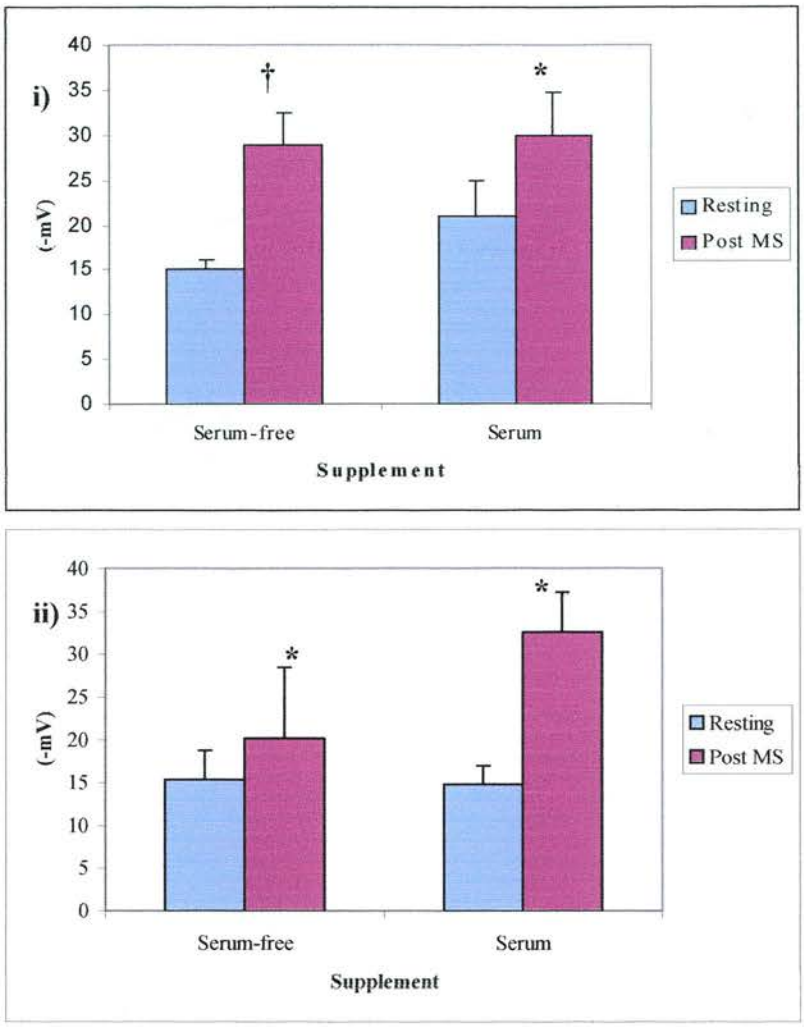

Figure 4.10. The effect of serum supplementation on the response of cyclic mechanical stimulated NCI-H441 cells. Electrophysological responses of NCI-H441 cells prior and following cyclic mechanical stimulation of 5000 □□, 25 Hz, for a period of 20 min, were measured. The effect of seeding experimental populations in the absence and presence of serum, on the cellular membrane potentials at rest and following mechanical stimulation were examined. The graphs are representative of two experiments i) and ii), + 1 Stdev, n=5. $p < 0.05$ * paired t-test, † Mann-U-Whitnney test

4.4.2.1 Results

Statistically significant membrane hyperpolarisation was seen in both experiments in all cell culture populations following 20 minutes of cyclic mechanical stimulation, 0.25 Hz, 5000 με.

In experiment i) in the absence of serum, the cells has a resting membrane potential of 15.00 ± 1.23 –mV and following mechanical stimulation the membrane potential was 29.00 ±3.42 –mV. This represents a mean relative percentage change of 89 ± 27.80 %, $p = 0.001$. In comparison, in the presence of serum the resting membrane potential was 21.00 ± 3.94 –mV and following mechanical stimulation 30.00 ± 4.80. This equates to a mean relative percentage change in membrane potential of 45.40 ± 49.90 %, $p = 0.0367$. Experiment ii) demonstrated that, in the absence of serum, the mean resting membrane potential of the NCI – H441 cells was 15.38 ± 3.43 –mV and following mechanical stimulation 20.17 ± 8.28 – mV. This represents a significant membrane hyperpolarisation response with a mean relative change of 141.20 ± 41.20%, $p = 0.003$. Following 24 hours of incubation with serum the resting membrane potential was 14.80 ± 2.17 – mV and after mechanical stimulation the membrane potential was 32.60 ± 4.62 –mV. This is a percentage change of 50.00 ± 27.40 %, $p = 0.011$. The NCI –H441 cells in each experiment appeared to degranulate following cyclic mechanical stimulation (Table 4.2).

It was decided that for all subsequent mechanotransduction experiments, NCI – H441 cells would be seeded on the relevant matrix in DMEM: F12 medium supplemented with 10 % foetal bovine serum, 1 % penicillin/streptomycin, 1 % L-glutamine for twenty –four hours, then 30 minutes in serum –free medium. This decision was based on the observation that NCI –H441 cells seeded in the presence of serum were easier to impale during electrophysiological recording

Table 4.2 The effect of 0.25 Hz, 5000 me cyclic mechanical strain on the membrane potential of the NCI –H441 cell line

i) n = number of cells, P – values were calculated from paired t – test, † value calculated with Mann-U-Whitnney test

		Membrane Potential (-mV) (mean ± SD)			
	n	Resting (mV)	Post MS	% Relative Change	P value
4 hour Incubation	5	25.20 ± 2.86	46.40 ± 6.80	86.90 ± 41.2	0.0122†
24 hour incubation	5	15.00 ± 1.23	29.00 ± 3.42	89.00 ± 27.8	0.0010
Serum-free	5	15.00 ± 1.23	29.00 ± 3.42	89.0± 27.8	0.0010
Serum	5	21.00 ± 3.94	30.00 ± 4.80	45.40± 49.90	0.0367†

		Membrane Potential (-mV) (mean ± SD)			
	n	Resting	Post MS	% Relative Change	P value
4 hour Incubation	5	14.83 ± 3.76	29.29 ± 4.86	124.00 ± 45.80	0.000
24 hour incubation	5	15.38 ± 3.43	20.17 ± 8.28	141.20 ± 41.20	0.003
Serum-free	5	15.38 ± 3.43	20.17 ± 8.28	141.20 ± 41.20	0.003
Serum	5	14.80 ± 2.17	32.60 ± 4.62	50.00 ± 27.40	0.011

ii) n = number of cells, P – values were calculated from paired t - test

4.5 The effect of extracellular matrix substrate on electrophysiological response cyclic mechanically stimulated NCI – H441 cells

Previous studies on epithelial cells from different locations in the body indicate that the ECM modulates the cell responses to mechanical stimulation (202)). To ascertain whether similar effects in cell function may be seen in alveolar epithelium, a human type II pneumocyte cell line NCI – H441 was cultured on different extracellular matrices and subjected to physiological cyclic mechanical strain.

NCI-H441 cells were seeded at 5 x 10^4 cells ml^{-1} on two different extracellular substrates collagen IV (CIV) and fibronectin (FN), and bovine serum albumin (BSA) coated dishes as a negative control. The NCI - H441 cells were subjected to mechanical cyclical stimulation at a frequency of 0.25 Hz (2 seconds on, 2 seconds off) for 20 minutes. Pressure pulses of 1.5 atm above atmospheric pressure were used, which resulted in a maximum of 5000 microstrain ($\mu\varepsilon$) on the base of the 58 mm plastic culture dish.

Transmembrane potentials were sampled from 5-10 individual cells in each dish before (resting) and following (post MS) mechanical stimulation.

The data was analysed to determine the effects of the three substrata conditions on resting membrane potential and relative percentage change in membrane potential response and statistical analysis undertaken as before. A summary of membrane responses is given in Table 4.3.

4.5.1 Resting membrane potential of the NCI –H441 Cell Line, cultured on collagen IV and fibronectin

There was a variation in the resting membrane potential of the cells on the different matrices, but this did not reach statistical significance. The mean resting membrane potential of NCI – H441 cells cultured on BSA was 23.67 ± 11.33 (-mV) in experiment i) and 14.00 ± 0.71 (-mV) in experiment ii). The mean resting membrane potentials of NCI –H441 cell culture populations seeded on CIV were 22.00 ± 4.30 (-mV) in experiment i) and 22.60 ± 9.94 (-mV) in the experiment ii). The mean resting membrane potential of NCI – H441 cells

innoculated onto FN coated substrata were 15.86 ± 5.52 (-mV) and 14.60 ± 2.79 (-mV) in experiments i) and ii) respectively.

Using Kruskal –Wallis analysis, no statistical significant difference between the resting membrane potentials of the ECM proteins CIV, FN and the coating control BSA were found. In experiment i) when comparing the resting membrane potential medians p = 0.300 and in ii) p =0.188 (Refer to Appendix)

4.5.2 Cyclic mechanical stimulation elicits significant membrane hyperpolarisation responses in NCI – H441 cultured on collagen IV and fibronectin

Consistent trends in membrane potential response to cyclical mechanical stimulation were observed between experiments. Statistically significant depolarisation of the NCI- H441 cells cultured on BSA occurred following cyclical mechanical stimulation In experiment i) following cyclic mechanical stimulation, the sampled membrane potential of NCI – H441 on BSA rose from 23.67 ± 11.33 – mV to 11.50 ± 4.90 – mV. This represents a significant membrane depolarisation response, equal to a relative change of – 35.10 ± 25.40 %, p = 0.0163. In experiment ii) the membrane potential of cells on BSA changed from 14.00 ±0.707 – mV to 9.00 ± 3.24 - mV, equivalent to a membrane relative change of –41.82 ± 25.40 %, p = 0.008.

In experiment i) mechanically stimulated NCI – H441 cells cultured on CIV demonstrated a hyperpolaristion of the membrane potential that did not reach statistical significance, from 22.00 ± 4.30 – mV to 34.00 ± 3.39 –mV post stimulation, a relative change of 98.00 ± 92.90 %, p = 0.054. However, the mechanically stimulated NCI – H441, CIV cell population of experiment ii) responded with a statistically significant membrane hyperpolarisation. The membrane potential of NCI – H441 fell from 22.60 ± 9.94 –mV resting membrane potential to 39.00 ± 12.51 –mV following mechanical stimulation, a significant mean relative change of 59.8 ± 38.1 %, p = 0.0122. A membrane hyperpolarisation of statistical significance was elicited in response to cyclic mechanical stimulation in both of the NCI – H441 cell cultures seeded on FN. The membrane potentials of NCI –H441 cultured on FN following mechanical stimulation in experiment i) were 15.86 ± 5.52 – mV at rest and following

mechanical stimulation 25.00 ± 7.92 –mV and in experiment ii) were 14.60 ± 2.79 – mV resting and 31.60 ± 13.37 –mV following mechanical stimulation. The membrane hyperpolarisation responses in experiments i) and ii) were mean relative changes of 112.00 ± 58.00 %, $p = 0.163$ and 75.70 ± 77.60 %, $p = 0.035$, respectively. The cells seeded on CIV and FN apparently degranulated following cyclic mechanical stimulation. The pattern of cell degranulation matched the pattern of strain that the base of the dish experiences. Maximum degranulation of the mechanically stimulated NCI –H441 cells was witnessed midway between the centre and the periphery of the petri dishes.

4.5.3 Relative change in NCI – H441 cells membrane potential, cultured on BSA, CIV, FN, following cyclical mechanical stimulation

A relative membrane depolarisation response of –35.10 ± 25.40 % SD was evident in the mechanically stimulated NCI –H441 cells of experiment i) cultured on BSA. The NCI – H441 cell culture seeded on BSA demonstrated a similar depolarisation membrane response with a relative membrane change of –41.82 ± 25.40 %. Overall, the NCI-H441 cells cultured on CIV displayed a trend of hyperpolarisation membrane response to cyclic mechanical stimulation. During experiment i) the mean relative change of 98.00 ± 92.90 % was evident and in experiment ii) 59.8 ± 38.10 %. The cell populations cultured on FN demonstrated relative change of 112.00 ± 58.00 % and 75.70 ± 77.60 % to cyclic mechanical stimulation in experiments i) and ii) respectively.

Kruskall –Wallace analysis of the median relative percentage changes in membrane potential of cyclical mechanically stimulated NCI – H441 cells seeded on BSA, CIV and FN, demonstrates a statistical significance of $p = 0.009$, $p = 0.013$ for experiments i) and ii). This suggests a significant difference between the responses elicited on the matrices.

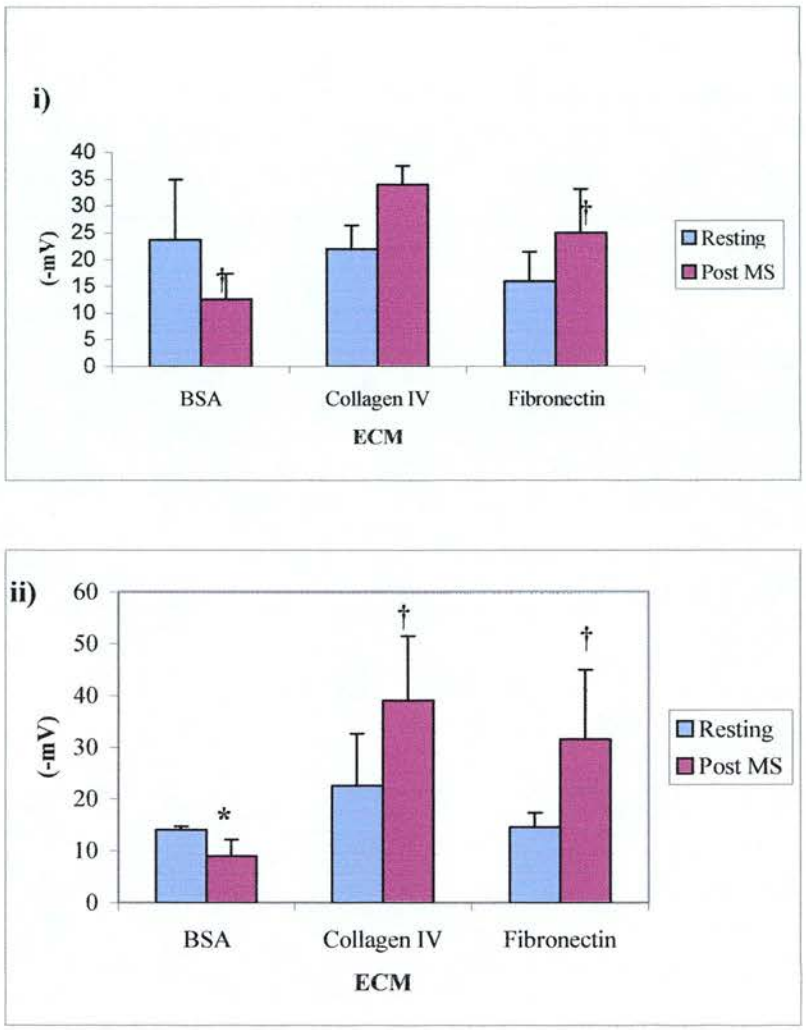

Figure 4.11. The effect of extracellular matrix protein coated substrata on the membrane potential of NCI – H441 mechanically stimulated at 0.25 Hz, 5000με. The membrane potentials of NCI-H441 cells cultured on bovine serum albumin(BSA), collagen IV and fibronectin, were measured prior and following cyclic mechanical stimulation. Graphs are representative of two experiments i) and ii), + 1 Stdev, n=5. $p < 0.05$ *paired t-test, † Mann-U-Whitnney test

Table 4.3 The effect of extracellular matrix protein coated sustrata on the membrane potential of NCI – H441 mechanically stimulated at 0.25 Hz, 5000με

i)

		Membrane potential (-mV) (mean ± SD)			
Substratum	n	Resting	Post MS	% Relative Change	P - value
BSA	5	23.67 ± 11.33	11.50 ± 4.90	-35.1 ± 25.4	0.0163†
Collagen IV	5	22.00 ± 4.30	34.00 ± 3.39	98.0 ± 92.9	0.054
Fibronectin	5	15.86 ± 5.52	25.00 ± 7.92	112.0 ± 58.0	0.0163†

		Membrane potential (-mV) (mean ± SD)			
Substratum	n	Resting	Post MS	% Relative Change	P - value
BSA	5	14.00 ± 0.707	9.00 ± 3.24	-41.82 ± 25.4	0.008
Collagen IV	5	22.60 ± 9.94	39.00 ± 12.51	59.8 ± 38.1	0.0122†
Fibronectin	5	14.60 ± 2.79	31.60 ± 13.37	75.7± 77.6	0.0350†

ii)

n = number of cells sampled, P – values calculated by a paired t- test, † = Mann – U – Whitney test

4.6 Discussion

The NCI –H441 cell line exhibits a number of classic respiratory epithelial cell characteristics. They express mRNA for the surfactant specific protein A. They also stain positive for alkaline phosphatase, surfactant specific proteins A and B and cytoplasmic cytokeratin. Under electron microsopic examination NCI –H441 cells display the morphological characteristics of human primary type II pneumocytes; apical microvilli and lamellar bodies.

Considering the morphological and phenotypic similarities between the human type II pneumocytes and the NCI – H441 cell line, it can be suggested that this cell line makes a good substitute cell model for primary type II pneumocyte cultures. Under the scrutiny of electron microscopy apical microvilli and dark osmiophillic lamellar bodies are evident (Figure 4.7). The NCI-H441 cell line stains positive for alkaline phosphatase activity; a recognised marker of the type II pneumocyte (190). Also there is positive evidence of the expression of SP-A mRNA and cytoplasmic production of SP-A and SP-B proteins (Figure 4.4.), by NCI-H441 cells. The fact that only a minority of the NCI –H441 cells within the surfactant protein immunocytochemistry stained positive does not mean that the majority of cells do not produce surfactant specific proteins A and B. It might be that the antibodies are not sensitive enough to show small quantities of protein in this immunocytochemical study procedure. Alternatively, the cell line could be expressing the mRNA but not necessarily produce the respective proteins. Additional studies using immunogold electron microscopy may be of value to further characterise NCI – H441. The majority of NCI-H441 cells stain positively by immunocytochemistry for cytokeratin expression, which is a typical marker of the epithelial cell but is not specific.

Primary human type II pneumocytes cultured on fibronectin display a significant membrane hyperpolarisation response to 20 minutes of cyclic mechanical strain at 5000 με, 0.25 Hz. In addition, the comparable responses observed between a primary culture of human type II pneumocytes and NCI –H441 to 0.25 Hz, 5000 με, 20 minutes of mechanical stimulation add weight to this conclusion and demonstrate a potential for the future use of this cell line in pulmonary epithelial cell mechanotransduction investigations.

Electrophysiological impalement of NCI – H441 is easier if cells are seeded in medium supplemented with serum. There was no statistically significant difference in resting membrane potential of cells cultured on the different substrata. The NCI –H441 cell line demonstrates a membrane hyperpolarisation response to twenty minutes cyclic mechanical stimulation of 5000 με, 0.25 Hz when seeded on collagen IV and fibronectin. However, membrane depolarisation responses were elicited within populations of NCI-H441 cultured on BSA coated substratum. The different responses elicited in response to substrata could be a reflection of the type of cell to substrate interaction experienced by the cell. Alternatively, or in addition, the responses could be a reflection of the differentiation status of the cells. Cyclic mechanically stimulated fibroblasts demonstrate a depolarisation response under conditions, which elicit a membrane hyperpolarisation in chondrocytes (92). Membrane potential itself is a natural phenomena occurring as the result of the dynamic movement of ions and molecules across the plasma membrane of a cell. The membrane responses to mechanical stimulation of chondrocytes have been attributed to small conductance calcium activated potassium channels and sodium tetrodoxtin ion channels. Whether or not similar ion channels are responsibility for the membrane responses of mechanically stimulated NCI – H441 and type II pneumocytes has yet to discovered.

Over the past decade, mechanotransduction in vitro studies utilising chondrocytes and osteoblasts have successfully elucidated novel signalling pathways for the transduction of molecular information to and from the cells as a result mechanical strain (93; 103; 127). Consequently, this body of work has led to the discovery of key differences in these signalling pathways in instances of disease, such as osteoarthritis (103; 203-205). The main features of this chondrocyte mechanotransduction model are: the role of the integrin $\alpha 5\beta 1$, stretch – activated ion channels; and small conductance calcium - activated potassium and sodium tetradrodoxtin ion channels, the autocrine/ paracrine action of interleukins 4 and IL-1β, increased expression of aggrecan mRNA, and decreased matrixmetalloproteinase 3 mRNA phosphorylation of the tyrosine kinase focal adhesion kinase (FAK125), paxillin and β - catenin; the involvement of phospholipase C and protein kinase C (206).

Monitoring membrane potential of cells subject to mechanical strain has been pivotal in the elucidation of signalling mechanisms in osteoarticular mechanobiology. Previous studies on osteoblasts (93; 207)chondrocytes (107) and fibroblasts (92) in vitro demonstrate significant

changes in membrane potential occur following cyclic mechanical stimulation of these cells. Also evidence from the human foetal intestinal epithelial cell line Intestinal 407 demonstrates a hyperpolarisation membrane response to mechanical stimulation (208), which suggests there is potentially a use for the exploitation of the methodology in other cell systems such as pulmonary epithelium.

The exact significance of the membrane potential responses elicited by cyclic mechanical strain is unknown. However, the possibility exists that the phenomena of membrane potential change could be a viability effect of cell function (207). Previous studies investigating the anti-apoptotic actions of Bcl-2 in the human B-cell lymphoma cell line PW and leukemia cell line HL60 demonstrated hyperpolarisation of the resting membrane potential was associated with a resistance to apoptosis (209). Similarly, resistance to apoptosis by a viability promoting protein of the Bcl-2 family, mcl-1, was mediated by membrane hyperpolarisation that had been induced by K^+ channel activation. TNF - α, an apoptosis - inducing agent, has been shown to cause membrane depolarisation responses in oligodendrocytes, by reducing the expression of K^+ channels (210). The main contributor to the resting membrane potential of a cell is the Na^+/K^+ ATP ase ion pump (211). The activity of a Na^+/K^+ ATP ase ion pump increases, and subunits have been shown to be translocated from intracellular stores to the basolateral membrane of murine lung epithelial cell line MLE-12 in response to cyclic mechanical strain (73). A single static strain of primary rat type II pneumocytes enhances secretion of phosphatidylcholine and transiently increases cytoplasmic concentrations of calcium ions (4). Subsequently, in vitro, rat type II pneumocyte, have demonstrated highly sensitive threshold levels of intracellular calcium in the secretion of lamellar bodies (212).

The different membrane potential responses elicited in mechanically stimulated NCI – H441 cells by the presence of an ECM protein coated substrata suggest that interactions with ECM proteins could indeed play a regulatory role in type II pneumocyte mechanobiology. The involvement of a mechanoreceptor in alveolar epithelial mechanotransduction awaits further investigation. In vivo ECM contributes to a number of cellular functions such as proliferation, differentiation, apoptosis, and organogenesis. Previously studies have demonstrated that epithelial cells from several different tissues require ECM proteins to suppress apoptosis. Cells cultured without an ECM coated substrata more readily undergo apoptosis than cells cultured on an adhesive ECM - coated sustratum (213). Therefore, ECM is thought to contribute survival signals for cells, in addition to those from specific growth factors, cytokines and interleukins. Rodent type II pneumocyte enriched populations

maintained on a tissue culture substratum rapidly lose their differentiated phenotypic characteristics, such as the expression of surfactant specific protein mRNAs (129; 214; 215), (176).

The complexity of respiratory movements and cell biology of the alveolus necessitate the development of robust physiological in vitro assays of the normal alveolus. The inability to maintain isolated human type II pneumocytes in a differentiated phenotype hampers the validity of study into pulmonary disease with in vitro models.
Current postulation is that type II pneumocytes proliferate and transdifferentiate into type I pneumocytes following injury to the alveolus. However, despite repeated examples of the plasticity of rat type II pneumocyte differentiation in response to strain (11; 216), (217) contraction (70), or different substrata (38; 145; 218), little has been achieved with human in vitro cultures. The assumption that all advances achieved with rodent type II pneumocyte culture will be applicable to human respiratory epithelium could be misleading. Already it has been shown that the antibody raised against rat type I pneumocyte antigen RTI46, does not recognise the equivalent human antigen HTI56 (217) nor does the rat type II pneumocyte specific antibody mmc4 recognise human type II cells (M^{c}Elroy personal communication). The cytokeratin expression profile of rodent alveolar epithelium differs markedly from that of a human (182). In addition to a quadrapedal gait, rodents lack an entire order of airways (219), and their respiratory frequency and amplitude would differ according to their needs. The normal quiet breathing rate of a rat is ~ 40 breaths per minute (0.66 Hz), whereas for a human is approximately 15 breaths per minute (0.25 Hz). The changes in rat epithelial basement membrane surface area and lung volume are described as 13-30 % between inflation at functional residual capacity (RFC) to 75 – 100 % total lung capacity (TLC) (46). In human studies between RFC – TLC estimates of distension and relaxation are increases of 16 % (220) to 34 % (45) alveolar surface area. Many investigators apply non – physiological respiratory frequencies (65; 198) or static strain (4) to their cultures, or fail to scale amplitude of strain according to the original species' of the cell culture under investigation. The quantity of strain postulated to be experienced by type II pneumocytes in vivo during normally breathing is 1 - 5 % (221), which was applied to the cultures within this study.

The human type II pneumocyte cell line NCI –H441 cultured on FN, demonstrates a significant membrane hyperpolarisation response to cyclic mechanical strain, which is comparable to human primary isolated type II pneumocytes stimulated in a similar fashion. The in vitro mechanical strain system utilised within this series of experiments offers unique

opportunities to investigate the apparatus of mechanotransduction in alveolar epithelium during normal breathing, and potentially, lung injury.

CHAPTER 5 THE EFFECT OF CYCLIC MECHANICAL STRAIN ON GENE EXPRESSION AND SURFACTANT SPECIFIC PROTEIN LEVELS IN THE NCI – H441 CELL LINE

5.1 The effect of cylic mechanical strain on gene expression and surfactant protein levels in the NCI – H441 cell line

Currently, belief is that the pulmonary epithelium plays a pivotal role in pro – inflammatory responses to injury and infection (13; 222). Surfactant specific protein and cytokines are important in lung epithelium homeostasis and remodelling in disease processes. Mechanical stimulation and extracellular matrix content may affect the capability of the epithelium to produce these molecules.

The alveolar epithelium possesses multiple homeostatic functions within the alveolus (13). It is widely accepted that type II pneumocytes in vivo act as stem cells of adult alveolar epithelium (10; 13). Type II pneumocytes maintain alveolar fluid balance. Membrane – associated water channels and ion pumps and in the regulation fluids and serum proteins within the alveolus (13). The production and secretion of surfactant by the type II pneumocyte acts to lower surface tension and prevent alveolar collapse (223; 224). Previous studies of type II pneumocytes co – cultured with fibroblasts have demonstrated an apoptotic effect of surfactant lipids. However, a partial reversal of fibroblast apoptosis was achieved with the application surfactant specific protein – A (SP – A) (225). Surfactant specific proteins SP – A and SP –D produced by type II pneumocytes are able to participate in the innate immune response and the removal of pathogens (226; 227). Recent studies have also reported evidence of the bacteriostatic function of the surfactant specific proteins SP – A and SP – D, toward Gram - negative bacteria by increasing the membrane permeability of the pathogen (228).SP - A potentially regulates oxygen radical release (229), and nitric oxide from macrophages (230).

The presence of particles within in vitro cultures of rat type II pneumocyte cultures induces the secretion of interleukin – 1β. This cytokine increases the expression of adhesion molecules, promotes chemotaxis of macrophages and neutrophils and enhances the activation of other immune cells (231). Evidence from previous studies in vitro suggests that type II pneumocytes potentially also produce the cytokines IL – 6 and IL – 8, which potentiate the differentiation of leukocytes (68; 232; 233). The discovery of MHC class II receptor expression on type II pneumocytes suggests a role in T –lymphocyte activation (234). Zissel and coworkers supported this suggestion with a human type II pneumocyte in vitro study (153). Previous studies show that type II pneumocytes inhibit proliferation of lymphocytes without modulating the activation state (235). Primary human type II pneumocytes and the cell line A549 can be stimulated with TNF - α which induces secretion of MCP – 1 and RANTES in vitro. Simultaneously the expression of

the adhesion molecules ICAM 1 and VCAM are increased. These characteristics could promote the migration of monocytes (236). In 1988 von Berthman and coworkers reported increased amounts of inflammatory cytokines TNF – α and IL – 6 with mechanical ventilation of isolated murine lungs (237). A rat model of ventilator – induced lung injury demonstrates the increased release of the inflammatory cytokines TNF – α and MIP – 2 (238).

Previous studies noted marked alterations in the basal lamina of human fibrotic lung. Compared to normal lung, fibrotic lungs possess an increased deposition of the extracellular protein fibronectin (35). Increased deposition of collagens III and V are also seen within fibrotic lung samples (31). In vitro investigation of foetal rat lung cells has demonstrated the differential regulation of mRNA and protein synthesis as the result of mechanical stimulation. Cyclic mechanical stimulation of the rat lung cells leads to a reduction in procollagen – α1 (I) and biglycan, an increase in collagen – α (IV) and α2 mRNA. The levels of laminin β mRNA remained constant in response to mechanical strain. However, an increase in the production of type I, IV collagen and biglycan was detected (57).

The main aims of the following work were to identify the expression of interleukin (IL) – 1β, IL 4, IL – 6, IL – 8, SOCS3, SP – A and within the NCI – H441 cell line, and to ascertain the influences of fibronectin and mechanical strain on the gene expression of these molecules.

5.2 Basal gene expression levels by NCI – H441 cell Line

Samples of total RNA from NCI – H441 cells previously cultured on tissue culture plastic were initially probed for IL - 1β, IL – 4, IL – 6, IL – 8, SP – A and SOCS3 gene expression with two step multiplex real time polymerase chain reactions (RTPCR). Details of the average cycle threshold values are given within Table 5.1.

Detail of extracting RNA from monolayer cell culture is given in section 2.8.1. Extracted RNA samples were DNase treated as detailed in section 2.8.4. Subsequent to DNase - treatment a standard GAPDH polymerase chain reaction (PCR) and agarose gel electrophoresis was run on all samples to check for contamination as detailed in sections 2.8.6. – 7,. The process of probing samples via TaqMan® real time polymerase chain reactions is detailed in section 2.9. Details of the average cycle threshold values are given within Table 5.1. The NCI –H441 cell line was found to express IL –4, IL –6, IL – 8, SP –A and SOCS3 mRNA, but not IL – 1β.

Gene	Gene Average Ct	GAPDH Average Ct	ΔCt gene-GAPDH
IL - 1β	40*	27	-
IL - 4	22	16.11	5.885
IL - 6	27	16	10.96
IL - 8	27	21.3	11.665
SOCS3	29	13	15.825
SP - A	27.75	14.71	12.95

Table. 5.1. Basal gene expression values of NCI – H441.

Samples of NCI – H441 cell line were probed for the basal expression of interleukin – 1 β (IL – 1β), IL – 4, IL – 6, IL – 8, suppressor of cytokine signalling 3 (SOCS3) and surfactant protein – A (SP- A). The values shown are expressed as relative to endogenous GAPDH gene expression, and normalised against the relevant reference. (n=2). * a Ct value of 40 or above is indicative of no amplification.

5.3 The effect of culture on fibronectin coated substrata on NCI – H441 cell line gene expression

RNA samples derived from NCI – H441 cells seeded on FN, cultured over a timecourse of five days were examined for the levels of relevant positive gene expression.
NCI –H441 cells were seeded at a concentration of 5 x 10^4 cells/ml of DMEM: F12 medium supplemented with 10 % FBS, 2 mM L – glutamine, 100 I. U. /ml penicillin and 100 µg/ml streptomycin onto fibronectin (FN) coated 58 mm petri dishes and cultured over a period of five days at 37°C, 5 %CO_2. RNA was extracted from NCI –H441 cells immediately before seeding, at twenty – four hours, three and five days following seeding. DMEM:F12 medium supplemented with 10 % FBS, 2 mM L – glutamine, 100 I. U./ml penicillin and 100 µg/ml streptomycin was replaced every 48 hours. Detail of extracting RNA from monolayer cell culture is given in Section 2.8.1 and the DNase treatment of RNA in Section 2.8.4. RNA over the timecourse were examined for levels of the relevant positive gene expression.

The relative quantitative analysis of levels of cytokine gene expression, in NCI – H441 cells on a FN coated substratum, over a five-day time course demonstrated an overall reduction in all genes probed for. At timepoint 6 hours, the relative level of IL – 4 mRNA expression was at a value of 1.60, which decreased to 0.09 at 24 hours. An outlier reading of 64.02 was gained at 72 hours and a further value of 0.05 was detected at 120 hours. The overall trend for the expression of relative IL – 4 mRNA for the timecourse was a decrease (Fig 5.1.). In the instance of IL – 6 mRNA expression at 6 hours a relative level of 0.644 was measured and at 24 hours the level of expression had decreased to 0.227. The relative values of IL –6 mRNA expression levels were 0.007 and 0.003 at the 72 and 120 hour timepoints respectively (5.2.). The pattern of IL – 8 mRNA expression also followed a decline in relative values. At the 6 hour timepoint a value of 0.785 was measured. Following 24 hours the relative value of IL- 8 mRNA declined to 0.179 and at 72 hours further declined to 0.012. After 120 hours the relative level of IL – 8 mRNA was 0.008 (Figure 5.3). Surfactant specific protein A (SP – A) mRNA relative expression levels at the 6-hour timepoint were 0.537 and declined to 0.035 after 24 hours. The relative levels of SP – A mRNA expression plateaued at values of 0.040 and 0.041, at 72 and 120 hours respectively (Figure 5.4.).

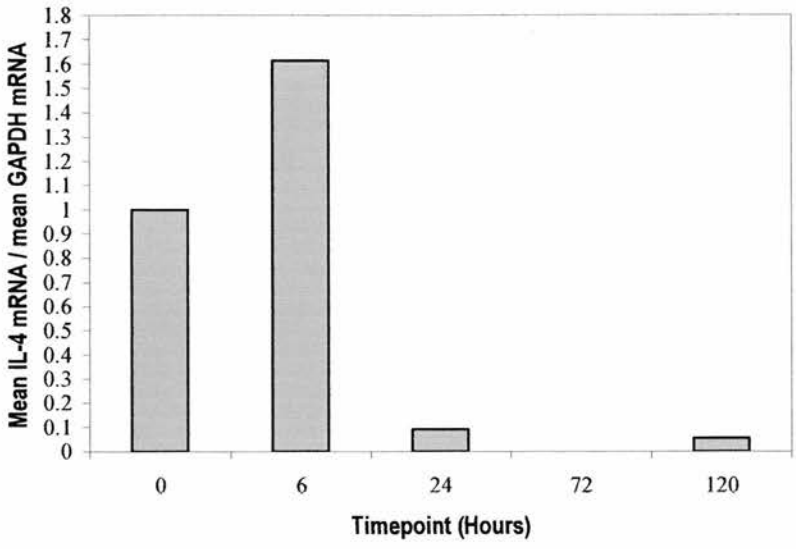

Figure 5.1. The effect of fibronectin substratum in NCI-H441 in cultured, over five days on IL-4 mRNA gene expression. The gene expression levels are representative of the intensity of IL – 4 mRNA probe, relative to an endogenous GAPDH reference. Total RNA was extracted at timepoints of 0, 6, 24, 72 and 120 hours from monolayer cultures of NCI – H441 cells adherent to a fibronectin coated substratum, and subject to real time polymerase chain reaction, to probe the levels of IL – 4 mRNA. (n = 1)

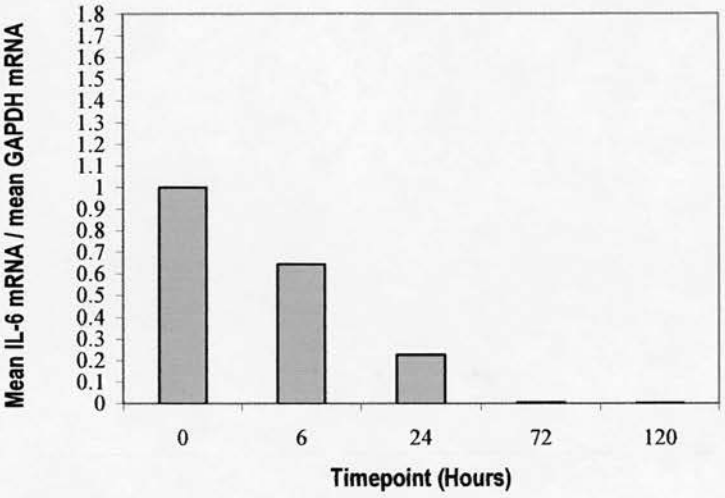

Figure 5.2. The effect of fibronectin substratum in NCI-H441 in cultured, over five days on IL-6 mRNA gene expression. The gene expression levels are representative of the intensity of IL – 6 mRNA probe, relative to an endogenous GAPDH reference. Total RNA was extracted at timepoints of 0, 6, 24, 72 and 120 hours from monolayer cultures of NCI – H441 cells adherent to a fibronectin coated substratum, and subject to real time polymerase chain reaction, to probe the levels of IL – 6 mRNA. (n = 1)

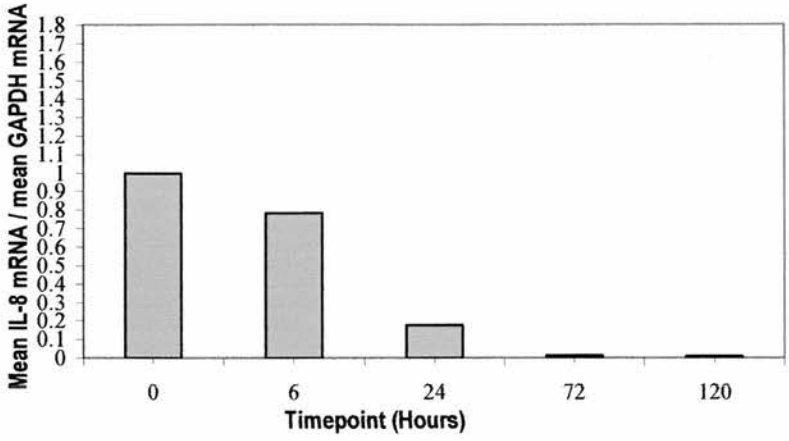

Figure 5.3. The effect of fibronectin substratum in NCI-H441 in cultured, over five days on IL-8 mRNA gene expression. The gene expression levels are representative of the intensity of IL – 8 mRNA probe, relative to an endogenous GAPDH reference. Total RNA was extracted at timepoints of 0, 6, 24, 72 and 120 hours from monolayer cultures of NCI – H441 cells adherent to a fibronectin coated substratum, and subject to real time polymerase chain reaction, to probe the levels of IL – 8 mRNA. (n = 1)

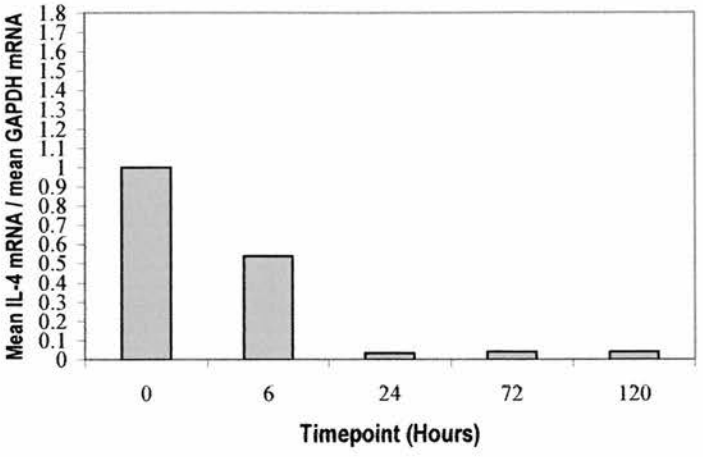

Figure 5.4. The effect of fibronectin substratum in NCI-H441 in cultured, over five days on SP –A mRNA gene expression. The gene expression levels are representative of the intensity of SP – A mRNA probe, relative to an endogenous GAPDH reference. Total RNA was extracted at timepoints of 0, 6, 24, 72 and 120 hours from monolayer cultures of NCI – H441 cells adherent to a fibronectin coated substratum, and subject to real time polymerase chain reaction, to probe the levels of SP – A mRNA. (n = 1)

5.4 The effect of cyclic mechanical stimulation on gene expression levels in NCI –H441

The effect of cyclic mechanical stimulation on the gene expression levels of IL – 6, IL – 8, SP – A, SOCS3 was investigated in NCI - H441 cells cultured on a BSA coated substrata. NCI – H441 cells were seeded onto 58 mm petri dishes coated with bovine serum albumin (BSA) at a density of 5 x 10^4 cells/ml of DMEM:F12 medium supplemented with 10 % FBS, 2 mM L – glutamine, 100 I. U./ml penicillin and 100 μg/ml streptomycin. Subsequent to overnight incubation at 37°C, 5 %CO_2, dishes were carefully rinsed twice with DMEM:F12 medium supplemented with 2 mM L – glutamine, 100 I. U./ml penicillin and 100 μg/ml streptomycin. The NCI –H441 cultures were subject to cyclic mechanical stimulation of 5000 microstrain (με), at a frequency of 0.25 Hz (2 seconds on and 2 seconds off), for twenty minutes. RNA was extracted from the mechanically stimulated cell cultures and the matching unstimulated controls over a timecourse of twenty – four hours. Detail of extracting RNA from monolayer cell culture is given in Section 2.8.1 and the DNase treatment of RNA in Section 2.8.4

NCI – H441 cells cultured on BSA coated substratum were found to possess a relative level of 0.687 immediately following cyclic mechanical stimulation, compared to resting control cell cultures 1.513 (Fig 5.5). An hour after stimulation of the cell cultures the relative level of IL –6 mRNA expression increased to 2.078 versus the control value of 1.322. Three hours after the application of cyclic mechanical strain the mean relative value of IL- 6 mRNA expression in stimulated cells is 1.292 with a mean value 0.128 in control NCI –H441 cell cultures. At 24 hours the levels of IL –6 mRNA expression were 1.505 in stimulated cell cultures compared to 2.976 of the control NCI – H441 cells cultured on a BSA coated substratum.

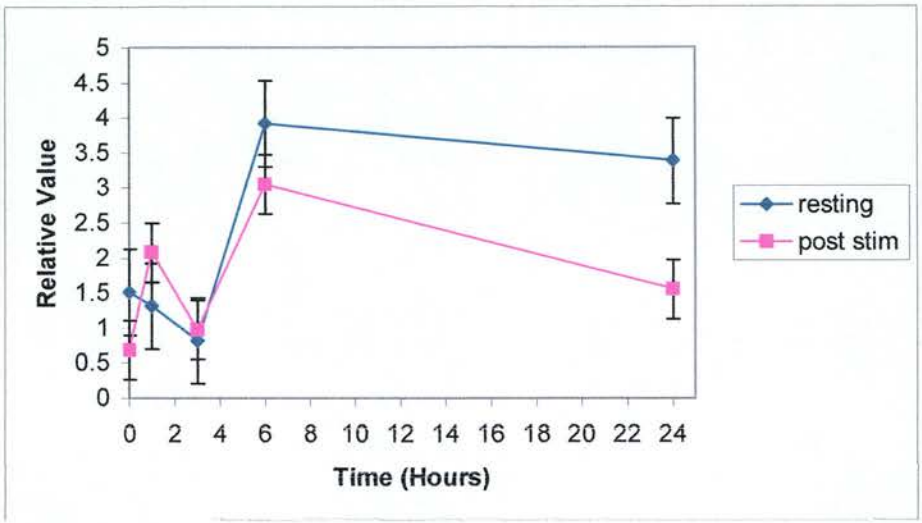

Figure 5.5 Effects of Cyclic Mechanical Stimulation on Gene Expression of IL – 6, in the NCI – H441 Cell Line, On a BSA coated Substratum. The gene expression levels are expressed as relative values of IL –6 intensity to the endogenous GAPDH reference ± SEM. RNA was extracted immediately following cyclic mechanical stimulation (0 timepoint) and at timepoints of 1, 3, 6, 24 hours, from monolayer cultures of NCI-H441 cells (stimulated) adherent to BSA coated substrata. NCI –H441 monolayer cultures not subject to mechanical strain (resting) acted as controls and RNA was isolated at the relevant time points (n = 3).

In the case of IL –8 mRNA the pattern of gene expression of resting NCI –H441 cell cultures versus stimulated NCI – H441 cell cultures is inverse throughout the 24 hours investigated (Fig 5.6). Immediately following cyclic mechanical stimulation (timepoint 0) the level of IL – 8 mRNA is 0.452 compared with the relative IL –8 mRNA expression levels in resting cultures of 2.165. After 1 hour the relative gene expression levels of IL –8 mRNA increases to 1.240, whereas the relative gene expression levels in resting cultures decrease to 0.641. Similarly, at 3 hours, stimulated cell cultures decrease to 0.637 compared to an increase in IL – 8 mRNA expression levels in unstimulated cell cultures to 2.131. At 6 hours the stimulated cell cultures have elevated levels of IL – 8 mRNA expression, with a value of 2.265, compared with an unstimulated value of 0.682. At the 24 hours the levels of IL – 8 mRNA expression in stimulated NCI – H441 cell cultures falls to 0.132 with unstimulated cell cultures, having a value of 0.821.

The trend of surfactant protein –A (SP –A) mRNA expression in NCI –H441 cell cultures subject to cyclic mechanical stimulation approximates closely with the relative gene expression levels demonstrated by unstimulated NCI – H441 cell cultures over a 24 hour timecourse (Fig 5.7). Immediately following the application of cyclic mechanical stimulation the NCI – H441 cells cultured on BSA had a relative value of SP –A mRNA expression of 0.749 compared to 0.751 in resting control cell cultures. Following an hour the stimulated population of cells possessed a value of 0.784 versus the control mean relative value of 0.828 in resting cell cultures. At 3 hours the mean relative value of SP – A mRNA expression was 0.780 and the resting control of the populations sampled was 0.999. Cell cultures subject to cyclic mechanical stimulation possessed a mean relative value of 0.624 at 6 hours compared to 0.721 of control NCI –H441 cell cultures. Finally, at 24 hours mean relative values of 0.422 and 0.509 were measured respectively in stimulated and resting control cultures

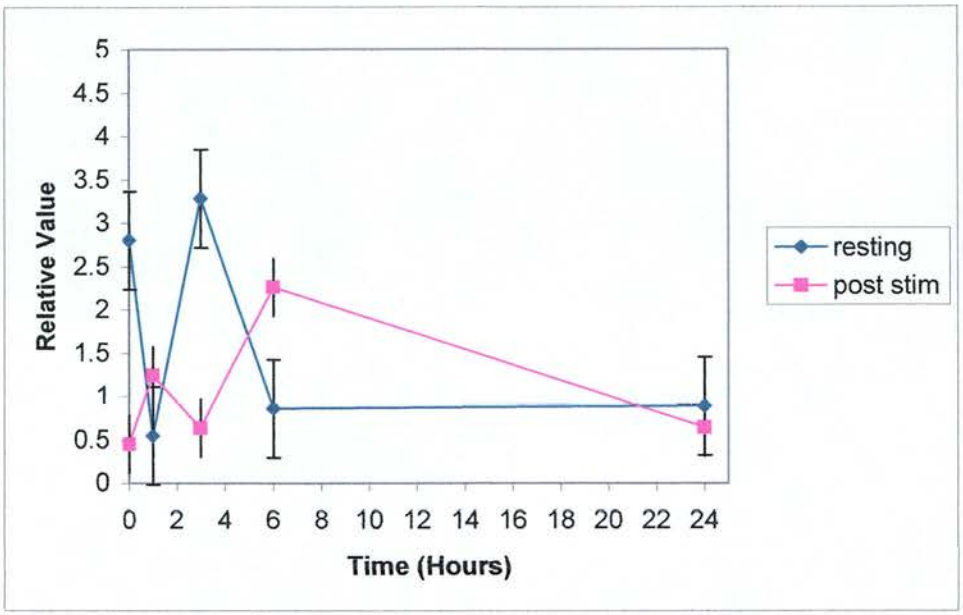

Figure 5.6 The effect of cyclic mechanical stimulation on the gene expression levels of IL – 8 in NCI – H441 cell line on a bovine serum albumin coated substratum. The gene expression levels are expressed as relative values of IL –8 intensity, to the endogenous GAPDH reference ± SEM. RNA was extracted immediately following cyclic mechanical stimulation (0 timepoint) and at timepoints of 1, 3, 6, 24 hours, from monolayer cultures of NCI-H441 cells (stimulated) adherent to BSA coated substrata. NCI – H441 monolayer cultures not subject to mechanical strain (resting) acted as controls and RNA was isolated at the relevant time points (n = 3).

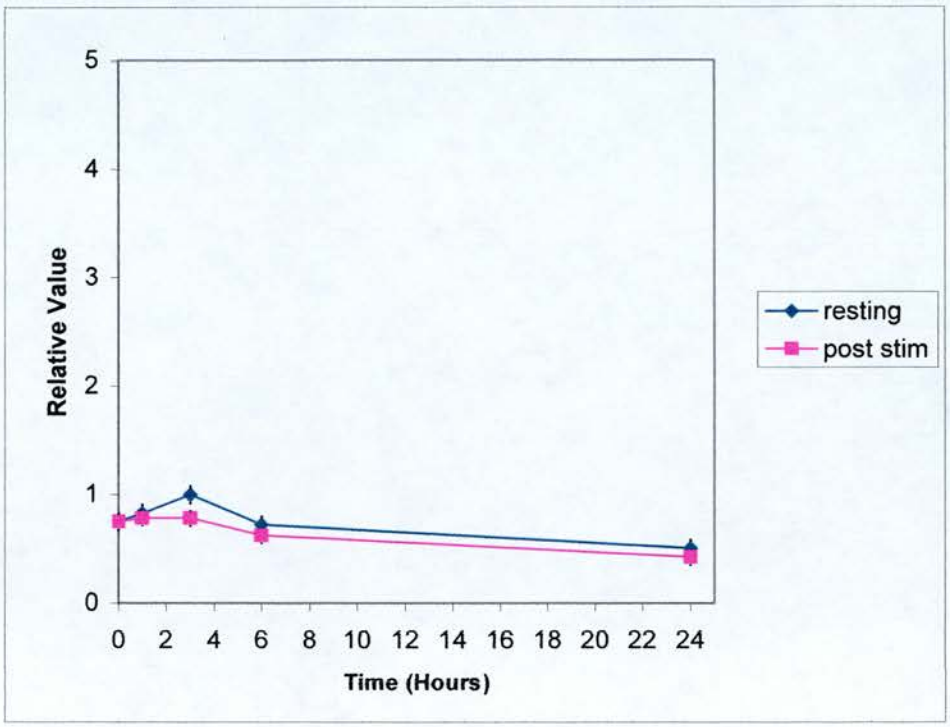

Figure 5.7 The effect of mechanical stimulation on the gene expression of SP – A in NCI – H441 cell line, on a bovine serum albumin coated on substratum. The gene expression levels are expressed as relative values of SP –A intensity, to the endogenous GAPDH reference ± SEM. RNA was extracted immediately following cyclic mechanical stimulation (0 timepoint) and at timepoints of; 1, 3, 6, 24 hours, from monolayer cultures of NCI-H441 cells (stimulated) adherent to BSA coated substrata. NCI –H441 monolayer cultures not subject to mechanical strain (resting) acted as controls and RNA was isolated at the relevant time points (n = 3).

An inverse pattern of relative suppressor of cytokine signalling –3 (SOCS3) gene expression is demonstrated in cyclic mechanical stimulated NCI – H441 cell cultures in comparison to unstimulated NCI – H441 cell cultures over a 24 hour time period (Fig 5.8). Subsequent to the application of cyclic mechanical strain a mean relative value of 0.543 SOCS3 mRNA was obtained, versus 0.745 in control resting NCI – H441 cell cultures. At one hour, the mean level of SOCS3 mRNA is 0.656 within stimulated cultures and 1.515 in resting control cell cultures of NCI – H441. At 3 hours, expression within stimulated cell cultures is 0.963 compared with 0.953 in resting control NCI – H441 cell cultures. However, at the 6-hour timepoint in stimulated cell cultures the mean relative value is 2.525 versus 0.303 within the resting control cell population sampled. Finally, at 24 hours similar values of 0.578 and 0.555 were obtained for the stimulated and resting control NCI – H441 cell populations respectively,

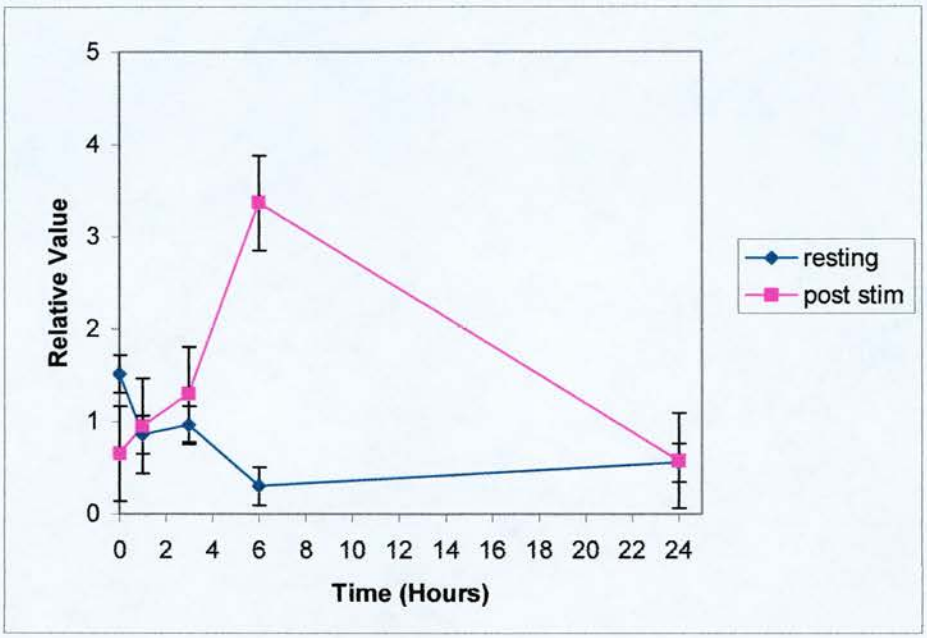

Figure 5.8 The effect of cyclic mechanical stimulation on the gene expression of SOCS3 in NCI –H441 cell line, on a bovine serum albumin coated substratum. The gene expression levels are expressed as relative values of SOCS3 intensity, to the endogenous GAPDH reference ± SEM. RNA was extracted immediately following cyclic mechanical stimulation (0 timepoint) and at timepoints of 1, 3, 6, 24 hours, from monolayer cultures of NCI-H441 cells (stimulated) adherent to BSA coated substrata. NCI – H441 monolayer cultures not subject to mechanical strain (resting) acted as controls and RNA was isolated at the relevant time points (n = 3).

5.5 The effect of cyclic mechanical stimulation on gene expression levels in NCI –H441 cultured on fibronectin

The effect of cyclic mechanical stimulation on the gene expression levels of IL – 6, IL – 8, SP – A, SOCS3 were investigated in NCI - H441 cells cultured on a FN coated substrata. The details of the experimental layout are as in Section 5., with the exception of the FN coated substrata of the petri dishes, which are given in Section 2.1.

Immediately following 20 minutes of cyclic mechanical strain on NCI –H441 cells cultured on a fibronectin substratum displayed a relative IL – 6 mRNA expression level of 1.117 versus a control population of 0.395. One hour subsequent to stimulation the relative mRNA expression level of IL – 6 in NCI –H441 cells had risen to 1.472, with the unstimulated control population of NCI –H441 cell line possessing a relative value of 1.618. At the timepoint of 3 hours, following cyclic mechanical stimulation the relative value of 0.726 within the stimulated NCI – H441 cell populations compared with the unstimulated control value of 0.582. Six hours after cyclic mechanical stimulation the relative mRNA expression level of IL –6 were 0.958 and 0.552 within the stimulated and unstimulated control NCI – H441 populations respectively. Twenty – four hours following cyclic mechanical stimulation a mean relative value of 0.499 was obtained from stimulated cells versus a mean relative value of 1.040 within the unstimulated control NCI – H441 cell populations (Fig. 5.9)

For IL – 8 gene expression, a mean relative value of 3.485 was detected from cyclic mechanical stimulated NCI –H441 cells, immediately following stimulation. However, unstimulated cells yielded a mean relative value of 12.759. One hour following cyclic mechanical stimulation the mean relative IL – 8 mRNA value of 19.723 was measured within stimulated cell populations compared with 4.400 with the unstimulated NCI – H441 cell populations (Fig 5.10). Further values at later timepoints were not ascertained .

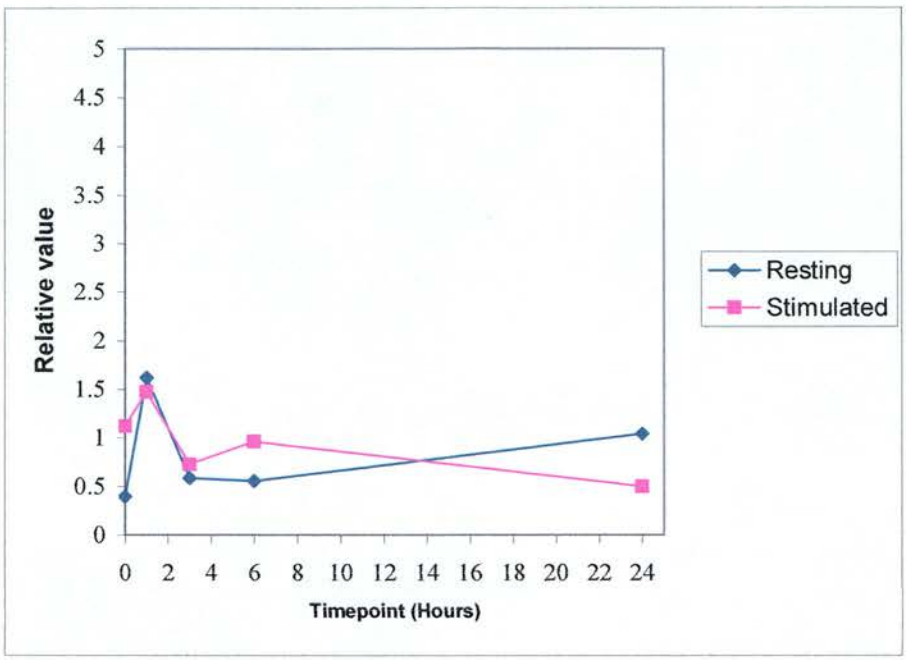

Figure 5.9 The effect of cyclic mechanical stimulation on gene expression of Il – 6, in the NCI – H441 cell line, on a fibronectin coated substratum. The gene expression levels are expressed as relative values of IL –6 intensity, to the endogenous GAPDH reference. RNA was extracted immediately following cyclic mechanical stimulation (0 timepoint) and at timepoints of 1, 3, 6, 24 hours, from monolayer cultures of NCI-H441 cells (stimulated) adherent to BSA coated substrata. NCI –H441 monolayer cultures not subject to mechanical strain (resting) acted as controls and RNA was isolated at the relevant time points (n = 2).

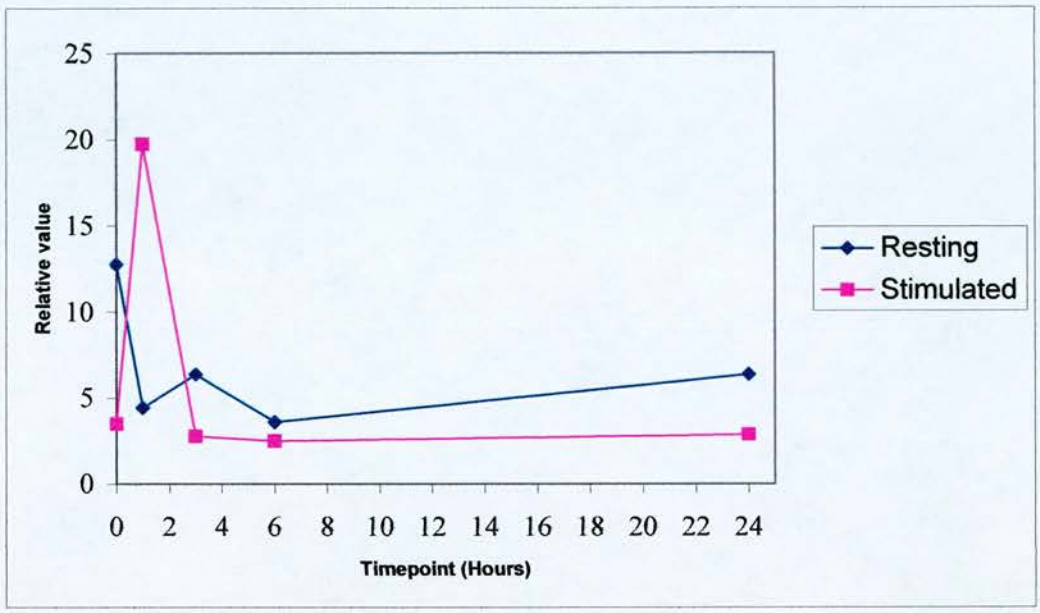

Figure 5.10 The effects of cyclic mechanical stimulation on gene expression of IL – 8, in the NCI – H441 cell line, on fibronectin coated substratum. The gene expression levels are expressed as relative values of IL –8 intensity to the endogenous GAPDH reference. RNA was extracted immediately following cyclic mechanical stimulation (0 timepoint) and at timepoints of 1, 3, 6, 24 hours, from monolayer cultures of NCI-H441 cells (stimulated) adherent to FN coated substrata. NCI –H441 monolayer cultures not subject to mechanical strain (resting) acted as controls and RNA was isolated at the relevant time points (n = 2).

The mean relative expression pattern over 24 hours of SOCS3 mRNA in NCI – H441 cells cultured on fibronectin is as follows (Figure 5.7). Immediately following cyclic mechanical stimulation the mean relative value of stimulated cells was 1.067 compared with a relative value of 0.856 for SOCS3 expression from unstimulated cells. The apparent mean relative mRNA expression value, an hour subsequent to cyclic mechanical stimulation was 0.860 versus 2.834 in stimulated and resting cells respectively. Three hours subsequent to cyclic mechanical stimulation within the stimulated and control populations of cells demonstrated mean relative values of 0.660 and 0.738, respectively. The NCI – H441 cells cultured on fibronectin 6 hours following subjection to cyclic mechanical stimulation demonstrated a mean relative value of 0.674 SOCS3 mRNA expression compared with a control mean value of 0.435. Finally, after 24 hours subsequent to cyclic mechanical stimulation the mean relative value of SOCS3 mRNA expression of 0.429 was from stimulated NCI – H441 cell populations. The mean relative value for SOCS3 mRNA expression in control populations in NCI – H441 cells cultured on fibronection-coated substrata subsequent to 24 hours was 0.507 (Fig. 5.11).

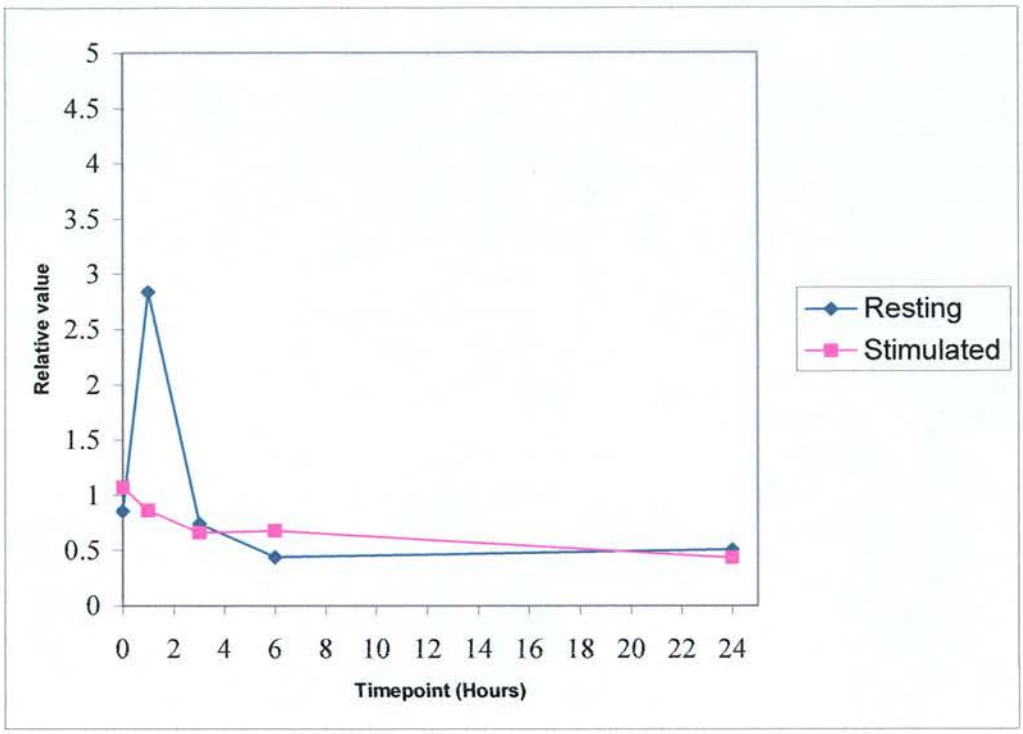

Figure 5.11 The effects of cyclic mechanical stimulation on the gene expression of SOCS3 in NCI – H441 cell line, on a fibronectin coated substratum. The gene expression levels are expressed as relative values of SOCS3 intensity, to the endogenous GAPDH reference. RNA was extracted immediately following cyclic mechanical stimulation (0 timepoint) and at timepoints of 1, 3, 6, 24 hours, from monolayer cultures of NCI-H441 cells (stimulated) adherent to FN coated substrata. NCI –H441 monolayer cultures not subject to mechanical strain (resting) acted as controls and RNA was isolated at the relevant time points (n = 2).

	Gene			
Cellular Substratum	**SP - A**	**IL - 6**	**IL - 8**	**SOCS3**
BSA	-	-	-	$\downarrow^{(6hours)}$
FN	n/d	-	$\uparrow(^{1hour})$ $\downarrow_{(3hours)}$	-

Table 5.2. Summary of the effects of cyclic mechanical stimulation on NCI –H441 cultured on fibronectin, on gene expression levels over twenty – four hours. (-) no change, (↑) increase in relative gene expression levels, (↓) decrease in relative gene expression level, (n/d) experiment not done. NCI – H441 cells cultured on two different substrata were subject to cyclic mechanical stimulation for 20 minutes and responses of selected genes over a twenty –four period monitored.

5.6 The effect of cyclic mechanical stimulation on surfactant specific protein – A in NCI – H441 cells

5.6.1 Cytoplasmic levels of SP A in cyclic mechanical stimulated NCI – H441

NCI – H441 cells were seeded onto 58 mm petri dishes coated with fibronectin (FN), at a density of 2 x 10^5 cells/ml of DMEM: F12 medium supplemented with 10 % FBS, 2 mM L – glutamine, 100 I. U. /ml penicillin and 100 μg/ml streptomycin. Subsequent to overnight incubation at 37°C, 5 %CO_2, dishes were carefully rinsed twice with DMEM: F12 medium supplemented with 2 mM L – glutamine, 100 I. U. /ml penicillin and 100 μg/ml streptomycin. The NCI –H441 cultures were subject to cyclic mechanical stimulation of 5000 microstrain (με), at a frequency of 0.25 Hz (2 seconds on and 2 seconds off), for twenty minutes. Protein extraction of NCI – H441 cell line, was undertaken as stipulated in Section 2.4.1. Details of the techniques utilised for resolution of surfactant specific protein – A (SP – A) are given in Section 2.5 –2.7.3. NCI – H441 protein extracts (40 μg per lane) were resolved by 12 % polyacrylamide SDS –PAGE under reducing conditions, transferred to PVDF, and probed with SP – A polyclonal (Chemicon AB3420) at a dilution of 1:1000. Subsequently, to check equal loading of protein, the membrane was stripped, washed, andreprobed with the loading control GAPDH mouse monoclonal antibody (Abcam clone: 6C5) at a dilution of 1: 5000. The x-ray films of both SP –A, and GAPDH were visualised under white light illumination.

Figure 5.12 depicts the relative values of cytoplasmic SP – A within stimulated and control NCI – H441 cell cultures whereas the western blots representative of the levels of SP –A and GAPDH are given within Figure 5.13. Immediately following cyclic mechanical stimulation the relative cytoplasmic value of SP – A in NCI – H441 cells cultured on fibronectin was 2.510. Unstimulated control NCI – H441 cells have a relative cytoplasmic value of SP – A of 2.210. Ten minutes subsequent to cyclic mechanical stimulation the relative cytoplasmic levels of SP – A are 1.679 and 2.589, within stimulated and control NCI – H441 cell populations respectively. Following 20 minutes NCI – H441 cells subject to cyclic mechanical stimulation the relative cytoplasmic value of SP –A was 1.218 versus 1.547 within control NCI – H441 cells, which were not stimulated. The relative value of cytoplasmic SP – A within NCI – H441 cell cultures, 60 minutes following subjection to cyclic mechanical was 2.631 versus 1.268 of unstimulated NCI – H441 control cells.

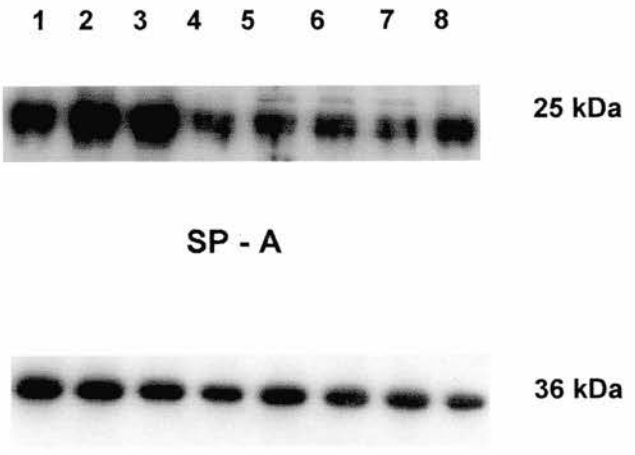

Figure 5.12 The effect of cyclic mechanical stimulation on cytoplasmic protein levels of SP – A in NCI – H441.

Monolayer cultures of the NCI –H441cell line cultured on fibronectin were subject to cyclic mechanical stimulation and cytoplasmic protein levels of SP – A subsequently analysed over a timecourse spanning one hour. Western blot was probed for SP –A with AB3420 (Chemicon), stripped and protein loading checked by probing for GAPDH with the clone 6C5 (Abcam). **1.** Negative control, **2.** 0 stimulated, **3.** 10 minutes negative control, **4.** 10 minutes following stimulation, **5.** 20 minutes negative control, **6.** 20 minutes following stimulation, **7.** 60 minutes negative control, **8.** 60 minutes following stimulation. (n = 1).

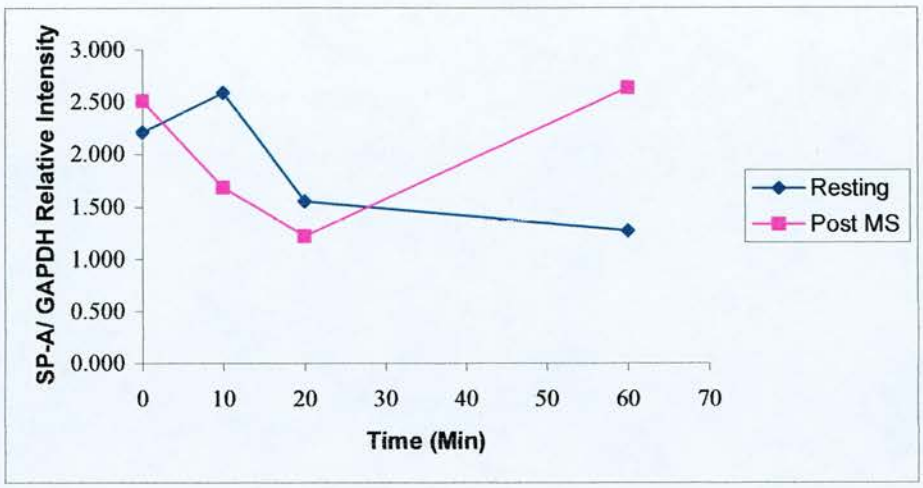

Figure 5.13The effect of cyclic mechanical stimulation on the cytoplasmic levels of SP – A in NCI – H441. The cytoplasmic levels of SP – A of NCI – H441 cells cultured on fibronectin and subject to cyclic mechanical stimulation were analysed. at timepoints immediately following cyclic mechanical stimulation, 10, 20, and 60 minutees following experimenttation, total cell protein was extracted. Levels of cytoplasmic SP – A are investigated with the aid of SDS – PAGE and western blotting. The values above are representative of the relative intensity ratio of SP – A bands to control GAPDH band intensity.

5.6.2 The effects of cyclic mechanical stimulation on SP – B secretion by the NCI – H441 cell line

Media samples were taken prior to and following mechanical stimulation of the NCI – H441 cell line cultures. Subsequently, quantification of SP – B protein levels in the samples was undertaken with Enzyme Linked Immunosorbent Assay (ELISA) by Dr Shirley O'Dea.

NCI-H441 cells cultured at 5 x 10^4 cells ml^{-1} on BSA, FN and CIV coated substrata in DMEM: F12, 1 % FCS, 1 % penicillin/streptomycin, 1 % L-glutamine, twenty –four hours, 37°C, 5 % CO_2. All cultures were rinsed with serum – free medium the following day and incubated for 30 minutes in serum –free media prior to experimentation. A cyclic mechanical strain regime of 0.25 Hz (2 seconds on, 2 seconds off) for 20 minutes was used with pressure pulses of 1.5 atm above atmospheric pressure, which resulted in a maximum of 5000 microstrain (με) on the base of the 58 mm plastic culture dish. Media samples were taken prior to and following mechanical stimulation, and at timepoints of 1, 3, 6 and 24 hours after mechanical stimulation.

A standard SP – B protein calibration graph was constructed using total protein extracted from a primary human lung sample; number 13963. Details of the protein extraction and total protein determination processes are given within Sections 2.4.1 and 2.4.2. respectively.

A limited number of media samples contained sufficient detectable protein to assay by sandwich SP – B ELISA. A surfactant specific protein - B concentration mean of 2175.862 ± 242.470 ng/ml was measured from resting NCI –H441 cells cultured on BSA. Immediately following mechanical stimulation the mean concentration of medium SP – B from NCI – H441 cultured on BSA was 113.108 ± 114.150 ng/ml. Within the sample taken from resting NCI –H441 cells cultured on fibronectin the concentration of surfactant specific protein – B was 113.210 ng/ml. In the instance of resting NCI – H441 cells cultured on collagen IV (CIV), the measured SP – B concentration was 243.360 ng/ml. The SP – B concentration from mechanically stimulated NCI – H441 cultured on CIV was 123.609 ± 66.26 ng/ml

5.7 Discussion

The analysis of the gene expression levels of the NCI – H441 cell line demonstrates that it bears similarities to current in vitro models and in vivo type II pneumocytes. The NCI –H441 cell line expresses IL – 4, IL – 6, IL – 8, SOCS3 and SP – A genes. The NCI – H441 cell line does not express the IL –1β gene. The expression of IL - 4 mRNA by the NCI – H441 cells cultured on a fibronectin coated sustratum is consistent with the detection of IL –4 mRNA during analysis of hyperplastic human type II pneumocytes from patients with chronic fibrosing alveolitis (CFA) (239). This is not the first evidence of a type II pneumocyte substitute expressing the IL –6 gene; previous investigations into rat type II pneumocytes gene expression demonstrate the expression of the cytokine IL – 6 (62; 232).

Similarly, known type II pneumocyte models are reported to demonstrate the expression of the IL – 8 gene. Witherden and coworkers demonstrated the basal protein secretion of moncyte interleukin (IL) – 8 from within in vitro cultures of human alveolar epithelium (240) et al. 2004). Mechanical strain of the human adenocarcinoma cell line A549 in vitro demonstrated the release of IL – 8 (61; 62). The presence of crocidolite asbestos fibres augments the release of IL – 8 during cyclic mechanical stimulation of the A549 cell line (61). Cyclic mechanical strain of the A549 cell line incubated with the cytokine tumour necrosis factor (TNF) - α, demonstrates a downregulation of IL – 8 gene expression compared with controls (79). SP – A is not unique to the type II pneumocyte, but it is known to be absent from neighbouring type I pneumocytes within the alveolus. Interestingly, the commonly used type II pneumocyte substitute A549 cell line does not express SP –A mRNA (201), (241; 242). Expression of SP – A mRNA within the NCI – H441 is again consistent with a type II pneumocyte phenotype. Investigations of rat type II pneumocyte culture demonstrate secretion of the cytokine IL – 1β, but only when stimulated with particles (231).

Growth of NCI –H441 cells on FN over 5 days led to the reduction in gene expression levels of IL – 4, IL – 6, IL – 8 and SP – A. These experimental results are without doubt limited, as the experiment was not replicated. To gain any significant meaning from this result the experiment would have to be repeated and in comparison with growth of NCI – H441 on BSA. On examination of the data from the investigation of the effects of mechanical strain on gene expression within the NCI – H441 cell line cultured on both BSA or FN, marked differences may be seen in the relative values of IL – 6 and IL – 8 over 24 hours (Figures 5.5 –5.11). The mean relative resting value of IL – 6 gene expression, on BSA and FN following 24 hours of cultures were 5.447 and 1.040 respectively.

The effects substrata elicit on gene expression levels in vitro would support the idea that remodelling or injury of ECM can modulate type II pneumocyte function in vivo. Fibronectin could itself affect other aspects of the alveolar epithelium. At the electron microscopic level the alveolar basement membrane stains continuously for FN, beneath type I and II pneumocytes, of normal human lung. Within samples of fibrotic human lung the intensity of staining for FN within the alveolar basement membrane is markedly increased (35). Hyperplastic type II pneumocytes such as those found in patients with CFA or lung injury (36) & Lamb 1996 express an altered pattern of cytokeratins compared with the pattern shown within normal lung type II pneumocytes (191). Intermediate pneumocytes which bear characteristics of both type I and II pnuemocytes are also found within the alveolar epithelium following lung injury (243). This phenomena can be replicated in in vitro rat type II cultures, where tissue culture plastic substrata can accelerate the transition of the culture toward the type I phenotype (38). Within the alveolus the progress of fibrotic lung disease is precipitated by an inflamatory response(23), (222).

Discrepancies between the basal gene expression levels seen within real time experiments could be due inherent problems with the technique. Multiplex real time PCR analysis relies on the reaction efficiency of both amplicon and normaliser genes being similar. When calculating the relative values of gene expression the readings are relative to the simultaneous evaluation of GAPDH expression and these readings normalised against a control sample. Recently doubts have arisen about the suitability of housekeeping genes in realtime PCR (244; 245). The stage of the cell cycle can effect the concentrations of GAPDH found within cells (246). A number of environmental conditions can affect the internal expression of GAPDH, such as hypoxia (247; 248), oxidative stress (249)the presence of insulin or retinoic acid (250)and food deprivation (251). However a tenet of mechanotransduction in many cell systems is the involvement of the cytoskeleton associated proteins (109; 111; 112; 126; 127; 252; 253). Therefore it would potentially be unwise to use a housekeeping gene such a β – actin.

The gene expression levels of selected genes probed for within the cyclic mechanically stimulated NCI – H441 cell line are summarised within Table 5.2. When the NCI – H441 cell line was cultured on BSA and subject to mechanical stimulation there was no significant alteration in the mean relative gene expression levels of SP – A, IL – 6 and IL – 8. A marked decrease in SOCS3 gene expression was apparent at the 6 hours within the sample of NCI – H441 cells cultured on FN and mechanically stimulated compared to the samples cultured on BSA. The suppressors of cytokine signalling (SOCS) family are a novel family of proteins

which regulate the Janus family of protein tyrosine kinases and STAT transcription factors (254). The SOCS3 protein is known to inhibit cytokines such as IL – 6. Interestingly, there has been an incidence where the loss of SOCS3 production within the liver cells promotes the development of fibrosis (255). The most significant changes in gene expression when the NCI – H441 cell line was cultured on FN was in the mean relative level of IL – 8 gene expression, specifically the levels of IL – 8 gene expression at the 1 and 3 hour timepoints. Transient fluctuations in the mean relative gene expression levels of both IL – 6 and IL – 8 were apparent when NCI – H441 cells were cultured on BSA and FN. Cyclic mechanical stimulated of human chondrocytes are reported to demonstrated transient fluctations in gene expression levels of aggrecan and matrixmetalloproteinase 3 over a 24 hour period (140). Therefore, the fluctuations of gene expression in themselves are not likely to be unique to this human pneumocyte cell line.

Previous mechanical strain investigations involving pulmonary epithelial cells have focused on the gene expression of IL – 8 mRNA (62; 79) (68) and IL – 8 protein secretion (61). Cyclic mechanical strain increases the gene expression of IL – 8 and activates src protein tyrosine kinase (79). Interestingly dos Santos and coworkers found that mechanical strain of A549 cells alone does not result in dramatic changes in many pro – inflammatory genes' expression, but enhances the effects of tumour necrosis factor - α. However, the gene expression of IL – 8 is increased two fold due to mechanical strain. Cyclic mechanical strain of A549 cells not only induces the expression of IL – 8 mRNA, but the production of IL – 6 and IL – 8 via oxidant release and inhibition by glutathione (GSH) of nuclear factor κB (NF – κB) and activator protein – 1 (AP – 1).

Recent data suggests that SP – A may act as an autocrine cytokine which specifically regulates the gene expression of the other surfactant proteins and c – fos (50). Cyclic mechanical stimulation of the NCI – H441 cell line is reported to increase the gene expression of SP – B and SP – A mRNA (72) two to four fold compared with controls, unlike the results found within this study. However, the reported study used a different apparatus to apply mechanical strain, a different frequency pattern of stimulation, cultured cells on collagen I and allowed the cells to grow to confluence. A static or continuous application of strain to rat type II pneumocyte culture in vitro has previously shown to result in a dramatic decrease in SP - A mRNA (Dobbs et al. 1998). Similarly, in vivo, 10 days of tracheal ligation of fetal sheep results in a dramatic reduction in the levels of SP –A protein (134).

One investigation of the changes in cytoplasmic levels of SP – A protein levels of NCI – H441 cells, in response to cyclic mechanical stimulation was carried out, which ideally should be repeated to gain further insight. Cytoplasmic levels of SP – A within NCI – H441 cells cultured on FN decline twenty minutes after cyclic mechanic stimulation. Sixty minutes following cyclic mechanical stimulation cytoplasmic levels of SP – A of NCI – H441 cells cultured on FN return to resting values. On examination of the medium from mechanically stimulated NCI – H441 cells a greater quantity of SP –B protein was detected within the medium of NCI – H441 cells cultured on BSA compared with those cell populations cultured on fibronectin or collagen IV. The quantity of extracellular SP – B detected within mechanically stimulated NCI – H441 cells cultured on BSA, was lower than that of unstimulated NCI – H441 cells cultured on BSA. A two - fold decrease in quantity of extracellular SP – B was detected within mechanically stimulated NCI – H441 cell cultures adhered on CIV, compared to an unstimulated control.

It is not apparent how the NCI – H441 cell line adhered to the BSA coated substrata. It is more than possible that ECM was synthesised de novo and laid down by the cells. Some evidence exists for the synthesis of ECM by isolated type II pneumocytes in vitro (256). The production of the major alveolar basement membrane proteins fibronectin, laminin, and type IV collagen has been noted in culture (257). Therefore, the possibility exists for the cells under these conditions to transduce mechanical stimuli through this provisional matrix via integrin receptors. Function blocking anti – integrin antibodies and RGD peptides could there be of use in future investigations of this hypothesis. Alternatively whether or not pulmonary epithelium function is regulated by stretch – activated ion channels during mechanotransduction could be investigated. Foetal lung cell mechanotransduction has been found to involve to actions of stretch – activated ion – channels through the application of gadolinium (51) as has chondrocyte mechanotransduction (107).

To date the presence and or identity of a pulmonary epithelial mechanoreceptor remains a mystery (258). There is a strong likelihood that integrin receptors are involved in the regulation of mechanotransduction within pumonary epithelium. The apparent differences in gene expression of cyclic mechanical stimulated NCI – H441 cells cultured on the ECM protein FN and in its absence (BSA) indicate an interaction with a receptor of some kind. A dynamic interaction with specific extracellular matrix ligands and integrin – mediated mechanotransduction within in vitro endothethelial cells was demonstrated to exist by Jalali and coworkers (259).

Within other tissues, the integrin family of receptors are implicated as mechanoreceptors. This family of receptors are heterodimeric glycoproteins that mediate links between the extracellular matrix and the intracellular environment. Cyclic mechanical stimulation of human osteoblasts at different frequencies elicits changes in membrane potential. These membrane responses can be abrogated by RGD – peptides, which is a consensus peptide sequence of the integrin. The human osteoblasts exhibit hyperpolarisation and depolarisation membrane responses when exposed to cyclic mechanical stimuli of 0.33 Hz and 0.104 Hz respectively. The membranse depolarisation membrane response to mechanical stimuli of human osteoblasts is inhibited by antibodies to αv, β1 and β5 integrin subunits, at 0.104 Hz. Hyperpolarisation of cyclic mechanical stimulation of human osteoblasts results in hyperpolarisation membrane response, which can be inhibited by antibodies to α5 and β1 (93). A demonstration of the involvement of the α5β1 integrin in the membrane hyperpolarisation response of mechanically stimulated human chondrocytes has been reported (107). An investigation into shear stress and endothelium NO – mediated vasodilation of coronary arterioles demonstrates a significant role for the integrin receptor in mechanotransduction. Synthetic RGD peptides and an antibody to β3 integrins significantly inhibited shear stress vasodilation (109).

The identification of an involvement of the integrin receptor in adult pulmonary epithelial mechanotransduction biology is yet to occur. However, a report of the receptors β1, α6 and α3, known participants in foetal lung development, has determined their involvement in mechanotransduction. The addition of function blocking antibodies to the system, toward β1 and α6 subunits inhibit the expression of the SP – C differentiation marker and cell adhesion, characteristics which both normally increase in response to mechanical strain. Similarly, a α3 antibody inhibited the alveolar pneumocyte differentiation, but not cell adhesion (83).

CHAPTER 6 SUMMARY

Summary

This final chapter briefly summarises the results, and suggest directions for future investigations.

The following points have arisen from the results of the work detailed within this thesis:

- This study demonstrated the effective isolation of primary human type II pneumocytes, utilizing a trypsin- DNase containing technique. The exclusion of DNase rendered the procedure ineffective in the extraction of primary human type II pneumocytes. Out of 14 extraction procedures excluding DNase, only one successfully yielded cells, which tested positive for alkaline phosphatase activity, a characteristic of type II pneumocytes. The four extraction procedures including DNase were all successful, with the cell yields testing positive for type II pneumocyte characteristics, by the use of electron microscopy, modified haematoxylin staining and immunocytochemistry.

- No individual characterization technique, unilaterally categorized an isolated population of primary human type II pneumocytes. The staining of alkaline phosphatase activity within primary type II pneumocytes was variable, depending on the substrate the cells were seeded. The primary type II pneumocytes cultured on BSA are spherical, on FN elliptical and on CIV uniformly spread. The degree of cell spreading made it difficult to distinguish between type II pneumocytes and contaminating macrophages, which do not stain positive for alkaline phosphatase activity.

- Morphological characterization with the aid of electron microscopy yields the simplest, non - contradictory data of populations' overall phenotype and content. I Antibodies with adequate specificity to appropriately characterize primary type II isolations are not yet widely available for use in immunocytochemistry. However, the modified haematoxylin technique gives the most rapid, sense of isolated populations' phenotype and cellular complement.

- The NCI – H441 cell line demonstrates numerous type II characteristics, such as dark lamellar body like structures and blunt microvilli as apparent under electron microscopic analysis. The NCI – H441 cell line stains positive for alkaline phosphatase activity, the expression of SP – A mRNA, presence of the SP – A and SP – B proteins was detected within the cells. Much lower expression of SP – A RT – PCR were detected within the NCI – H441 cell line than the control sample of primary human lung tissue. The test populations of NCI – H441 cells were 90 % positive for the presences of cytokeratins, as tested for with a pan – cytokeratin antibody MNF116.

- A previous pilot study of primary human type II pneumocytes demonstrated that cyclic mechanical stimulation of 5000 με, 0.25 Hz resulted in a statistically significant hyperpolarisation of the cellular membrane potential. Cyclic mechanical stimulation at 0.25 Hz, 5000 με for 20 minutes of the NCI – H441 cell line leads to significant membrane hyperpolarization, compared to unstimulated controls. The duration of culture before application of cyclic mechanical stimulation on NCI – H441 cells or addition of serum to culture media, before experimentation does not significantly affect the resulting response to mechanical stimulation. Similarly culture on different ECM including CIV, FN and BSA has no significant effects on resting membrane potential. Although cyclic mechanical stimulation elicited significant membrane hyperpolarisation response within NCI – H441 cell populations cultures on CIV and FN, no significant membrane depolarization response was elicited within cells cultured on BSA.

- The NCI – H441 cell line expresses the mRNA of the following cytokines: IL – 4, IL – 8, SP – A and SOCS3 but not IL -1β mRNA. The relative levels of cytokine mRNA expressed within NCI – H441 cells cultured on FN over 5 day shows a variable effect on cytokine, SOCS and SP-A mRNA levels varying with different cytokines and the substrate upon which cells are cultured.

It is indisputable that the three – dimensional structure and multicellular environment of the lungs, makes the study of pulmonary biology convoluted. In addition, to these environmental complexities of the lung the cells are subject to various patterns of mechanical stimulation, which regulate structure, function and metabolism. In short, mechanical strain is an integral and an essential part of the lungs' physiology. So why is the vast majority of in vitro pulmonary research carried out under static cultures? The most probable answer to this question arrived at during the course of this project is that basic fundamental knowledge of normal and abnormal pulmonary cell mechanotransduction is unknown. Therefore, the unusual stance of creating an in vitro model of normal cell mechanotransduction for the study of alveolar type II epithelial cell function, was undertaken.

With respect to the project aims, primary human type II pneumocytes were isolated in sufficient yields, which would suggest their potential for use in mechanotransduction studies. The NCI – H441 cell line demonstrated type II pneumocyte characteristics and reproducibly responded to cyclic mechanical strain with changes in membrane potential, dependant on ECM substratum, which suggests the involvement of cell surface to substratum interactions in the conduction of mechanical stimuli. In addition, cyclic mechanical stimulation of NCI – H441 cultured on fibronectin, at 0.25 Hz, 5000 με for 20 minutes, resulted in elevated levels of IL – 8 mRNA gene expression, one hour following the application of stimulus, which subsequently declined. Recently it was considered that the pulmonary epithelium plays a role in the progression of lung fibrosis through "epithelial mesenchymal transition" (EMT) (260). During this process the myofibroblasts pivotal in the production of lung fibrosis, are suggested to originate from the population of alveolar epithelium. The model presented within this not only makes headway into fundamental regulatory role of cyclic mechanical stimulation, during normal breathing, but could be used to investigate the role of EMT on alveolar epithelial cell function in future. Evidence would also suggest that NCI – H441 cell line is an adequate substitute for primary type II pneumocytes. Pulmonary mechanotransduction study is a rapidly growing area of research, which promises in future to shed light on all aspects of pulmonary disease, injury and infection.

Appendice I: Regent recipes

RNA extraction solutions

All solutions were made up in baked glassware.

RNA extraction medium (Stock solution)
Guanidine isothiocyanate(Sigma) 236.3 g
0.75 M Sodium citrate (Sigma) 3.68 g
10% n-lauroylsarcosine(Sigma) 2.5 g

Dissolve in 300 ml mQ dH_2O by heating to 65°C. Adjust to pH 7.0. Make up to

500 ml, and filter through Whatman no. 3 filter into sterile bottle.

RNA extraction medium (working solution)
Add 360 µl β-mercaptoethanol (Sigma) per 50 ml stock solution prior to use. Stored

working solution in fridge.

Western blotting solutions

Separating (Resolving) Gel Buffer

1.5 M Tris.HCl, 0.5% (w/v) SDS, pH 8.8.

Tris (Sigma) 90.75 g
Sodium dodecylsulfate (SDS) (Sigma) 2.5 g
Add approx. 400 ml distilled water and pH to 8.8 with 2 N HCl.
Make up to 500 ml, and store at room temperature.

Stacking Gel Buffer

0.5 M Tris.HCl, 0.5% (w/v) SDS, pH 6.8.

To make:
Tris (Sigma) 30.25 g
SDS (Sigma) 2.5 g
Add approx. 400 ml distilled water and pH to 6.8 with 2 N HCl.
Make up to 500 ml, and store at room temperature.

5x electrode buffer
0.125 M Tris.HCl, 0.95 M glycine, 0.5% (w/v) SDS.

To make:

Tris (Sigma)	7.5 g
Glycine (Sigma)	36.0 g
SDS (Sigma)	2.5 g

Add 400 ml distilled water to dissolve, then make up to 500 ml and store at room temperature.

Sample Buffer

to make up 8ml: 3.6ml ddw

1.0ml stacking gel buffer pH 6.8

1.6ml 10% SDS

800µl 1M DTT

800µl Glycerol

50µl 0.05% Bromophenol blue

Sample buffer may be made up and stored frozen

Transfer Buffer

0.025 M Tris, 0.19 M glycine, 20% (v/v) methanol, pH 8.3

To make (fresh):

Tris (Sigma)	3.03 g
Glycine (Sigma)	14.4 g
Methanol	200 ml

Make up to 1 l with distilled water. DO NOT ADJUST pH.

TBST (for washing blots)

Tris-buffered saline containing 1 ml/l Tween-20

To make (fresh):

10x Tris, pH 7.6	50 ml
Normal Saline	450 ml
(Tween-20) (Sigma)	0.5 ml

Protein extraction

Wash buffer

0.1 mM Na_3VO_4 (Sigma) in PBS

Make up 1 mM Na_3VO_4 stock in PBS, boil for 5 minutes and store at -20°C in 1 ml aliquots. Make up wash and lysis buffers using this stock.

Lysis Buffer

1% (v/v) Igepal (Sigma)

0.1 mM Na_3VO_4

1 Complete™ mini-protease inhibitor cocktail tablet (Roche) per 10 ml

made up in PBS

0.1N NaOH

Lowry protein assay

4g NaOH in 1l dH_2O

Alkaline carbonate solution

5 ml 1% copper sulphate (1 g $CuSO_4$ in 100 ml dH_2O)

5 ml 2% sodium potassium tartrate (2 g NaK tartrate in 100 ml dH_2O)

490 ml alkaline carbonate stock solution (20 g $NaHCO_3$, 4 g NaOH in 1l dH_2O)

Folin's reagent

10 ml stock solution diluted in 10 ml dH_2O, stored in the dark at 4°C.

:

PCR Stock solutions

Reaction buffer10x, supplied with enzyme. Better to buy the buffer with separate Mg. We buy ours from BioGene (£85 / 500U enzyme). Store at -20°C.

dNTPs	Pharmacia at 100 mM concentration for each and make up 10 mM mix of all of them. Store at -20°C.
$MgCl_2$	Depends where you buy the enzyme, some companies supply it at 25 mM, others at 50 mM. Store at -20°C.
Primers	Come lyophilised from Life Technologies. Resuspended to 50μM, aliquot into several tubes and make up working stock primer mix of 20 μM. Stored at -20°C.
BSA	Made up 0.2% in PCR water and store at 4°C for up to 1 month
Taq enzyme	Usually 5U/μl (250U or 500U). Store at -20°C

Primary type II pneumocyte isolation solutions

Reagents purchased Sigma
All solutions were filter sterilised before use

DNase-free method

PBS-
0.130 M NaCl
5.2 mM KCl
10.6 mM Hepes
2.6 mM Na_2HPO_4
0.1 mM EGTA
10 mM D-Glucose
pH adjusted to 7.4

+Ca/Mg working solution

0.9% NaCl
0.11 M $CaCl_2$
0.15 M KCl
0.15 M $MgSO_4$
0.10 M phosphate buffer, pH7.4
0.20 Hepes
11 mM glucose
pH 7.4,

-Ca/Mg working solution
As +Ca/ Mg solution, but without Ca/Mg
0.25 % w/ v Trypsin solution (made fresh before use),

Heavy gradient
1 ml solution 10 x –Ca.Mg solution
6.49 ml Percoll
0.05 ml FBS
2.51 ml ml distilled water

Light gradient
1 ml solution 10 x –Ca/Mg solution
2.72 ml Percoll
0.05 ml FBS
6.28 ml distilled water

Utilising DNase

Solution A

0.130 M NaCl
5.2 mM KCl
10.6 mM Hepes
2.6 mM Na_2HPO_4
0.1 mM EGTA
10 mM D-Glucose
pH adjusted to 7.4

Solution B as above with the inclusion 1.9 mM $CaCl_2$ and 1.29 mM $MgSO_4$

Solution C 10 x concentration of solution A

The discontinuous Percoll gradient comprises 10 ml of heavy gradient (1.089 g/ml) and 10 ml of light gradient (1.040 g/ml)

Heavy gradient
1 ml solution C
6.49 ml Percoll
0.05 ml FBS
2.51 ml ml distilled water

Light gradient
1 ml solution C
2.72 ml Percoll
0.05 ml FBS
6.28 ml distilled water

DNase 1 solution 200 U/g tissue
DNase 2 solution
2.5 mg DNase I (Boeringer Manheimeyr)
50 ml solution A
1% v/v penicillin / streptomycin solution (Invitrogen)

Table 2.1 Antibodies

Antigen	Clone/ Code No.	Supplier	Dilution	Isotype	Incubation Time (min)
Surfactant specific protein A (SP – A)	Polyclonal AB3426	Chemicon	1:5000	Rabbit IgG	30 RT or o/n 4°C
Surfactant specific protein B (SP – B)	Polyclonal AB3436	Chemicon	1:500	Rabbit IgG	30 RT or o/n 4°C
Normal Rabbit IgG	AB – 105 - C	R & D Systems	1:500 1:5000	Rabbit IgG	30 RT o/n 4°C
Rabbit IgG	P 0448	Dako	1:100	Goat Anti – Rabbit IgG, Peroxidase - Conjugated	30 RT
Human CD45, Leucocyte Common Antigen	2B11 + PD7/26	Dako	1:100 (cytospins) 1:200 (frozen sections)	Mouse IgG1κ	30 RT
Human Cytokeratin, (5, 6, 8, 17 and 19)	MNF116	Dako	1:100 (cytospins) 1:200 (frozen sections)	Mouse IgG1κ	30 RT
Mouse IgG1	DAK – GO1	Dako	1:100 (cytospins) 1:200 (frozen sections)	Mouse IgG1κ	30 RT
Mouse IgG1, IgG2a, IgG2b, IgG3, IgA, IgM	P 0260	Dako	1:200	Rabbit Anti-Mouse IgG, Peroxidase - Conjugated	30 RT

Table 2.2 Protein sample constituents for construction of calibration graph

Protein	Protein Quantitity (μg)	Volume of Protein solution (μl)	Volume of 0.1 N NaOH (μl)
BSA (1 mg/ml)	0	0	200
	25	5	195
	50	10	190
	75	15	185
	100	15	180
	125	20	175
	150	25	170
	175	35	165
	200	40	160
	400	80	120
Sample	unknown	5	195

RT-PCR recipes

Amplicon "master mix"

10 x *Taq* reaction buffer	1.8μl	
10 mM dNTP mix		0.2 μl
2.5 mM $MgCl_2$	5.0 μl	
20 μM primer mix		1.0 μl
0.02 % BSA		1.0 μl
$mQdH_2O$		to make volume up to 18 μl
cDNA		2.0 μl
volume per tube	18 μl	

Taq DNA polymerase "master mix"
1 x *Taq* reaction buffer
1U *Taq* DNA polymerase
$mQdH_2O$ to make volume up to 2.0 μl per reaction

SP – A and GAPDH cycle

94°C for 1 min
60°C* for 1 min
72°C for 1 min 30 sec
} x 35 cycles
72°C for 10 min

Table 2.3. Primer Sequence Details

Amplicon	Primer code	Genbank Access Nc	Sequence (5' to 3') S= sense, AS = antisense	Product size (bp)	Ref
Glyceralde 3 – phosphate dehydrogenase GAPDH	GAPDH 1	JO438	S = cca ccc atg gca aat tcc atg gca	600	(140)
	GAPDH 2		AS = tct aga cgg cag gtc agg tcc acc		
Surfactant protein A SP -A	SP – A 1	L10123	S = ctt ccc tgt tct tca tct ggc	400	in house design
	SP – A 2		AS = tgt gct cta cct gag cag gc		

Real time – PCR recipes

Amplicon Master mix

2x Taqman®Universal PCR master mix	12.50 µl
20x Target Primers and Probe	1.25 µl (IL – 1β, 4, 6, 8) / 7.00 µl (SP – A and SOCS3)
20x Control Primers and Probe (18s)	1.25 µl
RNase free – mQdH_2O	to make final volume up
cDNA volume	5 µl
Total volume	50 µl

Thermal Cycler Conditons

50°C for 2 minutes
95°C for 10 minutes } Initial steps
95°C for 15 seconds
60°C for 1 minute } 40 Cycles

	1 M Acetic Acid 100 ml/l 0.5 M EDTA pH 8.0
10 x TBE	0.9 M Tris 0.9 M Boric Acid 20 ml/l 0.5 M EDTA pH 8.0
PCR loading dye (10x)	0.25 % Orange G 50 % (v/v) Glycerol

Table 2.5. DNA Marker fragment sizes

Fragment sizes of DNA digested with λHindIII and EcoRI (bp)
21226
5148
4973
4277
3530
2027
1904
1584
1330
983
831
564
125

Table 3.1. Summary of primary human type II pneumocyte isolations

Ref	n	Enzymes	Purification method	No. cells x 10^6/gram tissue	% Type II	Purity Assay
(154)	13	Elastase, 30 U/ml[b]	Density gradient (Metrizamide)	[a]	[a]	Pap stain, tannic acid and polychrome stain, EM, Acridine orange stain
(155)		Dispase, 1.2 units/ml (1 g tissue: 1 ml) DNase, 10 μg/ml	Density gradient (Metrizamide) + adherence	1_3	80_90	Pap stain
(156)	10	Dispase , 2.5 mg/ml	Density gradient (Metrizamide) +panning on IgG coated dishes	0.5-1.0 x10^6	80-95	Pap stain

Table3.1. Continued

(146)	6	Crystalline Trypsin type I, 2.5 mg/ml (25ml/g tissue) DNase I, 4000 U/ml (200 -500 U/g tissue)	Adherence + Density gradient (Percoll)	2.3+/-1.1 SEM	1) 75+/-6 SEM 2) 83+/-2.6 SEM 3) 97+/-1 SEM 4) 89+/-4 SEM	1)AP 2) EM 3) LB counts of Pap stain post 24 hours 4) AP +ve post 24 hours culture
(153)	45	Dispase II, 2.5 mg/ml DNase, 2 mg/ml	Density gradient (Ficoll) + adherence 1) O/n collagen R, washing + trypsinization 2) O/n collagen R as in 1) + CD3 and CD14 antbodies + anti-idiotype MACS 3) CD3 and CD14 antbodies + anti-idiotype MACS	absolute relative yield 2.0+/-6.2 x 10^5 [5.2 x10^4-4x10^6] 1) 1.2 x10^5 [2.5x10^3-1.1x10^6] 2) 7.8x10^4 [2.5x10^3-1.1x10^6] 3) 1.3x10^5 [9.5x10^3-9.1x10^5][b]	Flow cytometry- HLA-DR= 44 [4-77], CD54=55 [16-89], CD2+CD58 = 44 [12-78], CD28(CD80, B7-1; 38 [0-77], CD86, B7-2;40 [4-68]) AEC type I lectin -ve 1) 73 [82-87] 3) 87 [75-96]	Flow cytometry Immuno EM
(157)	15	Trypsin type I, 5 mg/ml Elastase, 0.022 mg/ml	Adherence + Density gradient (Percoll) + MACS	2.3	81+/-1	AP

aNumerical yield and purity not given. bUnits in orcein/elastin units. cData expressed as the median and range. AEC type I lectin=Bauhinia purpurea, AP=Alkaline Phosphatase Stain, EM=Electron microscopy, Immuno=Immunocytochemistry, MACS=Magnetic Activated Cell Sorting, Pap stain=Modified Papanicalaou stain, SEM=Standard error of the mean

Appendice 2: Original data

The membrane potential of cyclically mechanicall stimulated primary type II pneumocytes

Resting (-mV)	Post strain (-mV)
22	42
16	45
12	32
24	43
34	33
17	34
28	34
23	
mean	**mean**
22	37.57142
SD	SD
7.030545	5.503245
sem	sem
2.5	2.1
var	var
49.42857	30.28571

The effects of time and serum on the membrane responses of cyclicall mechanically stimulated NCI – H441 cells

i)

4 hours serum-free		24 hours serum free		24 hours 10% FBS+1/2 hour serum-free	
Resting (-mV)	Post stim (-mV)	Resting (-mV)	Post stim (-mV)	Resting (-mV)	Post stim (-mV)
23	38	15	30	22	30
29	42	16	27	26	23
25	51	15	23	17	34
27	46	13	29	23	24
22	55	16	32	17	33
mean	mean	mean	mean	mean	mean
25.2	46.2	15	28.2	21	29
Stdev	Stdev	Stdev	Stdev	Stdev	Stdev
2.864	6.804	1.225	3.421	3.937	4.796
sem	sem	sem	sem	sem	sem
1.281	3.043	0.548	1.529	1.761	2.145
var	var	var	var	var	var
8.2	46.3	1.5	11.7	15.5	23

4 hours serum-free		24 hours serum free		24 hours 10% FBS+1/2 hour serum-free	
Resting (-mV)	Post stim (-mV)	Resting (-mV)	Post stim (-mV)	Resting (-mV)	Post stim (-mV)
15	31	14	20	17	34
12	33	20	15	16	32
15	24	12	14	12	37
22	23	22	36	13	25
13	35	12	21	16	35
12	26	12	15		
	33	17			
		15			
		16			
		17			
mean	mean	mean	mean	mean	mean
14.833	29.285	15.7	20.166	14.8	32.6
Stdev	Stdev	Stdev	Stdev	Stdev	Stdev
3.763	4.855	3.433	8.28	2.168	4.615
sem	sem	sem	sem	sem	sem
1.537	1.086	3.38	0.869		
var	var	var	var	var	var
14.167	23.5714	11.789	68.567	4.7	21.3

The effects of ECM on the membrane responses of cyclically mechanically stimulated NCI-H441 cells

i)

BSA		Collagen IV		Fibronectin	
Resting	Post MS	Resting	Post MS	Resting	Post MS
18	9	18	39	12	14
25	13	25	35	26	13
20	8	19	30	14	30
45	25	28	32	14	28
12	10	20	34	21	29
22	15			11	30
	12			13	31
	11				
	9				
	13				
n-1	n-1	n-1	n-1	n-1	n-1
5	9	4	4	6	6
mean	mean	mean	mean	mean	mean
23.666	12.5	22	34	15.857	25
stdev	stdev	stdev	stdev	stdev	stdev
11.325	4.905	4.301	3.391	5.520	8.1731
sem	sem	sem	sem	sem	sem
2.236	3	2	2	2.449	2.449
var	var	var	var	var	var
128.266	24.055	18.5	11.5	30.476	62.666

ii)

BSA		Collagen IV		Fibronectin	
resting (-mV)	post strain (-mV)	resting (-mV)	post strain (-mV)	resting(-mV)	post strain (-mV)
13	12	32	51	17	30
14	7	24	40	12	18
14	13	15	51	12	28
15	7	32	30	18	54
14	6	10	23	14	28
mean	mean	mean	mean	mean	mean
14	9	22.6	39	14.6	31.6
stdev	stdev	stdev	stdev	stdev	stdev
0.707	3.240	9.939	12.51	2.792	13.371
sem	sem	sem	sem	sem	sem
0.353	1.6201	4.969	6.254	1.396	6.685
var	var	var	var	var	var
0.5	10.5	98.8	156.5	7.8	178.8

4 hours serum-free		24 hours serum free		24 hours 10% FBS+1/2 hour serum-free	
Resting (-mV)	Post stim (-mV)	Resting (-mV)	Post stim (-mV)	Resting (-mV)	Post stim (-mV)
15	31	14	20	17	34
12	33	20	15	16	32
15	24	12	14	12	37
22	23	22	36	13	25
13	35	12	21	16	35
12	26	12	15		
	33	17			
		15			
		16			
		17			
mean	mean	mean	mean	mean	mean
14.833	29.285	15.7	20.166	14.8	32.6
Stdev	Stdev	Stdev	Stdev	Stdev	Stdev
3.763	4.855	3.433	8.28	2.168	4.615
sem	sem	sem	sem	sem	sem
1.537	1.086	3.38	0.869		
var	var	var	var	var	var
14.167	23.5714	11.789	68.567	4.7	21.3

Reference List

1. **Wirtz HR and Dobbs LG.** The effects of mechanical forces on lung functions. *Respir Physiol* 119: 1-17, 2000.

2. **Kitterman JA.** The effects of mechanical forces on fetal lung growth. *Clin Perinatol* 23: 727-740, 1996.

3. **Sachs F.** Mechanical transduction in biological systems. *Crit Rev Biomed Eng* 16: 141-169, 1988.

4. **Wirtz HR and Dobbs LG.** Calcium mobilization and exocytosis after one mechanical stretch of lung epithelial cells. *Ciba Found Symp* 250: 1266-1269, 1990.

5. **Weibel, E. R.** Morphometry of the human lung. 1963. Berlin, Springer.

6. **Crapo JD, Barry BE, Gehr P, Bachofen M and Weibel ER.** Cell number and cell characteristics of the normal human lung. *Am Rev Respir Dis* 126: 332-337, 1982.

7. **Castranova V, Rabovsky J, Tucker JH and Miles PR.** The alveolar type II epithelial cell: a multifunctional pneumocyte. *Toxicol Appl Pharmacol* 93: 472-483, 1988.

8. **Askin FB and Kuhn C.** The cellular origin of pulmonary surfactant. *Lab Invest* 25: 260-268, 1971.

9. **Kikkawa Y and Yoneda K.** The type II epithelial cell of the lung. I. Method of isolation. *Lab Invest* 30: 76-84, 1974.

10. **Uhal BD.** Cell cycle kinetics in the alveolar epithelium. *Am J Physiol* 272: L1031-L1045, 1997.

11. **Flecknoe S, Harding R, Maritz G and Hooper SB.** Increased lung expansion alters the proportions of type I and type II alveolar epithelial cells in fetal sheep. *Am J Physiol Lung Cell Mol Physiol* 278: L1180-L1185, 2000.

12. **Evans MJ, Cabral LJ, Stephens RJ and Freeman G.** Renewal of alveolar epithelium in the rat following exposure to NO2. *Annu Rev Physiol* 70: 175-198, 1973.

13. **Fehrenbach H.** Alveolar epithelial type II cell: defender of the alveolus revisited. *Respir Res* 2: 33-46, 2001.

14. **Evans MJ, Cabral LJ, Stephens RJ and Freeman G.** Transformation of alveolar type 2 cells to type 1 cells following exposure to NO2. *Exp Mol Pathol* 22: 142-150, 1975.

15. **Corrin, Bryan and .** Pathology of the Lungs.

1, 1-31. 1999. Churchhill Livingstone. Pathology of the Lungs.

16. **Desmouliere A, Geinoz A, Gabbiani F and Gabbiani G.** Transforming growth factor-beta 1 induces alpha-smooth muscle actin expression in granulation tissue myofibroblasts and in quiescent and growing cultured fibroblasts. *J Cell Biol* 122: 103-111, 1993.

17. **Mattey DL, Dawes PT, Nixon NB and Slater H.** Transforming growth factor beta 1 and interleukin 4 induced alpha smooth muscle actin expression and myofibroblast-like differentiation in human synovial fibroblasts in vitro: modulation by basic fibroblast growth factor. *Ann Rheum Dis* 56: 426-431, 1997.

18. **Kuhn C and McDonald JA.** The roles of the myofibroblast in idiopathic pulmonary fibrosis. Ultrastructural and immunohistochemical features of sites of active extracellular matrix synthesis. *Annu Rev Physiol* 138: 1257-1265, 1991.

19. **Zhang K, Rekhter MD, Gordon D and Phan SH.** Myofibroblasts and their role in lung collagen gene expression during pulmonary fibrosis. A combined immunohistochemical and in situ hybridization study. *Annu Rev Physiol* 145: 114-125, 1994.

20. **Phan SH.** The myofibroblast in pulmonary fibrosis. *Chest* 122: 286S-289S, 2002.

21. **Zhang K and Phan SH.** Cytokines and pulmonary fibrosis. *Biol Signals* 5: 232-239, 1996.

22. **Darby I, Skalli O and Gabbiani G.** Alpha-smooth muscle actin is transiently expressed by myofibroblasts during experimental wound healing. *Lab Invest* 63: 21-29, 1990.

23. **Crouch E.** Pathobiology of pulmonary fibrosis. *Am J Physiol* 259: L159-L184, 1990.

24. **Isakson BE, Lubman RL, Seedorf GJ and Boitano S.** Modulation of pulmonary alveolar type II cell phenotype and communication by extracellular matrix and KGF. *Am J Physiol Cell Physiol* 281: C1291-C1299, 2001.

25. **Wadsworth SJ, Freyer AM, Corteling RL and Hall IP.** Biosynthesized matrix provides a key role for survival signaling in bronchial epithelial cells. *Am J Physiol Lung Cell Mol Physiol* 286: L596-L603, 2004.

26. **Yurchenco PD and O'Rear JJ.** Basal lamina assembly. *Curr Opin Cell Biol* 6: 674-681, 1994.

27. **Dunsmore SE, Lee YC, Martinez-Williams C and Rannels DE.** Synthesis of fibronectin and laminin by type II pulmonary epithelial cells. *Am J Physiol* 270: L215-L223, 1996.

28. **Ekblom P, Ekblom M, Fecker L, Klein G, Zhang HY, Kadoya Y, Chu ML, Mayer U and Timpl R.** Role of mesenchymal nidogen for epithelial morphogenesis in vitro. *Development* 120: 2003-2014, 1994.

29. **Hudson BG, Reeders ST and Tryggvason K.** Type IV collagen: structure, gene organization, and role in human diseases. Molecular basis of Goodpasture and Alport syndromes and diffuse leiomyomatosis. *J Biol Chem* 268: 26033-26036, 1993.

30. **Pierce RA, Griffin GL, Mudd MS, Moxley MA, Longmore WJ, Sanes JR, Miner JH and Senior RM.** Expression of laminin alpha3, alpha4, and alpha5 chains by alveolar epithelial cells and fibroblasts. *Am J Respir Cell Mol Biol* 19: 237-244, 1998.

31. **Madri JA and Furthmayr H.** Collagen polymorphism in the lung. An immunochemical study of pulmonary fibrosis. *Hum Pathol* 11: 353-366, 1980.

32. **Sannes PL.** Differences in basement membrane-associated microdomains of type I and type II pneumocytes in the rat and rabbit lung. *J Histochem Cytochem* 32: 827-833, 1984.

33. **Lwebuga-Mukasa JS.** Matrix-driven pneumocyte differentiation. *Am Rev Respir Dis* 144: 452-457, 1991.

34. **Furuyama A and Mochitate K.** Assembly of the exogenous extracellular matrix during basement membrane formation by alveolar epithelial cells in vitro. *J Cell Sci* 113 (Pt 5): 859-868, 2000.

35. **Torikata C, Villiger B, Kuhn C, III and McDonald JA.** Ultrastructural distribution of fibronectin in normal and fibrotic human lung. *Lab Invest* 52: 399-408, 1985.

36. **Wallace WA, Howie SE, Lamb D and Salter DM.** Tenascin immunoreactivity in cryptogenic fibrosing alveolitis. *J Pathol* 175: 415-420, 1995.

37. **Guo Y, Alford AI, Martinez-Williams C and Rannels DE.** Extracellular matrix modulates expression of connexin messenger RNA and protein by alveolar epithelial cells. *Chest* 120: 17S-19S, 2001.

38. **Reynolds LJ, McElroy M and Richards RJ.** Density and substrata are important in lung type II cell transdifferentiation in vitro. *Int J Biochem Cell Biol* 31: 951-960, 1999.

39. **Gutierrez JA, Gonzalez RF and Dobbs LG.** Mechanical distension modulates pulmonary alveolar epithelial phenotypic expression in vitro. *Am J Physiol* 274: L196-L202, 1998.

40. **Newton DA, Rao KM, Dluhy RA and Baatz JE.** Hemoglobin is expressed by alveolar epithelial cells. *J Biol Chem* 281: 5668-5676, 2006.

41. **Dunnill MS.** Postnatal growth of the lung. *Thorax* 17: 329-333, 1962.

42. **Gil J, Bachofen H, Gehr P and Weibel ER.** Alveolar volume-surface area relation in air- and saline-filled lungs fixed by vascular perfusion. *J Appl Physiol* 47: 990-1001, 1979.

43. **Bachofen H and Schurch S.** Alveolar surface forces and lung architecture. *Comp Biochem Physiol A Mol Integr Physiol* 129: 183-193, 2001.

44. **Mercer RR, Laco JM and Crapo JD.** Three-dimensional reconstruction of alveoli in the rat lung for pressure-volume relationships. *J Appl Physiol* 62: 1480-1487, 1987.

45. **Mercer RR and Crapo JD.** Spatial distribution of collagen and elastin fibers in the lungs. *J Appl Physiol* 69: 756-765, 1990.

46. **Tschumperlin DJ and Margulies SS.** Alveolar epithelial surface area-volume relationship in isolated rat lungs. *J Appl Physiol* 86: 2026-2033, 1999.

47. **Uhlig S.** Ventilation-induced lung injury and mechanotransduction: stretching it too far? *Am J Physiol Lung Cell Mol Physiol* 282: L892-L896, 2002.

48. **Vogel, S.** Comparative biomechanics:life's a physical world. 2003. Princeton, New Jersey, USA, Princeton university press.

49. **Hamm H, Kroegel C and Hohlfeld J.** Surfactant: a review of its functions and relevance in adult respiratory disorders. *Respir Med* 90: 251-270, 1996.

50. **Korutla L and Strayer DS.** SP-A as a cytokine: surfactant protein-A-regulated transcription of surfactant proteins and other genes. *Pharm Res* 178: 379-386, 1999.

51. **Liu M, Skinner SJ, Xu J, Han RN, Tanswell AK and Post M.** Stimulation of fetal rat lung cell proliferation in vitro by mechanical stretch. *Am J Physiol* 263: L376-L383, 1992.

52. **Liu M, Xu J, Souza P, Tanswell B, Tanswell AK and Post M.** The effect of mechanical strain on fetal rat lung cell proliferation: comparison of two- and three-dimensional culture systems. *In Vitro Cell Dev Biol Anim* 31: 858-866, 1995.

53. **Liu M, Xu J, Liu J, Kraw ME, Tanswell AK and Post M.** Mechanical strain-enhanced fetal lung cell proliferation is mediated by phospholipase C and D and protein kinase C. *Am J Physiol* 268: L729-L738, 1995.

54. **Xu J, Liu M, Tanswell AK and Post M.** Mesenchymal determination of mechanical strain-induced fetal lung cell proliferation. *Am J Physiol* 275: L545-L550, 1998.

55. **Xu J, Liu M, Liu J, Caniggia I and Post M.** Mechanical strain induces constitutive and regulated secretion of glycosaminoglycans and proteoglycans in fetal lung cells. *J Cell Sci* 109 (Pt 6): 1605-1613, 1996.

56. **Mourgeon E, Xu J, Tanswell AK, Liu M and Post M.** Mechanical strain-induced posttranscriptional regulation of fibronectin production in fetal lung cells. *Am J Physiol* 277: L142-L149, 1999.

57. **Xu J, Liu M and Post M.** Differential regulation of extracellular matrix molecules by mechanical strain of fetal lung cells. *Am J Physiol* 276: L728-L735, 1999.

58. **Mourgeon E, Isowa N, Keshavjee S, Zhang X, Slutsky AS and Liu M.** Mechanical stretch stimulates macrophage inflammatory protein-2 secretion from fetal rat lung cells. *Am J Physiol Lung Cell Mol Physiol* 279: L699-L706, 2000.

59. **Brown TD.** Techniques for mechanical stimulation of cells in vitro: a review. *J Biomech* 33: 3-14, 2000.

60. **Hasegawa S, Sato S, Saito S, Suzuki Y and Brunette DM.** Mechanical stretching increases the number of cultured bone cells synthesizing DNA and alters their pattern of protein synthesis. *Calcif Tissue Int* 37: 431-436, 1985.

61. **Tsuda A, Stringer BK, Mijailovich SM, Rogers RA, Hamada K and Gray ML.** Alveolar cell stretching in the presence of fibrous particles induces interleukin-8 responses. *Am J Respir Cell Mol Biol* 21: 455-462, 1999.

62. **Jafari B, Ouyang B, Li LF, Hales CA and Quinn DA.** Intracellular glutathione in stretch-induced cytokine release from alveolar type-2 like cells. *Respirology* 9: 43-53, 2004.

63. **Yamamoto H, Teramoto H, Uetani K, Igawa K and Shimizu E.** Stretch induces a growth factor in alveolar cells via protein kinase. *Respir Physiol* 127: 105-111, 2001.

64. **Yamamoto H, Teramoto H, Uetani K, Igawa K and Shimizu E.** Cyclic stretch upregulates interleukin-8 and transforming growth factor-beta1 production through a protein kinase C-dependent pathway in alveolar epithelial cells. *Respirology* 7: 103-109, 2002.

65. **Oswari J, Matthay MA and Margulies SS.** Keratinocyte growth factor reduces alveolar epithelial susceptibility to in vitro mechanical deformation. *Am J Physiol Lung Cell Mol Physiol* 281: L1068-L1077, 2001.

66. **Banes AJ, Gilbert J, Taylor D and Monbureau O.** A new vacuum-operated stress-providing instrument that applies static or variable duration cyclic tension or compression to cells in vitro. *J Cell Sci* 75: 35-42, 1985.

67. **Torday JS and Rehan VK.** Stretch-stimulated surfactant synthesis is coordinated by the paracrine actions of PTHrP and leptin. *Am J Physiol Lung Cell Mol Physiol* 283: L130-L135, 2002.

68. **Vlahakis NE, Schroeder MA, Limper AH and Hubmayr RD.** Stretch induces cytokine release by alveolar epithelial cells in vitro. *Am J Physiol* 277: L167-L173, 1999.

69. **Upadhyay D, Correa-Meyer E, Sznajder JI and Kamp DW.** FGF-10 prevents mechanical stretch-induced alveolar epithelial cell DNA damage via MAPK activation. *Am J Physiol Lung Cell Mol Physiol* 284: L350-L359, 2003.

70. **Gutierrez JA, Suzara VV and Dobbs LG.** Continuous mechanical contraction modulates expression of alveolar epithelial cell phenotype. *Am J Respir Cell Mol Biol* 29: 81-87, 2003.

71. **Correa-Meyer E, Pesce L, Guerrero C and Sznajder JI.** Cyclic stretch activates ERK1/2 via G proteins and EGFR in alveolar epithelial cells. *Am J Physiol Lung Cell Mol Physiol* 282: L883-L891, 2002.

72. **Sanchez-Esteban J, Tsai SW, Sang J, Qin J, Torday JS and Rubin LP.** Effects of mechanical forces on lung-specific gene expression. *Am J Med Sci* 316: 200-204, 1998.

73. **Waters CM, Ridge KM, Sunio G, Venetsanou K and Sznajder JI.** Mechanical stretching of alveolar epithelial cells increases Na(+)-K(+)-ATPase activity. *J Appl Physiol* 87: 715-721, 1999.

74. **Edwards YS, Sutherland LM and Murray AW.** NO protects alveolar type II cells from stretch-induced apoptosis. A novel role for macrophages in the lung. *Am J Physiol Lung Cell Mol Physiol* 279: L1236-L1242, 2000.

75. **Sanchez-Esteban J, Wang Y, Cicchiello LA and Rubin LP.** Cyclic mechanical stretch inhibits cell proliferation and induces apoptosis in fetal rat lung fibroblasts. *Am J Physiol Lung Cell Mol Physiol* 282: L448-L456, 2002.

76. **Chess PR, Toia L and Finkelstein JN.** Mechanical strain-induced proliferation and signaling in pulmonary epithelial H441 cells. *Am J Physiol Lung Cell Mol Physiol* 279: L43-L51, 2000.

77. **Sanchez-Esteban J, Wang Y, Gruppuso PA and Rubin LP.** Mechanical stretch induces fetal type II cell differentiation via an epidermal growth factor

receptor-extracellular-regulated protein kinase signaling pathway. *Am J Respir Cell Mol Biol* 30: 76-83, 2004.

78. **Rose F, Zwick K, Ghofrani HA, Sibelius U, Seeger W, Walmrath D and Grimminger F.** Prostacyclin enhances stretch-induced surfactant secretion in alveolar epithelial type II cells. *Am J Respir Crit Care Med* 160: 846-851, 1999.

79. **Dos Santos CC, Han B, Andrade CF, Bai X, Uhlig S, Hubmayr R, Tsang M, Lodyga M, Keshavjee S, Slutsky AS and Liu M.** DNA microarray analysis of gene expression in alveolar epithelial cells in response to TNFalpha, LPS, and cyclic stretch. *Physiol Genomics* 19: 331-342, 2004.

80. **Gilbert JA, Weinhold PS, Banes AJ, Link GW and Jones GL.** Strain profiles for circular cell culture plates containing flexible surfaces employed to mechanically deform cells in vitro. *J Biomech* 27: 1169-1177, 1994.

81. **Gutierrez JA, Ertsey R, Scavo LM, Collins E and Dobbs LG.** Mechanical distention modulates alveolar epithelial cell phenotypic expression by transcriptional regulation. *Am J Respir Cell Mol Biol* 21: 223-229, 1999.

82. **Oudin S and Pugin J.** Role of MAP Kinase Activation in Interleukin-8 Production by Human BEAS-2B Bronchial Epithelial Cells Submitted to Cyclic Stretch. *Am J Respir Cell Mol Biol* 27: 107-114, 2002.

83. **Sanchez-Esteban J, Wang Y, Filardo EJ, Rubin LP and Ingber DE.** Integrins beta1, alpha6, and alpha3 contribute to mechanical strain-induced differentiation of fetal lung type II epithelial cells via distinct mechanisms. *Am J Physiol Lung Cell Mol Physiol* 290: L343-L350, 2006.

84. **Chapman KE, Sinclair SE, Zhuang D, Hassid A, Desai LP and Waters CM.** Cyclic mechanical strain increases reactive oxygen species production in pulmonary epithelial cells. *Am J Physiol Lung Cell Mol Physiol* 289: L834-L841, 2005.

85. **Tschumperlin DJ and Margulies SS.** Equibiaxial deformation-induced injury of alveolar epithelial cells in vitro. *Am J Physiol* 275: L1173-L1183, 1998.

86. **Singer W, Frick M, Haller T, Bernet S, Ritsch-Marte M and Dietl P.** Mechanical forces impeding exocytotic surfactant release revealed by optical tweezers. *Sheng Wu Hua Xue Yu Sheng Wu Wu Li Xue Bao (Shanghai)* 84: 1344-1351, 2003.

87. **Cavanaugh KJ, Jr., Oswari J and Margulies SS.** Role of stretch on tight junction structure in alveolar epithelial cells. *Am J Respir Cell Mol Biol* 25: 584-591, 2001.

88. **Isakson BE, Evans WH and Boitano S.** Intercellular Ca2+ signaling in alveolar epithelial cells through gap junctions and by extracellular ATP. *Am J Physiol Lung Cell Mol Physiol* 280: L221-L228, 2001.

89. **Berrios JC, Schroeder MA and Hubmayr RD.** Mechanical properties of alveolar epithelial cells in culture. *J Appl Physiol* 91: 65-73, 2001.

90. **Trepat X, Grabulosa M, Puig F, Maksym GN, Navajas D and Farre R.** Viscoelasticity of human alveolar epithelial cells subjected to stretch. *Am J Physiol Lung Cell Mol Physiol* 287: L1025-L1034, 2004.

91. **Ohata H, Seito N, Yoshida K and Momose K.** Lysophosphatidic acid sensitizes mechanical stress-induced Ca2+ mobilization in cultured human lung epithelial cells. *Life Sci* 58: 29-36, 1996.

92. **Wright MO, Stockwell RA and Nuki G.** Response of plasma membrane to applied hydrostatic pressure in chondrocytes and fibroblasts. *Connect Tissue Res* 28: 49-70, 1992.

93. **Salter DM, Robb JE and Wright MO.** Electrophysiological responses of human bone cells to mechanical stimulation: evidence for specific integrin function in mechanotransduction. *J Bone Miner Res* 12: 1133-1141, 1997.

94. **Durvasula RV, Petermann AT, Hiromura K, Blonski M, Pippin J, Mundel P, Pichler R, Griffin S, Couser WG and Shankland SJ.** Activation of a local tissue angiotensin system in podocytes by mechanical strain. *Kidney Int* 65: 30-39, 2004.

95. **Hipper A and Isenberg G.** Cyclic mechanical strain decreases the DNA synthesis of vascular smooth muscle cells. *Pflugers Arch* 440: 19-27, 2000.

96. **Alenghat FJ and Ingber DE.** Mechanotransduction: all signals point to cytoskeleton, matrix, and integrins. *Sci STKE* 2002: E6, 2002.

97. **Dos Santos CC and Slutsky AS.** Mechanotransduction, ventilator-induced lung injury and multiple organ dysfunction syndrome. *Intensive Care Med* 26: 638-642, 2000.

98. **Ingber DE.** Cellular basis of mechanotransduction. *Biol Bull* 194: 323-325, 1998.

99. **Oddou C, Wendling S, Petite H and Meunier A.** Cell mechanotransduction and interactions with biological tissues. *Biorheology* 37: 17-25, 2000.

100. **Vlahakis NE and Hubmayr RD.** Response of alveolar cells to mechanical stress. *Curr Opin Crit Care* 9: 2-8, 2003.

101. **Riley DJ, Rannels DE, Low RB, Jensen L and Jacobs TP.** NHLBI Workshop Summary. Effect of physical forces on lung structure, function, and metabolism. *Am Rev Respir Dis* 142: 910-914, 1990.

102. **Guharay F and Sachs F.** Stretch-activated single ion channel currents in tissue-cultured embryonic chick skeletal muscle. *J Physiol* 352: 685-701, 1984.

103. **Millward-Sadler SJ and Salter DM.** Integrin-dependent signal cascades in chondrocyte mechanotransduction. *Ann Biomed Eng* 32: 435-446, 2004.

104. **Chen KD, Li YS, Kim M, Li S, Yuan S, Chien S and Shyy JY.** Mechanotransduction in response to shear stress. Roles of receptor tyrosine kinases, integrins, and Shc. *J Biol Chem* 274: 18393-18400, 1999.

105. **Ingber DE.** Integrins, tensegrity, and mechanotransduction. *Gravit Space Biol Bull* 10: 49-55, 1997.

106. **Liu M, Xu J, Tanswell AK and Post M.** Inhibition of mechanical strain-induced fetal rat lung cell proliferation by gadolinium, a stretch-activated channel blocker. *Pharm Res* 161: 501-507, 1994.

107. **Wright M, Jobanputra P, Bavington C, Salter DM and Nuki G.** Effects of intermittent pressure-induced strain on the electrophysiology of cultured

human chondrocytes: evidence for the presence of stretch-activated membrane ion channels. *Clin Sci (Lond)* 90: 61-71, 1996.

108. **Hynes RO.** Integrins: versatility, modulation, and signaling in cell adhesion. *Cell* 69: 11-25, 1992.

109. **Muller JM, Chilian WM and Davis MJ.** Integrin signaling transduces shear stress--dependent vasodilation of coronary arterioles. *Circ Res* 80: 320-326, 1997.

110. **D'Angelo G, Mogford JE, Davis GE, Davis MJ and Meininger GA.** Integrin-mediated reduction in vascular smooth muscle [Ca2+]i induced by RGD-containing peptide. *Am J Physiol* 272: H2065-H2070, 1997.

111. **Schmidt C, Pommerenke H, Durr F, Nebe B and Rychly J.** Mechanical stressing of integrin receptors induces enhanced tyrosine phosphorylation of cytoskeletally anchored proteins. *J Biol Chem* 273: 5081-5085, 1998.

112. **MacKenna DA, Dolfi F, Vuori K and Ruoslahti E.** Extracellular signal-regulated kinase and c-Jun NH2-terminal kinase activation by mechanical stretch is integrin-dependent and matrix-specific in rat cardiac fibroblasts. *J Clin Invest* 101: 301-310, 1998.

113. **Brehm P, Kidokoro Y and Moody-Corbett F.** Acetylcholine receptor channel properties during development of Xenopus muscle cells in culture. *J Physiol* 357: 203-217, 1984.

114. **Sachs F.** Mechanical transduction by ion channels: how forces reach the channel. *Soc Gen Physiol Ser* 52: 209-218, 1997.

115. **Ghazi A, Berrier C, Ajouz B and Besnard M.** Mechanosensitive ion channels and their mode of activation. *Biochimie* 80: 357-362, 1998.

116. **Gu CX, Juranka PF and Morris CE.** Stretch-activation and stretch-inactivation of Shaker-IR, a voltage-gated K+ channel. *Sheng Wu Hua Xue Yu Sheng Wu Wu Li Xue Bao (Shanghai)* 80: 2678-2693, 2001.

117. **Adamson IY and Young L.** Alveolar type II cell growth on a pulmonary endothelial extracellular matrix. *Am J Physiol* 270: L1017-L1022, 1996.

118. **Calabrese B, Tabarean IV, Juranka P and Morris CE.** Mechanosensitivity of N-type calcium channel currents. *Sheng Wu Hua Xue Yu Sheng Wu Wu Li Xue Bao (Shanghai)* 83: 2560-2574, 2002.

119. **Casado M and Ascher P.** Opposite modulation of NMDA receptors by lysophospholipids and arachidonic acid: common features with mechanosensitivity. *J Physiol* 513 (Pt 2): 317-330, 1998.

120. **Salter DM, Wright MO and Millward-Sadler SJ.** NMDA receptor expression and roles in human articular chondrocyte mechanotransduction. *Biorheology* 41: 273-281, 2004.

121. **Kawakubo T, Naruse K, Matsubara T, Hotta N and Sokabe M.** Characterization of a newly found stretch-activated KCa,ATP channel in cultured chick ventricular myocytes. *Am J Physiol* 276: H1827-H1838, 1999.

122. **Datta SR, Dudek H, Tao X, Masters S, Fu H, Gotoh Y and Greenberg ME.** Akt phosphorylation of BAD couples survival signals to the cell-intrinsic death machinery. *Cell* 91: 231-241, 1997.

123. **Orazizadeh , M.** The role of PKB signalling in chondrocyte mechanotransduction. 2006.

Ref Type: Personal Communication

124. **Liu M, Liu J, Buch S, Tanswell AK and Post M.** Antisense oligonucleotides for PDGF-B and its receptor inhibit mechanical strain-induced fetal lung cell growth. *Am J Physiol* 269: L178-L184, 1995.

125. **Woodruff ML, Chaban VV, Worley CM and Dirksen ER.** PKC role in mechanically induced Ca2+ waves and ATP-induced Ca2+ oscillations in airway epithelial cells. *Am J Physiol* 276: L669-L678, 1999.

126. **Liu M, Qin Y, Liu J, Tanswell AK and Post M.** Mechanical strain induces pp60src activation and translocation to cytoskeleton in fetal rat lung cells. *J Biol Chem* 271: 7066-7071, 1996.

127. **Lee HS, Millward-Sadler SJ, Wright MO, Nuki G and Salter DM.** Integrin and mechanosensitive ion channel-dependent tyrosine phosphorylation of focal adhesion proteins and beta-catenin in human articular chondrocytes after mechanical stimulation. *J Bone Miner Res* 15: 1501-1509, 2000.

128. **Agarwal S, Deschner J, Long P, Verma A, Hofman C, Evans CH and Piesco N.** Role of NF-kappaB transcription factors in antiinflammatory and proinflammatory actions of mechanical signals. *Arthritis Rheum* 50: 3541-3548, 2004.

129. **Rannels DE.** Role of physical forces in compensatory growth of the lung. *Am J Physiol* 257: L179-L189, 1989.

130. **Joe P, Wallen LD, Chapin CJ, Lee CH, Allen L, Han VK, Dobbs LG, Hawgood S and Kitterman JA.** Effects of mechanical factors on growth and maturation of the lung in fetal sheep. *Am J Physiol* 272: L95-105, 1997.

131. **Flecknoe SJ, Wallace MJ, Cock ML, Harding R and Hooper SB.** Changes in alveolar epithelial cell proportions during fetal and postnatal development in sheep. *Am J Physiol Lung Cell Mol Physiol* 285: L664-L670, 2003.

132. **Bishop JE, Mitchell JJ, Absher PM, Baldor L, Geller HA, Woodcock-Mitchell J, Hamblin MJ, Vacek P and Low RB.** Cyclic mechanical deformation stimulates human lung fibroblast proliferation and autocrine growth factor activity. *Am J Respir Cell Mol Biol* 9: 126-133, 1993.

133. **Dietl P, Haller T, Mair N and Frick M.** Mechanisms of surfactant exocytosis in alveolar type II cells in vitro and in vivo. *News Physiol Sci* 16: 239-243, 2001.

134. **Lines A, Nardo L, Phillips ID, Possmayer F and Hooper SB.** Alterations in lung expansion affect surfactant protein A, B, and C mRNA levels in fetal sheep. *Am J Physiol* 276: L239-L245, 1999.

135. **Torday JS, Sanchez-Esteban J and Rubin LP.** Paracrine mediators of mechanotransduction in lung development. *Am J Med Sci* 316: 205-208, 1998.

136. **Millward-Sadler SJ, Wright MO, Lee H, Nishida K, Caldwell H, Nuki G and Salter DM.** Integrin-regulated secretion of interleukin 4: A novel pathway of mechanotransduction in human articular chondrocytes. *J Cell Biol* 145: 183-189, 1999.

137. **Pasternack M, Jr., Liu X, Goodman RA and Rannels DE.** Regulated stimulation of epithelial cell DNA synthesis by fibroblast-derived mediators. *Am J Physiol* 272: L619-L630, 1997.

138. **McAdams RM, Mustafa SB, Shenberger JS, Dixon PS, Henson BM and Digeronimo RJ.** Cyclic stretch attenuates the effects of hyperoxia on cell proliferation and viability in human alveolar epithelial cells. *Am J Physiol Lung Cell Mol Physiol* 2006.

139. **Copland IB, Reynaud D, Pace-Asciak C and Post M.** MECHANOTRANSDUCTION OF STRETCH-INDUCED PROSTANOID RELEASE BY FETAL LUNG EPITHELIAL CELLS. *Am J Physiol Lung Cell Mol Physiol* 2006.

140. **Millward-Sadler SJ, Wright MO, Davies LW, Nuki G and Salter DM.** Mechanotransduction via integrins and interleukin-4 results in altered aggrecan and matrix metalloproteinase 3 gene expression in normal, but not osteoarthritic, human articular chondrocytes. *Arthritis Rheum* 43: 2091-2099, 2000.

141. **Flecknoe SJ, Wallace MJ, Harding R and Hooper SB.** Determination of alveolar epithelial cell phenotypes in fetal sheep: evidence for the involvement of basal lung expansion. *J Physiol* 542: 245-253, 2002.

142. **Flecknoe SJ, Wallace MJ, Cock ML, Harding R and Hooper SB.** Changes in alveolar epithelial cell proportions during fetal and postnatal development in sheep. *Am J Physiol Lung Cell Mol Physiol* 285: L664-L670, 2003.

143. **Adamson IY and Bowden DH.** Derivation of type 1 epithelium from type 2 cells in the developing rat lung. *Lab Invest* 32: 736-745, 1975.

144. **Mercurio AR and Rhodin JA.** An electron microscopic study on the type I pneumocyte in the cat: differentiation. *Am J Anat* 146: 255-271, 1976.

145. **Dobbs LG.** Isolation and culture of alveolar type II cells. *Am J Physiol* 258: L134-L147, 1990.

146. **Murphy SA, Dinsdale D, Hoet P, Nemery B and Richards RJ.** A comparative study of the isolation of type II epithelial cells from rat, hamster, pig and human lung tissue. *Methods Cell Sci* 21: 31-38, 1999.

147. **Boone CW, Harell GS and Bond HE.** The resolution of mixtures of viable mammalian cells into homogeneous fractions by zonal centrifugation. *J Cell Biol* 36: 369-378, 1968.

148. **Crapo JD and Greeley DA.** Estimation of the mean caliper diameter of cell nuclei. II. Various cell types in rat lung. *J Microsc* 114: 41-48, 1978.

149. **Haies DM, Gil J and Weibel ER.** Morphometric study of rat lung cells. I. Numerical and dimensional characteristics of parenchymal cell population. *Am Rev Respir Dis* 123: 533-541, 1981.

150. **Finkelstein JN and Mavis RD.** Biochemical evidence for internal proteolytic damage during isolation of type II alveolar epithelial cells. *Lung* 156: 243-254, 1979.

151. **Goodman BE and Crandall ED.** Dome formation in primary cultured monolayers of alveolar epithelial cells. *Am J Physiol* 243: C96-100, 1982.

152. **Cunningham AC, Milne DS, Wilkes J, Dark JH, Tetley TD and Kirby JA.** Constitutive expression of MHC and adhesion molecules by alveolar epithelial

cells (type II pneumocytes) isolated from human lung and comparison with immunocytochemical findings. *J Cell Sci* 107 (Pt 2): 443-449, 1994.

153. **Zissel G, Ernst M, Rabe K, Papadopoulos T, Magnussen H, Schlaak M and Muller-Quernheim J.** Human alveolar epithelial cells type II are capable of regulating T-cell activity. *J Investig Med* 48: 66-75, 2000.

154. **Robinson PC, Voelker DR and Mason RJ.** Isolation and culture of human alveolar type II epithelial cells. Characterization of their phospholipid secretion. *Am Rev Respir Dis* 130: 1156-1160, 1984.

155. **Papadopoulos T, Ionescu L, Dammrich J, Toomes H and Muller-Hermelink HK.** Type I and type IV collagen promote adherence and spreading of human type II pneumocytes in vitro. *Lab Invest* 62: 562-569, 1990.

156. **Guzman J, Izumi T, Nagai S and Costabel U.** Immunocytochemical characterization of isolated human type II pneumocytes. *Acta Cytol* 38: 539-542, 1994.

157. **Fuchs S, Hollins AJ, Laue M, Schaefer UF, Roemer K, Gumbleton M and Lehr CM.** Differentiation of human alveolar epithelial cells in primary culture: morphological characterization and synthesis of caveolin-1 and surfactant protein-C. *Cell Tissue Res* 311: 31-45, 2003.

158. **Voelker, D. R. and Mason, R. J.** Alveolar type II epithelial cells. Massaro, D. (41), 487-538. 1987. New York, USA, Marcel Dekker, Inc. Lung biology in health and Disease. Lenfant, C.

159. **Wilson JS, Steinkamp JA and Lehnert BE.** Isolation of viable type II alveolar epithelial cells by flow cytometry. *Cytometry* 7: 157-162, 1986.

160. **Leary JF, Finkelstein JN, Notter RH and Shapiro DL.** Isolation of type II pneumocytes by laser flow cytometry. *Am Rev Respir Dis* 125: 326-330, 1982.

161. **Guttentag SH, Beers MF, Bieler BM and Ballard PL.** Surfactant protein B processing in human fetal lung. *Am J Physiol* 275: L559-L566, 1998.

162. **Gonzales LW, Angampalli S, Guttentag SH, Beers MF, Feinstein SI, Matlapudi A and Ballard PL.** Maintenance of differentiated function of the surfactant system in human fetal lung type II epithelial cells cultured on plastic. *Pediatr Pathol Mol Med* 20: 387-412, 2001.

163. **Mason RJ, Walker SR, Shields BA, Henson JE and Williams MC.** Identification of rat alveolar type II epithelial cells with a tannic acid and polychrome stain. *Am Rev Respir Dis* 131: 786-788, 1985.

164. **Campbell L, Hollins AJ, Al Eid A, Newman GR, von Ruhland C and Gumbleton M.** Caveolin-1 expression and caveolae biogenesis during cell transdifferentiation in lung alveolar epithelial primary cultures. *Biochem Biophys Res Commun* 262: 744-751, 1999.

165. **Kasper M, Reimann T, Hempel U, Wenzel KW, Bierhaus A, Schuh D, Dimmer V, Haroske G and Muller M.** Loss of caveolin expression in type I pneumocytes as an indicator of subcellular alterations during lung fibrogenesis. *Histochem Cell Biol* 109: 41-48, 1998.

166. **Dobbs LG, Williams MC and Brandt AE.** Changes in biochemical characteristics and pattern of lectin binding of alveolar type II cells with time in culture. *Biochim Biophys Acta* 846: 155-166, 1985.

167. **Greenleaf RD, Mason RJ and Williams MC.** Isolation of alveolar type II cells by centrifugal elutriation. *In Vitro* 15: 673-684, 1979.

168. **Walker SR, Williams MC and Benson B.** Immunocytochemical localization of the major surfactant apoproteins in type II cells, Clara cells, and alveolar macrophages of rat lung. *J Histochem Cytochem* 34: 1137-1148, 1986.

169. **Williams MC, Hawgood S, Schenk DB, Lewicki J, Phelps MN and Benson B.** Monoclonal antibodies to surfactant proteins SP28-36 label canine type II and nonciliated bronchiolar cells by immunofluorescence. *Am Rev Respir Dis* 137: 399-405, 1988.

170. **Shannon JM, Emrie PA, Fisher JH, Kuroki Y, Jennings SD and Mason RJ.** Effect of a reconstituted basement membrane on expression of surfactant apoproteins in cultured adult rat alveolar type II cells. *Am J Respir Cell Mol Biol* 2: 183-192, 1990.

171. **Phelps DS and Floros J.** Localization of pulmonary surfactant proteins using immunohistochemistry and tissue in situ hybridization. *Exp Lung Res* 17: 985-995, 1991.

172. **Kalina M, Mason RJ and Shannon JM.** Surfactant protein C is expressed in alveolar type II cells but not in Clara cells of rat lung. *Am J Respir Cell Mol Biol* 6: 594-600, 1992.

173. **Beers MF, Kim CY, Dodia C and Fisher AB.** Localization, synthesis, and processing of surfactant protein SP-C in rat lung analyzed by epitope-specific antipeptide antibodies. *J Biol Chem* 269: 20318-20328, 1994.

174. **Corrin B and King E.** Experimental endogenous lipid pneumonia and silicosis. *J Pathol* 97: 325-330, 1969.

175. **Mason RJ and Williams MC.** Type II alveolar cell. Defender of the alveolus. *Am Rev Respir Dis* 115: 81-91, 1977.

176. **Dobbs LG, Pian MS, Maglio M, Dumars S and Allen L.** Maintenance of the differentiated type II cell phenotype by culture with an apical air surface. *Am J Physiol* 273: L347-L354, 1997.

177. **Shannon JM, Jennings SD and Nielsen LD.** Modulation of alveolar type II cell differentiated function in vitro. *Am J Physiol* 262: L427-L436, 1992.

178. **Bui KC, Buckley S, Wu F, Uhal B, Joshi I, Liu J, Hussain M, Makhoul I and Warburton D.** Induction of A- and D-type cyclins and cdc2 kinase activity during recovery from short-term hyperoxic lung injury. *Am J Physiol* 268: L625-L635, 1995.

179. **Brody JS, Vaccaro CA and Joyce-Brady MF.** Human pulmonary alveolar type 2 cells contain an apical membrane glycoprotein common to malignant cells. *Lab Invest* 59: 522-530, 1988.

180. **Boylan GM, Pryde JG, Dobbs LG and McElroy MC.** Identification of a novel antigen on the apical surface of rat alveolar epithelial type II and Clara cells. *Am J Physiol Lung Cell Mol Physiol* 280: L1318-L1326, 2001.

181. **Newman V, Gonzalez RF, Matthay MA and Dobbs LG.** A novel alveolar type I cell-specific biochemical marker of human acute lung injury. *Am J Respir Crit Care Med* 161: 990-995, 2000.

182. **Kasper M and Singh G.** Epithelial lung cell marker: current tools for cell typing. *Histol Histopathol* 10: 155-169, 1995.

183. **Kasper M, Haroske G and Muller M.** Species differences in lectin binding to pulmonary cells: Soybean agglutinin (SBA) as a marker of type I alveolar epithelial cells and alveolar macrophages in mini pigs. *Acta Histochem* 96: 63-73, 1994.

184. **McBride S, Tatrai E, Blundell R, Kovacikova Z, Cardozo L, Adamis Z, Smith T and Harrison D.** Characterisation of lectin binding patterns of mouse bronchiolar and rat alveolar epithelial cells in culture. *Histochem J* 32: 33-40, 2000.

185. **Taatjes DJ, Barcomb LA, Leslie KO and Low RB.** Lectin binding patterns to terminal sugars of rat lung alveolar epithelial cells. *J Histochem Cytochem* 38: 233-244, 1990.

186. **Sarker AB, Koirala TR, Aftabuddin, Jeon HJ and Murakami I.** Lectin histochemistry of normal lung and pulmonary carcinoma. *Indian J Pathol Microbiol* 37: 29-38, 1994.

187. **Chu PG and Weiss LM.** Keratin expression in human tissues and neoplasms. *Histopathology* 40: 403-439, 2002.

188. **Blobel GA, Moll R, Franke WW and Vogt-Moykopf I.** Cytokeratins in normal lung and lung carcinomas. I. Adenocarcinomas, squamous cell carcinomas and cultured cell lines. *Virchows Arch B Cell Pathol Incl Mol Pathol* 45: 407-429, 1984.

189. **Broers JL, de Leij L, Rot MK, ter Haar A, Lane EB, Leigh IM, Wagenaar SS, Vooijs GP and Ramaekers FC.** Expression of intermediate filament proteins in fetal and adult human lung tissues. *Differentiation* 40: 119-128, 1989.

190. **Edelson JD, Shannon JM and Mason RJ.** Alkaline phosphatase: a marker of alveolar type II cell differentiation. *Am Rev Respir Dis* 138: 1268-1275, 1988.

191. **Iyonaga K, Miyajima M, Suga M, Saita N and Ando M.** Alterations in cytokeratin expression by the alveolar lining epithelial cells in lung tissues from patients with idiopathic pulmonary fibrosis. *J Pathol* 182: 217-224, 1997.

192. **Jonas E, Sargent TD and Dawid IB.** Epidermal keratin gene expressed in embryos of Xenopus laevis. *Proc Natl Acad Sci U S A* 82: 5413-5417, 1985.

193. **Paine R, Ben Ze'ev A, Farmer SR and Brody JS.** The pattern of cytokeratin synthesis is a marker of type 2 cell differentiation in adult and maturing fetal lung alveolar cells. *Dev Biol* 129: 505-515, 1988.

194. **Li CY, Ziesmer SC, Wong YC and Yam LT. Diagnostic accuracy of the immunocytochemical study of body fluids.** ***Acta Cytol* 33: 667-673, 1989.**

195. **Pulido R, Cebrian M, Acevedo A, de Landazuri MO and Sanchez-Madrid F.** Comparative biochemical and tissue distribution study of four distinct CD45 antigen specificities. *J Immunol* 140: 3851-3857, 1988.

196. **Freshney, R. I.** Culture of animal cell; a manual of basic technique. 4th, 149-175. 2000. New York, USA, John - Wiley & Sons, Inc.

197. **Maas-Szabowski N, Shimotoyodome A and Fusenig NE.** Keratinocyte growth regulation in fibroblast cocultures via a double paracrine mechanism. *J Cell Sci* 112 (Pt 12): 1843-1853, 1999.

198. **Edwards YS, Sutherland LM, Power JH, Nicholas TE and Murray AW.** Cyclic stretch induces both apoptosis and secretion in rat alveolar type II cells. *FEBS Lett* 448: 127-130, 1999.

199. **Brower M, Carney DN, Oie HK, Gazdar AF and Minna JD.** Growth of cell lines and clinical specimens of human non-small cell lung cancer in a serum-free defined medium. *Cancer Res* 46: 798-806, 1986.

200. **Gazdar AF, Linnoila RI, Kurita Y, Oie HK, Mulshine JL, Clark JC and Whitsett JA.** Peripheral airway cell differentiation in human lung cancer cell lines. *Cancer Res* 50: 5481-5487, 1990.

201. **Betz C, Papadopoulos T, Buchwald J, Dammrich J and Muller-Hermelink HK.** Surfactant protein gene expression in metastatic and micrometastatic pulmonary adenocarcinomas and other non-small cell lung carcinomas: detection by reverse transcriptase-polymerase chain reaction. *Cancer Res* 55: 4283-4286, 1995.

202. **Zhang J, Li W, Sanders MA, Sumpio BE, Panja A and Basson MD.** Regulation of the intestinal epithelial response to cyclic strain by extracellular matrix proteins. *FASEB J* 2003.

203. **Millward-Sadler SJ, Wright MO, Lee H, Caldwell H, Nuki G and Salter DM.** Altered electrophysiological responses to mechanical stimulation and abnormal signalling through alpha5beta1 integrin in chondrocytes from osteoarthritic cartilage. *Osteoarthritis Cartilage* 8: 272-278, 2000.

204. Millward-Sadler SJ, Wright MO, Flatman PW and Salter DM. ATP in the mechanotransduction pathway of normal human chondrocytes. *Biorheology* 41: 567-575, 2004.

205. Salter DM, Millward-Sadler SJ, Nuki G and Wright MO. Differential responses of chondrocytes from normal and osteoarthritic human articular cartilage to mechanical stimulation. *Biorheology* 39: 97-108, 2002.

206. Salter DM, Millward-Sadler SJ, Nuki G and Wright MO. Integrin-interleukin-4 mechanotransduction pathways in human chondrocytes. *Clin Orthop* S49-S60, 2001.

207. Salter DM, Wallace WH, Robb JE, Caldwell H and Wright MO. Human bone cell hyperpolarization response to cyclical mechanical strain is mediated by an interleukin-1beta autocrine/paracrine loop. *J Bone Miner Res* 15: 1746-1755, 2000.

208. Yada T and Okada Y. Electrical activity of an intestinal epithelial cell line: hyperpolarizing responses to intestinal secretagogues. *J Membr Biol* 77: 33-44, 1984.

209. Gilbert M and Knox S. Influence of Bcl-2 overexpression on Na+/K(+)-ATPase pump activity: correlation with radiation-induced programmed cell death. *Pharm Res* 171: 299-304, 1997.

210. Soliven B, Takeda M and Szuchet S. Depolarizing agents and tumor necrosis factor-alpha modulate protein phosphorylation in oligodendrocytes. *J Neurosci Res* 38: 91-100, 1994.

211. **Vasilets LA, Ohta T, Noguchi S, Kawamura M and Schwarz W.** Voltage-dependent inhibition of the sodium pump by external sodium: species differences and possible role of the N-terminus of the alpha-subunit. *Eur Biophys J* 21: 433-443, 1993.

212. **Haller T, Ortmayr J, Friedrich F, Volkl H and Dietl P.** Dynamics of surfactant release in alveolar type II cells. *Proc Natl Acad Sci U S A* 95: 1579-1584, 1998.

213. **Meredith JE, Jr., Fazeli B and Schwartz MA.** The extracellular matrix as a cell survival factor. *Mol Biol Cell* 4: 953-961, 1993.

214. **Diglio CA and Kikkawa Y.** The type II epithelial cells of the lung. IV. Adaption and behavior of isolated type II cells in culture. *Lab Invest* 37: 622-631, 1977.

215. **Mason RJ and Dobbs LG.** Synthesis of phosphatidylcholine and phosphatidylglycerol by alveolar type II cells in primary culture. *J Biol Chem* 255: 5101-5107, 1980.

216. **Sanchez-Esteban J, Cicchiello LA, Wang Y, Tsai SW, Williams LK, Torday JS and Rubin LP.** Mechanical stretch promotes alveolar epithelial type II cell differentiation. *J Appl Physiol* 91: 589-595, 2001.

217. **Dobbs LG and Gutierrez JA.** Mechanical forces modulate alveolar epithelial phenotypic expression. *Comp Biochem Physiol A Mol Integr Physiol* 129: 261-266, 2001.

218. **Rannels SR, Yarnell JA, Fisher CS, Fabisiak JP and Rannels DE.** Role of laminin in maintenance of type II pneumocyte morphology and function. *Am J Physiol* 253: C835-C845, 1987.

219. **Plopper CG, Mariassy AT and Lollini LO.** Structure as revealed by airway dissection. A comparison of mammalian lungs. *Am Rev Respir Dis* 128: S4-S7, 1983.

220. **Bachofen H, Schurch S, Urbinelli M and Weibel ER.** Relations among alveolar surface tension, surface area, volume, and recoil pressure. *J Appl Physiol* 62: 1878-1887, 1987.

221. **Chandel NS and Sznajder JI.** Stretching the lung and programmed cell death. *Am J Physiol Lung Cell Mol Physiol* 279: L1003-L1004, 2000.

222. **Kasper M and Haroske G.** Alterations in the alveolar epithelium after injury leading to pulmonary fibrosis. *Histol Histopathol* 11: 463-483, 1996.

223. **Pattle RE.** The relation between surface tension and area in the alveolar lining film. *J Physiol* 269: 591-604, 1977.

224. **Clements JA.** Surface tension of lung extracts. *Proc Soc Exp Biol Med* 95: 170-172, 1957.

225. **Vazquez dL, Becerril C, Montano M, Ramos C, Maldonado V, Melendez J, Phelps DS, Pardo A and Selman M.** Surfactant components modulate fibroblast apoptosis and type I collagen and collagenase-1 expression. *Am J Physiol Lung Cell Mol Physiol* 279: L950-L957, 2000.

226. **Pison U, Max M, Neuendank A, Weissbach S and Pietschmann S.** Host defence capacities of pulmonary surfactant: evidence for 'non-surfactant' functions of the surfactant system. *Eur J Clin Invest* 24: 586-599, 1994.

227. **Crouch EC.** Surfactant protein-D and pulmonary host defense. *Respir Res* 1: 93-108, 2000.

228. **Wu H, Kuzmenko A, Wan S, Schaffer L, Weiss A, Fisher JH, Kim KS and McCormack FX.** Surfactant proteins A and D inhibit the growth of Gram-negative bacteria by increasing membrane permeability. *J Clin Invest* 111: 1589-1602, 2003.

229. **Weissbach S, Neuendank A, Pettersson M, Schaberg T and Pison U.** Surfactant protein A modulates release of reactive oxygen species from alveolar macrophages. *Am J Physiol* 267: L660-L666, 1994.

230. **Stamme C, Walsh E and Wright JR.** Surfactant protein A differentially regulates IFN-gamma- and LPS-induced nitrite production by rat alveolar macrophages. *Am J Respir Cell Mol Biol* 23: 772-779, 2000.

231. **Blau H, Riklis S, Kravtsov V and Kalina M.** Secretion of cytokines by rat alveolar epithelial cells: possible regulatory role for SP-A. *Am J Physiol* 266: L148-L155, 1994.

232. **Finkelstein JN, Johnston C, Barrett T, Oberdorster G, Wright TW, Johnston CJ, Harmsen AG and Finkelstein JN.** Particulate-cell interactions and pulmonary cytokine expression

Analysis of cytokine mRNA profiles in the lungs of Pneumocystis carinii-infected mice. *Nutrition* 105 Suppl 5: 1179-1182, 1997.

233. **Kunkel SL and Strieter RM.** Cytokine networking in lung inflammation. *Hosp Pract (Off Ed)* 25: 63-66, 1990.

234. **Schneeberger EE, DeFerrari M, Skoskiewicz MJ, Russell PS and Colvin RB.** Induction of MHC-determined antigens in the lung by interferon-gamma. *Lab Invest* 55: 138-144, 1986.

235. **Paine R, III, Mody CH, Chavis A, Spahr MA, Turka LA and Toews GB.** Alveolar epithelial cells block lymphocyte proliferation in vitro without inhibiting activation. *Am J Respir Cell Mol Biol* 5: 221-229, 1991.

236. **Rosseau S, Hammerl P, Maus U, Walmrath HD, Schutte H, Grimminger F, Seeger W, Lohmeyer J, Rosseau S, Selhorst J, Wiechmann K, Leissner K, Maus U, Mayer K, Grimminger F, Seeger W and Lohmeyer J.** Phenotypic characterization of alveolar monocyte recruitment in acute respiratory distress syndrome

Monocyte migration through the alveolar epithelial barrier: adhesion molecule mechanisms and impact of chemokines. *Am J Physiol Lung Cell Mol Physiol* 279: L25-L35, 2000.

237. **von Bethmann AN, Brasch F, Nusing R, Vogt K, Volk HD, Muller KM, Wendel A and Uhlig S.** Hyperventilation induces release of cytokines from perfused mouse lung. *Am J Respir Crit Care Med* 157: 263-272, 1998.

238. **Tremblay L, Valenza F, Ribeiro SP, Li J and Slutsky AS.** Injurious ventilatory strategies increase cytokines and c-fos m-RNA expression in an isolated rat lung model. *J Clin Invest* 99: 944-952, 1997.

239. **Wallace WA and Howie SE.** Immunoreactive interleukin 4 and interferon-gamma expression by type II alveolar epithelial cells in interstitial lung disease. *J Pathol* 187: 475-480, 1999.

240. **Witherden IR, Vanden Bon EJ, Goldstraw P, Ratcliffe C, Pastorino U and Tetley TD.** Primary human alveolar type II epithelial cell chemokine release: effects of cigarette smoke and neutrophil elastase. *Am J Respir Cell Mol Biol* 30: 500-509, 2004.

241. **Phelps DS and Floros J.** Localization of surfactant protein synthesis in human lung by in situ hybridization. *Am Rev Respir Dis* 137: 939-942, 1988.

242. **Liley HG, White RT, Benson BJ, Ballard PL, Liley HG, Ertsey R, Gonzales LW, Odom MW, Hawgood S, Dobbs LG and Ballard PL.** Glucocorticoids both stimulate and inhibit production of pulmonary surfactant protein A in fetal human lung

Synthesis of surfactant components by cultured type II cells from human lung. *Proc Natl Acad Sci U S A* 85: 9096-9100, 1988.

243. **Adamson IY and Bowden DH.** The pathogenesis of bloemycin-induced pulmonary fibrosis in mice. *Annu Rev Physiol* 77: 185-197, 1974.

244. **Thellin O, Zorzi W, Lakaye B, De Borman B, Coumans B, Hennen G, Grisar T, Igout A and Heinen E.** Housekeeping genes as internal standards: use and limits. *J Biotechnol* 75: 291-295, 1999.

245. **Bustin SA.** Quantification of mRNA using real-time reverse transcription PCR (RT-PCR): trends and problems. *J Mol Endocrinol* 29: 23-39, 2002.

246. **Mansur NR, Meyer-Siegler K, Wurzer JC and Sirover MA.** Cell cycle regulation of the glyceraldehyde-3-phosphate dehydrogenase/uracil DNA glycosylase gene in normal human cells. *Nucleic Acids Res* 21: 993-998, 1993.

247. **Graven KK, McDonald RJ and Farber HW.** Hypoxic regulation of endothelial glyceraldehyde-3-phosphate dehydrogenase. *Am J Physiol* 274: C347-C355, 1998.

248. **Zhong H and Simons JW.** Direct comparison of GAPDH, beta-actin, cyclophilin, and 28S rRNA as internal standards for quantifying RNA levels under hypoxia. *Biochem Biophys Res Commun* 259: 523-526, 1999.

249. **Ito Y, Pagano PJ, Tornheim K, Brecher P and Cohen RA.** Oxidative stress increases glyceraldehyde-3-phosphate dehydrogenase mRNA levels in isolated rabbit aorta. *Am J Physiol* 270: H81-H87, 1996.

250. **Barroso I, Benito B, Garci-Jimenez C, Hernandez A, Obregon MJ and Santisteban P.** Norepinephrine, tri-iodothyronine and insulin upregulate glyceraldehyde-3-phosphate dehydrogenase mRNA during Brown adipocyte differentiation. *Eur J Endocrinol* 141: 169-179, 1999.

251. **Yamada H, Chen D, Monstein HJ and Hakanson R.** Effects of fasting on the expression of gastrin, cholecystokinin, and somatostatin genes and of various housekeeping genes in the pancreas and upper digestive tract of rats. *Biochem Biophys Res Commun* 231: 835-838, 1997.

252. **Glogauer M, Arora P, Yao G, Sokholov I, Ferrier J and McCulloch CA.** Calcium ions and tyrosine phosphorylation interact coordinately with actin to regulate cytoprotective responses to stretching. *J Cell Sci* 110 (Pt 1): 11-21, 1997.

253. **Wright MO, Nishida K, Bavington C, Godolphin JL, Dunne E, Walmsley S, Jobanputra P, Nuki G and Salter DM.** Hyperpolarisation of cultured human chondrocytes following cyclical pressure-induced strain: evidence of a role for alpha 5 beta 1 integrin as a chondrocyte mechanoreceptor. *J Orthop Res* 15: 742-747, 1997.

254. **Yasukawa H, Sasaki A and Yoshimura A.** Negative regulation of cytokine signaling pathways. *Annu Rev Immunol* 18: 143-164, 2000.

255. **Ogata H, Chinen T, Yoshida T, Kinjyo I, Takaesu G, Shiraishi H, Iida M, Kobayashi T and Yoshimura A.** Loss of SOCS3 in the liver promotes fibrosis by enhancing STAT3-mediated TGF-beta1 production. *Oncogene* 25: 2520-2530, 2006.

256. **Rannels DE, Dunsmore SE and Grove RN.** Extracellular matrix synthesis and turnover by type II pulmonary epithelial cells. *Am J Physiol* 262: L582-L589, 1992.

257. **Rannels SR, Fisher CS, Heuser LJ and Rannels DE.** Culture of type II pneumocytes on a type II cell-derived fibronectin-rich matrix. *Am J Physiol* 253: C759-C765, 1987.

258. **Edwards YS.** Stretch stimulation: its effects on alveolar type II cell function in the lung. *Comp Biochem Physiol A Mol Integr Physiol* 129: 245-260, 2001.

259. **Jalali S, del Pozo MA, Chen K, Miao H, Li Y, Schwartz MA, Shyy JY and Chien S.** Integrin-mediated mechanotransduction requires its dynamic interaction with specific extracellular matrix (ECM) ligands. *Proc Natl Acad Sci U S A* 98: 1042-1046, 2001.

260. Willis,B.C.; Liebler,J.M.; Luby-Phelps,K.; Nicholson,A.G.; Crandall,E.D.; du Bois,R.M.; Borok,Z. Induction of epithelial-mesenchymal transition in alveolar epithelial cells by transforming growth factor-beta1: potential role in idiopathic pulmonary fibrosis. *Am.J.Pathol.* 166 5 1321-1322, 2005.